A VISUAL INVESTIGATION OF THE INTERACTION OF SHOCK WAVES FROM A BODY IN CURVILINEAR DIVING FLIGHT BY SIMULATED SURFACE WAVES ON WATER

A Thesis Submitted to the Graduate Faculty
of the
University of Minnesota

by

Andrew Anthony Lemeshewsky
Lieutenant, United States Navy

In Partial Fulfillment of the Requirements

for the Degree of

Master of Science in Aeronautical Engineering

June, 1955

ACKNOWLEDGEMENTS

I wish to express my thanks to Professor John D. Akerman for his guidance and inspiration, to Mike Schonberg and Miles Mock for their help in the construction details, and to my wife, Carol, for her patience and understanding during the course of this investigation.

TABLE OF CONTENTS

INDEX OF FIGURES

Page

Page

Page

A VISUAL INVESTIGATION OF THE INTERACTION OF SHOCK WAVES FROM A BODY IN CURVILINEAR DIVING FLIGHT BY SIMULATED SURFACE WAVES ON WATER

SUMMARY

The problem investigated herein is the interaction of the shock waves from an aircraft moving in a curvilinear diving path. A pictorial presentation of these waves and their interactions, both in the vicinity of the body, and at distances beyond the influence of the body is given. Situations investigated include the interaction between the waves themselves as well as their interaction with other surfaces. These interactions are depicted both at constant and at changing Mach numbers.

The hydraulic analogy is used for the simulation of the problem. An outline of the basic theory behind the analogy is given. An experimental verification of the geometric accuracy of the shock wave patterns, as depicted by the surface water waves for the body under consideration, is presented.

The construction features of the water channel which was built for the tests are outlined. Specific emphasis is given the features which allow the simulation of curvilinear paths.

No attempt is made to gather quantitative data from the simulated shock wave interactions. Qualitative results relating to the major features of the interactions rather than to the minutiae are given.

The following conclusions are reached:

1. A water channel is a valuable aerodynamic research tool. In its simplest form it is very useful for the demonstration of known

aerodynamic phenomena and for the rapid and inexpensive checking of new theories and ideas. A channel made with precision and operated with care can furnish quantitive data. A water channel permits observation of transient phenomena associated with varying "flight" paths and velocities. High supersonic Mach numbers are easily simulated at water speeds of a few feet per second.

2. After extensive trial of the photographic techniques most frequently used in the study of surface water waves, i.e., refraction through and reflection from the water surface, it was found that they were generally not suitable for qualitative investigation of hydraulic jumps where phenomena occur over an area greater than two feet square. The method which allows the best visual and photographic observation of surface wave patterns uses light reflected from a water surface covered with aluminum powder.

3. For models with small flow deflection angles, the surface wave patterns formed in a water channel compare almost identically with the shock wave patterns for the same body in air.

4. In addition to the normal shock wave system associated with a particular body, under conditions of acceleration from a subsonic to a supersonic Mach number an additional tail wave is formed and shed by the body. This second tail wave trails astern until dissipated by viscous effects.

5. To achieve the full effect from the interaction of shock wave systems projected ahead of a suddenly decelerated body in flight, it is necessary that the body decelerate to a subcritical

Ma number and not only to a subsonic Mach number. Deceleration only to a supercritical subsonic Mach number results in the retention at the body of all the shock wave system aft of any small, local supercritical subsonic shock wave which may be formed on the body.

6. Planar interaction between an aircraft's shock wave system and any surface of a structure, regardless of whether it be horizontal, vertical or angled between, can be accomplished by a proper adjustment of flight conditions.

7. Regardless of the manner in which shock waves impinge on a surface of a structure, the transfer of energy is insufficient to cause even the slightest damage to the major structure. Planar interaction of the shock waves with glass areas, however, will usually result in the transfer of sufficient energy to shatter the glass.

This investigation was conducted by Lieutenant Andrew A. Lemeshewsky, United States Navy, in partial fulfillment of the requirements for the degree of Master of Science in Aeronautical Engineering from the University of Minnesota, during the academic year 1954-55.

SYMBOLS

a	speed of sound in gas; acceleration
C_p	specific heat at constant pressure
C_v	specific heat at constant volume
d	water depth
F	force
g	acceleration of gravity
m	mass
P	pressure of a gas
R	radius of curvature
T	absolute temperature
u, v	components of velocity in x-direction and y-direction, respectively
x, y	rectangular coordinate axes
V	velocity of flow
U	velocity of propagation of surface waves in fluid
ρ	mass density
γ	adiabatic gas constant, ratio of c_p to c_v of gas
ϕ	velocity potential in two-dimensional flow
λ	wave length of surface waves in liquid
σ	surface tension of liquid
θ	shock wave angle; hydraulic jump angle
δ	flow deflection angle

Subscripts:

o	value at stagnation
n	normal component
t	tangential component

A VISUAL INVESTIGATION OF THE INTERACTION OF SHOCK WAVES FROM A BODY IN CURVILINEAR DIVING FLIGHT BY SIMULATED SURFACE WAVES ON WATER

INTRODUCTION

The problem undertaken in this investigation is the simulation of the shock wave interactions from an aircraft in curvilinear diving flight. It is intended that these simulations represent, with reasonable geometric accuracy, the actual shock wave signatures associated with the aircraft performing certain specified actions.

A previous investigation[1]* has undertaken the experimental study of shock wave interactions from a body moving in straight line motion both at constant and changing Mach number. The purpose of this study is to reproduce some of the above results. In addition, it is intended to extend the study to include interactions along what is felt to be a typical curvilinear flight path associated with an aircraft performing a dive and pull-up. Further, the impingement of these shock wave signatures upon selected geometric surfaces is examined. A photographic record of these interactions is included herein.

The hydraulic analogy is used to represent the problem. In order to allow the simulation of curvilinear flight paths, a special water channel was constructed by the author. The basic construction features of this channel are outlined in the equipment section of this report.

---

*Numbers in parenthesis refer to the references at the end of this report.

THE THEORY

The analogy between compressible gas flow and the flow of liquids with a free surface, known as the hydraulic analogy, has been derived and tested by many investigators. Mathematical treatments of the analogy were first presented by Jouget and Riabouchinsky. Perhaps the most comprehensive investigation of the extent of the analogy, both theoretical and experimental, was first made by Preiswerk.[2] Much work has been done since then by numerous groups, among which are the National Advisory Committee for Aeronautics[3], North American Aviation[4], and the hydrodynamics laboratories of the various universities[5], [6], [7], to mention a few.

The basic relations signifying the hydraulic analogy have been derived and outlined in detail by the references above. For convenience, the results are gathered below.

Necessary assumptions for the gas:

1. Ideal
2. Adiabatic
3. Frictionless
4. Steady flow
5. Two-dimensional flow

Necessary assumptions for the liquid:

1. Incompressible
2. Adiabatic
3. Frictionless

4. Steady flow

5. Flow bounded by a flat surface on the bottom and by a free surface on the top.

6. Vertical accelerations of the free surface are negligible compared with the acceleration of gravity.

The analogous relations between compressible gas flow and the flow of liquids with a free surface can be obtained by considering some basic equations written in terms of the appropriate variables.

By the energy equation:

for a gas	for a liquid
$V^2 = 2gC_p (T_o - T)$	$V^2 = 2g (d_o - d)$
$V_{max} = (2gC_pT_o)^{1/2}$	$V_{max} = (2gd_o)^{1/2}$

Equating V/V_{max} for the gas to V/V_{max} for the liquid,

$$\frac{T_o - T}{T_o} = \frac{d_o - d}{d_o}$$

whence

$$\frac{T}{T_o} = \frac{d}{d_o}$$

By the continuity equation:

for a gas	for a liquid
$\frac{\partial (\rho u)}{\partial x} + \frac{\partial (\rho v)}{\partial y} = 0$	$\frac{\partial (d u)}{\partial x} + \frac{(d v)}{\partial y} = 0$

whence

$$\frac{\rho}{\rho_o} = \frac{d}{d_o}$$

For adiabatic isentropic flow in a gas:

$$\frac{\rho}{\rho_o} = \left(\frac{T}{T_o}\right)^{\frac{1}{\gamma-1}}$$

Using the previously derived relations between ρ, T and d, a direct substitution of variable yields:

$$\frac{d}{d_o} = \left(\frac{d}{d_o}\right)^{\frac{1}{\gamma-1}}$$

For the above equation to be satisfied, the analogy requires that the gas have $\gamma = 2.0$. It should be noted at this point that the analogy does not specify any value of γ for the liquid. Any liquid may be used in the application of the analogy. The results, however, represent the conditions which exist in a gas which has a value of $\gamma = 2.0$

From the relation:

$$\frac{P}{P_o} = \left(\frac{\rho}{\rho_o}\right)^{\gamma}$$

and since $\gamma = 2.0$,

$$\frac{P}{P_o} = \left(\frac{d}{d_o}\right)^{2}$$

By the velocity potential relation for a gas

$$\phi_{xx}\left(1-\frac{\phi_x^2}{a^2}\right)+\phi_{yy}\left(1-\frac{\phi_y^2}{a^2}\right)-2\phi_{xy}\frac{\phi_x\phi_y}{a^2}=0$$

and for a liquid:

$$\phi_{xx}\left(1-\frac{\phi_x^2}{gd}\right)+\phi_{yy}\left(1-\frac{\phi_y^2}{gd}\right)-2\phi_{xy}\frac{\phi_x\phi_y}{gd}=0$$

therefore, for the two to be identical,

$$a^2 = gd$$

By the foregoing, the disturbance propagation velocity, $(gd)^{1/2}$, in the liquid flow is shown to correspond to the velocity of sound in gas flow.

A disturbance in liquid, under the assumptions made, gives rise to two types of waves; gravity waves due to the force of gravity and capillary waves due to the surface-tension force of the liquid. The velocity of propagation of these waves is shown by Rouse[8] to be:

$$U = \left[\left(\frac{g\lambda}{2\pi} + \frac{2\pi\sigma}{\rho\lambda}\right) \tanh \frac{2\pi d}{\lambda}\right]^{1/2}$$

It has been shown[3], [4] that the velocity of propagation of capillary waves is nearly independent of liquid depth and hence they do not satisfy the analogy. The effect of the capillary waves on the disturbance propagation velocity becomes negligible as the wavelength of the disturbance increases and as the depth decreases. For these conditions, the velocity of propagation approaches the asymptote:

$$U = (gd)^{1/2}$$

making the long gravity waves in shallow water analogous to sound waves in air.

A disturbance of a given physical size, say a towed model, will have associated with it waves of a certain wavelength. In order for the propagation velocity to approach the required asymptotic value, then, it generally becomes necessary to reduce the depth of the liquid. It has been shown[4], for example, that in a liquid depth of 0.225 inches all wavelengths between approximately three-quarters of an inch and

infinity satisfy the analogy. By comparison, in a liquid depth of one inch the minimum wavelength satisfying the analogy is of the order of eleven inches. It has also been shown[4] that models being towed in shallow water have disturbance wavelengths proportional to their size. For reasonable model size, which, in turn, means reasonable water channel size, it is apparent that the liquid depth must be limited.

Certain specific terminology is used in the hydraulic analogy. For liquid flow which corresponds to subsonic gas flow the ratio $U/(gd)^{1/2}$ is less than one, and the liquid is said to be "streaming". For liquid flow which corresponds to supersonic gas flow the ratio $U/(gd)^{1/2}$ is greater than one, and the liquid is said to be "shooting". The gravity waves in the liquid corresponding to shock waves in a gas are termed "hydraulic jumps".

Summary of the analogy[3]:

Significant quantities and characteristics of two-dimensional compressible gas flow, $\gamma = 2.0$	Corresponding values in analogous liquid flow.
Temperature ratio, T/T_o	Liquid-depth ratio, d/d_o
Density ratio, ρ/ρ_o	Liquid-depth ratio, d/d_o
Pressure ratio, P/P_o	(Liquid-depth ratio)$^{1/2}$, $(d/d_o)^{1/2}$
Velocity of sound, $a=\left(\frac{\gamma P}{\rho}\right)^{1/2}$	Wave velocity, $(gd)^{1/2}$
Mach number, V/a	Mach number, $V/(gd)^{1/2}$
Subsonic flow	Streaming liquid
Supersonic flow	Shooting liquid
Shock wave	Hydraulic jump

Certain limitations to the use of the hydraulic analogy are apparent. Since the analogous relations depend on only one variable, i.e., the depth of liquid, the hydraulic analogy is limited to two-dimensional phenomena.

For subsonic flows the hydraulic analogy is limited only by the basic assumptions in the equations of motion. Direct application of the analogy is quite accurate for all practical purposes.

For supersonic flows the hydraulic analogy has two basic limitations. The first is the requirement that the gas have $\gamma = 2.0$. From Figure 1, it may be seen that this requirement does not introduce any appreciable error into the comparison between shock wave angles in liquid and those in air, if the deflection producing the shock is small.

A second anomaly is due to a loss of mechanical energy in hydraulic jumps. This loss is converted into an increase in the temperature of the liquid. Since liquid temperature has no analogous quantity in gas flow, a loss in total head will occur in hydraulic jumps that has no counterpart in shock waves. This loss is significant and must be allowed for if a true comparison is to be made. This study does not investigate the quantitative strength of hydraulic jumps, hence this anomaly is of no immediate interest. An indication of the extent of this limitation to the to the analogy may be obtained from reference (4). This reference makes a comparison between the total head in normal hydraulic jumps and the total head in normal shock waves for a gas with $\gamma = 2.0$ and for air.

EQUIPMENT

There are two main types of water channels in which investigations may be conducted. Each has its advantages and limitations. In general, the type of channel used depends upon the problem under consideration.

One type of channel is constructed to permit water to flow about a stationary model. The other type employs a model moving in quiet water. Flow results are the same in each case, but certain problems require one or the other type of channel for ease in gathering and interpreting the data.

The construction features and use of the moving water type of channel are described in detail by references (3), (5), (6) and (9). The construction features and use of the moving model type of water channel may be found in references (1) and (4). These latter references specifically describe water channels designed to explore phenomena associated with one-dimensional model motion, i.e., straight line motion. The problems investigated in this report required a water channel in which any desired curvilinear model path could be established. Such a water channel was designed and constructed by the author and is now established in the aerodynamics laboratory of the University of Minnesota.

Description of Water Channel

The present installation consists of:

1. A water basin and supporting framework.

2. A model track whose path may be adjusted.

3. A model carriage.

4. A means of towing the model and of regulating the model velocity.

Figures 2 and 3 show the installation as a whole.

One of the problems in the design of the water basin was to provide a structure which would be rigid enough to be dimensionally stable so as to provide accuracy of alignment and measurement, yet flexible enough to allow leveling at all points. In addition, the basin was to remain completely waterproof through all normal levelings. Also, for reasons explained in the discussion of photographic techniques, it was decided that the bottom of the water basin should be made of plate glass.

Figure 4 shows the plan view of the L-shaped water basin and the overall dimensions thereof. The bottom of the water basin is made up of two sheets of one-quarter inch plate glass, each sheet being eight feet long by four feet wide. The sides and ends of the basin are of three-quarter inch waterproof plywood. The junction of the plywood and glass is capped on the outside by an extruded aluminum angle, one inch by one inch by one-sixteenth inch. The plywood is rigidly joined to the angle by three-quarter inch No. 8 round-head brass screws spaced every six inches. Both the plywood and the glass are bedded on the aluminum angle in one-eighth inch of aquarium cement. This provides a semi-elastic, waterproof seal for the entire joint. The interior joint is further waterproofed, however, by the

application of a plastic based, leak-sealing aquarium compound.

The present design of the water basin has proved satisfactory and does not leak even after successive levelings of the supporting structure. An improvement and simplification of the design, however, would provide the replacement of both the plywood sides and the aluminum capping strip with a single extruded aluminum angle of appropriate height.

The supporting framework for the water basin is constructed of angle iron. A peripheral angle forms the surface upon which the water basin rests directly. Legs are spaced every two feet around the periphery to provide leveling points. Cross-piece angles fit between the legs to provide support for the glass bottom of the basin. Aquarium cement is used to cushion the glass on each cross-piece. Legs and cross-pieces are of 1-1/2 inch by 1-1/2 inch by one-eighth inch angle. The peripheral angle is one inch by one inch by one-sixteenth inch to provide some vertical flexibility for leveling. All units are bolted together by five-sixteenth inch bolts. Each leg is fitted with a one-half inch diameter, two inch long National Fine threaded bolt for leveling. Each bolt has a suitable nut for locking the adjustment.

Once the structure is leveled and tightened, additional rigidity is secured by bolting the sides of the water basin to the top of each leg at two points. This does not prevent further leveling if required. In addition, this has the double advantage of giving the sides of the water basin the additional dimensional stability necessary for

the support of the model track and of leaving the area beneath the water basin free of all structural cross-bracing so that photographic or lighting equipment may be installed, if desired.

All parts of the water basin and supporting framework are protected against moisture and rust.

Figure 5 shows the adjustable model track and the manner in which it is suspended over the water basin. The track is fashioned from an extruded aluminum bar one and three-quarter inches by one-eighth inch by fifteen feet long. It functions as a monorail, being suspended from overhead angle iron cross-pieces, one inch by one inch by one-eighth inch, which span the water basin every two feet along the length of the basin. These cross-pieces are individually adjustable in position along the basin length so as to allow an unobstructed view of any particular area required. Selected cross-pieces may be removed entirely, if desired, though this is not recommended.

Investigations may be conducted along both the straight and the curvilinear portions of the track.

The track suspension fittings are fabricated from one inch square aluminum. They are adjustable to any position along the suspension cross-pieces to allow alignment of the model track. They attach to one side of the track leaving the other side, the top and the bottom free for model carriage attachment and guidance. Where the track is to be capable of adjustment in curvature, the attachment bolts from the suspension fittings ride in slots in the track. This compensates for varying track length between suspension points.

Features of the model carriage are illustrated in Figures 6 and 7 B. Points to be noted are that the two lower wheels may be adjusted vertically to provide proper clearance with the rail. Guidance of the carriage and the prevention of any relative motion between the carriage and the track, except in the direction along the track, is provided by the particular grooving of the wheels. Each wheel runs along two edges of the track by means of two 45 degree surfaces grooved into each wheel.

Provision is made for the rapid interchange of models by means of two model attachment bolts. These bolts are threaded into the model and fit into slightly enlarged holes in the carriage. In this manner, the model may be aligned perpendicular to the water surface and may be adjusted vertically to provide proper clearance with the bottom of the basin.

No counter-balancing of the model carriage is required for models attached close to the main axle plate of the carriage as indicated in Figure 6. Models can not be offset forward or aft of the carriage when investigating phenomena on the curvilinear portion of the track. This arrangement would cause the model to slip or slide through the water, rather than follow true, as the carriage goes along the track. Models may be offset directly to the side of the carriage, however, without affecting the accuracy of the model's path when shock wave phenomena in the immediate vicinity of the model are of interest. For this arrangement, some counter-balancing is required.

The model towing system is composed of a power and velocity

control unit for the tow, and a closed circuit towline

The power and control unit is a 115 volt A.C. variable speed motor producing up to five inch-pounds of torque with an electronic speed adjustment. This unit is shown in Figure 7A. The speed of the motor is continuously variable from 15 to 230 rpm. A four inch pulley is mounted on the motor thereby yielding the range of tow velocities indicated in Figure 8. On this same figure the conversion of these velocities into corresponding Mach numbers for a water depth of one-quarter inch is made. Direction of motor rotation is reversible allowing the model to be controlled for test runs in either direction. The power and control unit is mounted at the foot of the "L" of the water basin and is shock mounted to eliminate the transmission of any vibration.

The towline is of waxed 25 pound test linen fishline. It forms a continuous closed circuit from the front of the model carriage, around the various line guides along the track, up and over the foot end of the basin through a system of ball bearing pulleys, down and around the motor pulley, and is then guided under the water basin and up and over the head of the "L" by other ball bearing pulleys to the back end of the model carriage. The complete circuit may be followed by reference to the figures which show the equipment components.

In order to tow at constant velocity along the path, the towline must be guided essentially parallel to the path at all points. In the straight portion of the track guide fittings are attached to each of the cross-pieces which support the track as shown in Figure 5. For

curvilinear portions of the track, additional guide fittings are attached directly to the track itself. These may also be seen in Figure 5. If required, these fittings may be attached at any point along the track.

Photographic Techniques and Equipment

The photographing of surface water waves in a manner which shows any great contrast between the crests and the troughs of the waves is an art. Considerable difficulty was experienced in recording on film what was clearly apparent to the eye of an observer. Transient phenomena of all descriptions may be noted with ease, but if these phenomena occur over a general area rather than at a specific point at which specialized lighting and photography may be used, then their capture is difficult. This particular requirement of area photography necessitated the use of techniques which most other investigations have found marginal in quality. For these particular circumstances, however, these techniques were the only ones which produced any results whatsoever.

Almost without exception, the photographic technique used most widely in all the references depends on the refraction of light rays passing through the water surface. The curvature of the surface water waves bends the light rays so they add and subtract from one another and form a pattern of highlights and shadows. The two most widely used types of light source have been diffuse lighting and spark lighting.

In order to make use of the above techniques, the curvilinear water channel constructed for this investigation was fitted with a plate glass bottom. Attempts to use the refraction photographic technique,

however, proved fruitless for the large surface areas under observation. It is still felt, though, that this technique holds promise for the area type of investigation, but that it would require an extensive and elaborate array of equipment.

The photographic technique used for the gathering of test run data in this investigation is a direct application of the reflection method described in reference (1). In this arrangement, the water surface is covered with a thin layer of aluminum powder. The surface area is then lighted by reflection. An observer or camera, in turn, receives the light reflected by the aluminum particles. Each particle acts as a tiny mirror. Depending upon the orientation of their reflecting planes due to the curvature of the water surface, the particles will transmit a varying amount of light, forming a pattern of highlights and shadows.

Although the placement of the light source was varied in a number of ways, the method which proved most satisfactory by far was to reflect the light from a white ceiling down to the water surface. More direct methods of reflection such as having the light reflect directly to the surface from the level of the surface or from an angle of 45 degrees to the surface proved much less effective.

The light source used varied from two to four No. 4 photoflood lights directed at the white ceiling, the number varying with the amount of surface area to be illuminated. Lights were adjusted to provide equal illumination for the whole test area. To an observer at one point above such a surface covered with aluminum powder, however,

the lighting will not appear uniform. The particles reflect in a direction perpendicular to the surface, so for a level surface the reflection will be most intense directly under the observer, gradually shading away as the eye is swept away from the vertical. For this reason, illumination sufficient for the photographing of phenomena at a considerable angle to the perpendicular will be too bright for proper contrast between wave crest and trough directly under the observer.

This condition can be noted in the sequence photographs of the various test runs where the pictures taken near the vertical show much less contrast than the following pictures in the sequence taken at an angle to the vertical.

In the evaluation of the other photographic techniques which preceded the selection of the above technique, a condition similar to the above was noted. All methods showed some contrast when the waves were viewed from an angle, but few gave significant contrast when viewed from directly above under the same lighting.

The camera used for Runs Nos. 1, 2, 4, 5 and 6 was a four by five Speed Graphic fixed directly above the point to be photographed. Film used was Kodak Super Pancro Press, Type B. Exposure was f 5.6 and 1/400 of a second. This procedure illustrates that photography from directly above a point can be satisfactorily done by the reflection technique if the lighting is of the proper intensity and adjustment.

A 35 mm Robot camera was used for the recording of all the

remaining tests. This camera automatically advances the film and cocks the shutter between pictures, allowing rapid sequence pictures to be taken. The camera was hand held, the operator following the path of the model. Film used was 35 mm Kodak Super Triple X. Exposure was f 8 and 1/500 of a second.

In general, it was necessary to view the model motion from relatively close range. This required high speed shutter times and did not allow the use of the slower high contrast film types.

Since it was also necessary to view each test from one vantage point rather than to travel with the model along the path, it was not considered feasible to use a normal movie camera for the photography. The maximum shutter speed generally available is about 1/100 of a second for slow motion photography. This is not sufficient to stop the model motion.

If the facilities were available, by far the best arrangement would be to provide for a movie camera mounted above the model carriage and riding along with it around the path. This, of course, would also necessitate a complete re-design of the model track suspension system. This arrangement was not considered feasible for this investigation.

PROCEDURE

Simulation of the Problem

The problem undertaken in this investigation is the simulation of the shock wave patterns and interactions from an aircraft in curvilinear diving flight. Reasonable geometric comparison between the hydraulic jumps associated with a model in the water channel and the shock waves associated with an aircraft performing the same maneuvers in air is desired.

As indicated by the theory upon which the hydraulic analogy is based, the analogy may be used only for the representation of two-dimensional phenomena. Certain assumptions are necessary to reduce the general three-dimensional aspects associated with an aircraft in curvilinear diving flight to a situation which may be simulated in a water channel.

It first becomes necessary to justify the use of a two-dimensional model to produce a representation of an aircraft's shock wave signature.

In its simplest form, the aircraft's shock wave signature may be visualized as consisting of two main shock envelopes. One of these is formed by the geometry of the forward edges of the aircraft, and the other by the geometry of the trailing edges of the aircraft. All interior shock waves are generally much smaller by comparison and may be neglected. These two envelopes alone, therefore, constitute a very good first order of approximation to the shock signature.

Each of these shock envelopes consists of two main portions; one contributed by the fuselage geometry and the other by the wing geometry. The relative portion contributed by each necessarily varies with their respective shapes. Any cross section of each envelope parallel to the aircraft's longitudinal axis, however, is wedge shaped. Lateral cross-sections vary only in wedge angle according to whether they belong to the fuselage or wing systems. For a first order of approximation, then, a wedge shaped envelope of constant average wedge angle can be used to represent each of the two main shock envelopes.

Any of the above references to a wedge shaped cross-section should be interpreted to apply equally well if the cross-section were of any other shape due to the particular geometry or velocity of the aircraft.

By these simplifications, any two dimensional model which produces a bow and a tail wave may be used to simulate an aircraft's shock wave signature. Figure 9 is a cross-sectional view of the model selected for this investigation. Included thereon is a tabulation of the comparison between the shock wave angles associated with the body for various Mach numbers in air, and the shock wave angles as determined experimentally. The double-wedge offers the advantage of producing two well-defined waves. In addition, the selection of a deflection angle of five degrees for the wedge should produce hydraulic jump signatures geometrically equal within one degree to the shock wave signatures for the same body in air. Further, the wedge thickness ratio is 8.7% which is the order of the average thickness ratio of a

typical high speed aircraft.

The second requirement in the simulation of the problem is the determination of a typical flight path for an aircraft performing a dive and pull-out.

First of all, except for minor variations of no significance, the entire flight path is planar. No third coordinate is necessary for its specification.

Secondly, all the various forces such as lift, drag, thrust and gravity which act on an aircraft in curvilinear planar flight combine to cause acceleration along and perpendicular to the path.

$$\begin{aligned} F &= ma \\ &= m(a_t^2 + a_n^2)^{1/2} \\ &= m(a_t^2 + \frac{V^2}{R})^{1/2} \end{aligned}$$

The pilot controls and adjusts for these forces by varying the aircraft's velocity and the pull-out "G" forces. These two pilot-controlled variables automatically compensate for the changing angular relations between the flight forces throughout the curvilinear path. These two alone, therefore, are sufficient to specify the exact path.

A pilot has several options as to the velocity variation during the dive and as to the "g" forces imposed in the pull-out. The particular technique selected depends upon the circumstances requiring the maneuver.

Consider first a constant velocity dive with a constant "g" pull-out.

Since constant velocity is assumed, there is no tangential acceleration component to the path. The radial acceleration is the resultant acceleration. It is, of course, perpendicular to the path at every point and directed toward the center of curvature. Using the above equations, there follows that

$$F = \frac{mV^2}{R}$$

where F is now the pull-out "g" force. The radius of curvature at each point in the path is thus determined. In this case, the radius is constant and the path is an arc of a circle.

In the more general case of varying velocity and pull-out "g" force, the path may best be determined graphically. Divide the dive into equal intervals of time, assigning each an appropriate value of average velocity and "g" for the interval according to the overall history desired for the path. With these values, calculate each radius of curvature and successively construct circular arcs as in the case above. Each arc has a length equal to the distance traveled during the time interval. The use of suitably small time intervals allows a smooth path to be faired through the arcs. The accuracy of the approximation, of course, increases as the time intervals are made smaller.

Consider an actual path. A common precision diving technique is to maintain constant Mach number during the dive and to pull-out at constant "g". Since air temperature generally increases with decreasing altitude, a constant Mach number represents an increasing velocity as the dive progresses. From the cases considered above,

it is apparent that at constant "g" pull-out this results in a continually increasing pull-out radius of curvature along the path, i.e., a "loosening" of the circular arc.

Another consideration which affects the above path is that normally the constant pull-out force is not applied suddenly at the commencement of the pull-out. A smooth, but generally rapid, build-up occurs; the actual rate of increase depending upon the particular circumstances. This action results in a continually decreasing radius of curvature for the flight path, i.e., a smooth transition from straight line flight to the arc representing the constant "g" portion of the path.

The above considerations were applied to establish a "typical" flight path for the model in the water channel. Any path so established will apply to a dive made at any constant Mach number and at any constant pull-out "g". There is no specific scale associated with the path itself, nor with the placement of the walls of the water channel with respect to the path. For any particular set of dive values, the altitudes and flight path radii of curvature are directly related and self-compensating.

Figure 4 is a scale drawing of the curvilinear path used for all the tests. Also indicated thereon is the plan view of the water channel showing certain construction members. When viewing the sequence photographs for each run, reference to the relative positions of the construction members in each picture will allow the specific placement of the model at points along the path.

Conditions Investigated

In general, the areas of interest during the investigation were the shock wave interactions

(i) between themselves, both in the vicinity of the body and at distances beyond the influence of the body;

(ii) with other surfaces, specifically planar interaction and fly-by interaction with the ground.

Each of the above areas of investigation were divided into three main categories which describe the variation of Mach number during that series of tests, i.e.,

A. Constant Mach number

B. Increasing Mach number

C. Decreasing Mach number

For each of the above categories, tests were conducted along two portions of the flight path:

1. Straight line path

2. Curvilinear diving path. (No specific grouping designating either planar or fly-by interaction has meaning here. The interactions as a whole may be discussed from one run.)

The following is a listing of the conditions investigated. For convenience, the figures showing the results of these runs are also indicated.

I. Shock wave interactions between themselves.

A. Constant Mach number.

1. Straight line path.

Run No. 1: M = 0.95 Figure 11

Run No. 2: M = 1.1 Figure 13

Run No. 3: M = 1.25 Figure 15

Run No. 4: M = 1.5 Figure 17

Run No. 5: M = 1.75 Figure 19

Run No. 6: M = 2.0 Figure 21

2. Curvilinear diving path.

Run No. 7: M = 1.1 Figure 23

Run No. 8: M = 1.5 Figure 25

Run No. 9: M = 2.0 Figure 27

B. Increasing Mach number.

1. Straight line path.

Run No. 10: Gradual acceleration from M = 0.85 to M = 2.0
Figure 29

2. Curvilinear diving path.

Run No. 11: Gradual acceleration from M = 0.85 to M = 1.5
Figure 31.

Run No. 12: Gradual acceleration from M = 0.85 to M = 2.0
Figure 33

C. Decreasing Mach number.

1. Straight line path.

Run No. 13: Sudden deceleration from M = 1.5 to
sub-critical Mach number. Figure 35

2. Curvilinear diving path.

Run No. 14: Sudden deceleration from M = 1.5 to a supercritical Mach number of 0.85. Figure 37.

Run No. 15: Sudden deceleration from M = 2.0 to subcritical Mach number. Figure 39.

II. Shock wave interactions with other surfaces.

A. Constant Mach number.

1. Straight line path

Run No. 16: Fly-by interaction, M = 1.25 Figure 41

Run No. 17: Fly-by interaction, M = 1.5 Figure 43

Run No. 18: Fly-by interaction, M = 2.0 Figure 45

Run No. 19: Planar interaction, M = 1.5 Figure 47

Run No. 20: Planar interaction, M = 2.0 Figure 49

2. Curvilinear diving path

Run No. 21: M = 1.1 Figure 23

Run No. 22: M = 1.5 Figure 25

Run No. 23: M = 2.0 Figure 27

B. Increasing Mach number.

These conditions may be investigated by inspection of Runs No. 16 through No. 23.

C. Decreasing Mach number.

1. Straight line path.

Run No. 24: Fly-by interaction. Sudden deceleration from M = 1.25 to sub-critical Mach number. Figure 51

Run No. 25: Fly-by interaction. Sudden deceleration

from M = 1.5 to sub-critical Mach number. Figure 53

Run No. 26: Fly-by interaction. Sudden deceleration from M = 2.0 to sub-critical Mach number. Figure 55

Run No. 27: Planar interaction. Sudden deceleration from M = 1.5 to sub-critical Mach number. Figure 57

2. Curvilinear diving path.

Run No. 28: Sudden deceleration from M = 1.5 to sub-critical Mach number. Figure 59-A

Run No. 29: Sudden deceleration from M = 2.0 to sub-critical Mach number. Figure 59-B

Sample calculation to determine the model tow velocity required in the water channel to simulate a selected Mach number:

$$M = \frac{V}{a}$$

$$= \frac{V}{(gd)^{1/2}}$$

for a water depth of one-quarter inch,

$$(gd)^{1/2} = \left(32.18 \frac{ft}{sec^2} \times 0.25 \text{ inches} \times \frac{1}{12} \frac{ft}{\text{inches}}\right)^{1/2}$$

$$= 0.82 \frac{ft}{sec}$$

To determine the model tow velocity to simulate M = 1.5, then

$$V = M (gd)^{1/2} = 1.5 \times 0.82 \text{ ft/sec}$$

$$= 1.23 \text{ ft/sec}$$

In the above manner, the Mach number may be related to the entire range of model tow velocities for any particular water depth. Figure 8 shows such a calibration curve for the water depth of one-quarter inch which was used in this investigation.

RESULTS AND DISCUSSION

The results of the various shock wave patterns and interactions simulated in this investigation, as outlined in the procedure section, are depicted in Figures 11 through 59. Accompanying each of these figures is a page of line drawings depicting the shock wave patterns in each picture. The figures may be divided into two groups; Figures 11 through 39 depicting shock wave interactions between themselves, and Figures 23 through 27 and 41 through 59 depicting shock wave interactions with other surfaces. It should be noted that due to the perspective necessary for the photography of the phenomena, the order of some of the sequence pictures in the figures is contrary to the ordinary method of presentation.

Figures 11 through 21 depict straight line motion at a constant Mach number. Their purpose is to verify the accuracy of the hydraulic analogy as it relates to this particular investigation by a comparison of shock wave patterns for the five degree double wedge model in the water channel and for the shock wave patterns as computed for the same model in air. Figure 9 tabulates these pattern angles. As indicated thereon, the comparison is excellent, being very nearly within the limits predicted by Figure 1 and well within the limits desired for the investigation. Any slight difference is believed to exist because of the difficulty of exactly locating some of the hydraulic jumps in the photographs. In addition, a small amount of perspective exists in some of the views.

A further purpose of Figures 11 through 21 is to allow for the determination of the amount of distortion existing in the following wave pattern sequences due to the perspective from which they were photographed.

This group of figures also illustrates the formation and change in the shock wave pattern associated with the model for various constant speeds through the transonic range into the supersonic range. Figure 11 clearly illustrates the presence of the small shock which forms somewhere on a body traveling subsonically above its critical velocity. Although this figure does not show the exact location of the shock, from the particular geometry of the model and from other views of the model at the same velocity, it may be seen that this shock is at the trailing edge.

Figures 23, 25 and 27 show the shock wave patterns associated with the model as it performs a curvilinear dive and pull-out at constant Mach numbers of 1.1, 1.5 and 2.0. The first picture in each sequence is taken very near the beginning of the pull-out so that the wave pattern very nearly corresponds to that existing in the straight line portion of the dive. The exact pattern in that portion, of course, is more clearly shown in the figure for the appropriate speed in the series of Runs No. 1 through No. 6. The last picture in each sequence is taken after the plane has completed its maneuver and is parallel with the ground and about to pull-up.

The overall pattern in each of the figures is quite similar. The only differences which do exist can be explained by the difference in

Mach number alone.

As the Mach number of a body increases, the strength of the shock waves associated with the body also increases, requiring greater energy to dissipate them in regions beyond the influence of the body. In the air, this dissipative energy is provided by the viscous effects of the air, and in the water by its viscous effects. Both the longer persistence of the stronger hydraulic jumps and their eventual dissipation is clearly indicated in the figures.

Another point to be noted is that on the inside of the arc the waves are dissipated much more rapidly than on the outside of the arc. This effect can be explained by considering that the model is actually emitting a disturbance at every point along its path. In the two-dimensional case these disturbances are propagated in the form of circular waves, the diameter of which increase with time. The envelope of these waves from a disturbance traveling at supersonic speed forms the shock waves associated with the disturbance. In the more familiar straight line motion of a disturbance, these waves generally assume some wedge or arc shape. Reference (1) presents a method of graphically and analytically determining the wave envelope for any curvilinear motion. For the case of a disturbance moving along an arc, the portions of the disturbance waves on the inside of the arc tend to subtract from one another and to form a cusp in the wave envelope. This cusp may be seen on the inside portion of the shock wave from the trailing edge of the model. The cusp for the inside portion of the shock wave from the leading edge of the model

is apparently dissipated in the expansion wave zone between the two shock waves before it can be seen.

Figure 29 depicts the build-up and change in the shock wave pattern about a body which accelerates from a supercritical subsonic Mach number to a supersonic Mach number of 2.0 along a straight line path. It may be seen that the basic bow and tail wave patterns are identical with the steady state patterns for the same body at the same Mach numbers.

One major point of difference may be noted, however. In Figures 29b, c, d and e the presence of a second tail wave may be noted which is more normal to the model path than the other waves and which is joined at its extremities to the main tail wave. As the Mach number increases, this second tail wave falls progressively further behind the model until it is dissipated by viscous effects. The formation and shedding of this second tail wave is a phenomenon associated only with the process of acceleration. The presence of this wave may be noted visually on every occasion that the model is accelerated from a subsonic Mach number to a supersonic Mach number. It is not present in any of the steady state conditions, nor does it reappear upon deceleration if it has once been dissipated. Because of this, it is believed that this second tail wave is actually the supercritical subsonic shock wave which is formed before the main shock system develops. When the main system develops, this wave can no longer find conditions favorable to its existence on the body and must seek these conditions in the trailing stream, where it remains until overcome by viscous effects.

Figures 31 and 33 depict the build-up and change in the shock wave pattern about a body which accelerates from a supercritical subsonic Mach number to supersonic Mach numbers of 1.5 and 2.0 along a curvilinear diving path. Comparing these figures with pictures for the same conditions along a straight path reveals no new differences of any importance. Both the presence of the cusp in the shock wave envelope as previously observed in Figures 25 and 27 and the presence of a second trailing tail wave as observed in Figure 29 may be noted. The apparent presence of multiple trailing tail waves can not be explained. It is believed they represent additional shock envelopes formed by the interaction of the original trailing tail wave with the disturbance circles emitted by the model along its path as previously explained. In any case, the effects are considered secondary to the major features depicted.

Figures 35, 37 and 39 depict the conditions which exist when a body which has been traveling at supersonic speed is suddenly decelerated to some subcritical speed. Figure 35 specifically depicts a body traveling at an original Mach number of 1.5 along a straight line path. The typical wedge shaped shock wave pattern associated with the body at this Mach number is shown in Figure 35a. Figure 35b is taken just after deceleration and shows the shock waves leaving the body. At this point it may be noted that the wedge pattern has already begun to transform into an arc in the center portions of the waves. The final picture in the sequence shows the continuation of the process. In this picture the center section arc has extended further from the center

line, and it may be definitely noted that the wave angle of both the shocks has increased. Further, the leading edge shock wave is moving faster, leaving the trailing edge shock behind. This is due to the region of expansion waves between the two shock systems. It should also be noted that there is no formation of a second trailing tail wave upon deceleration as there was upon acceleration.

Figures 37 and 39 depict conditions of sudden deceleration for a body traveling along a curvilinear diving path at original Mach numbers of 1.5 and 2.0. In each case, the wave pattern changes follow the same sequence of formation as depicted along the straight line path and with the same features to be noted.

One apparently minor change is made in the conditions which are simulated for Figure 37 and which is not made for the other two tests of this series. Instead of suddenly decelerating the model to a subcritical speed, in which case, of course, there are no shock waves associated with the model, deceleration was made to a supercritical Mach number of approximately 0.85. In this case, the trailing edge shock wave system never detaches itself from the body. The presence of the small, local supercritical wave is apparently sufficient to retain the trailing edge shock at the body, leaving only the leading edge shock to proceed ahead of the body. Any later interaction effects between the shock waves and other surfaces would, therefore, be approximately half of the normal interaction.

The remaining tests to be discussed concern the interactions between shock waves and other surfaces.

Figures 41, 43 and 45 depict the shock wave interactions from an aircraft flying in a straight line path parallel to the ground and at constant Mach numbers of 1.25, 1.5 and 2.0. The basic patterns are similar in each case and serve to verify that the interactions with the parallel surface conform to classical form. The sequences indicate that each point on the ground receives an identical pressure-time pattern as the model passes by.

A point to be noted in the interpretation of the pictures is that the reflected leading edge shock wave is dissipated to some extent in the expansion wave region and is, therefore, somewhat more difficult to follow than the trailing edge shock.

Figures 47 and 49 depict the shock wave interactions from an aircraft flying in a straight line path parallel to the ground and at constant Mach numbers of 1.5 and 2.0. At some point along this path some structure, such as a roof, may be oriented in such a manner as to receive a planar interaction with the shock waves as the aircraft passes by. These figures clearly show this type of interaction.

The effects in this case are quite different from those in the three preceding figures. In the former circumstances, only a small increment of a structure at any one time is affected by the pressure differences of the shock wave system. The structure as a whole may readily absorb the impulse acting on an increment of the structure. In the present case, however, the planar interaction of the shock waves with the entire surface of a structure may possibly result in the transfer of sufficient energy to cause the structure to fail.

In order to investigate this effect further, consider a body of revolution with a fineness ratio of 10% flying a few hundred feet above the ground. Reference (1) gives the pressure rise across the bow shock wave at ground level as being approximately thirty pounds per square foot for all Mach numbers in the range 1.5 to 3.0. The approximate pressure rise across both the bow and tail waves would then be sixty pounds per square foot if they both interacted at essentially the same time. Average roof structures are constructed to wishstand from twenty to forty pounds per square foot of STATIC pressure. The impulse delivered by the DYNAMIC loading from shock waves would, therefore, be insufficient to cause any structural damage even to the lightest of frame structures since the interval of time during which they act upon the structure is so small. The impulse would be sufficient, however, to break glass or to cause damage to similar materials in the structure.

Runs No. 21, 22 and 23 were designed to investigate the shock wave interactions with other surfaces which may be expected from an aircraft in curvilinear diving flight at constant Mach numbers of 1.1, 1.5 and 2.0. Figures 23, 25 and 27 can be used for this study. Although no particular interacting surfaces are depicted in the pictures, it may readily be seen that both the planar and fly-by types of interactions are likely to occur during one maneuver. The specific interactions would not be unlike those depicted for straight line flight, and since they are most clearly seen in those sequences, need not be repeated.

Figures 51, 53, 55 and 57 depict the conditions which exist when a body which has been traveling at supersonic speed is suddenly decelerated to some subcritical speed and the projected shock wave system is allowed to interact with other surfaces. The first three of these figures specifically depict a body traveling at original Mach numbers of 1.25, 1.5 and 2.0 along a straight line path, with fly-by interactions occuring. Figure 57 depicts the body performing the same maneuver along a curvilinear diving path with an original Mach number of 1.5, but with a planar interaction with some angled structure.

The phenomena in this group of figures are a straightforward combination of the deceleration and interaction phenomena previously observed. One difference resulting from this combination which should be noted is that as the detached waves travel ahead of the body in straight line flight, the intersection of the shocks with the ground surface becomes more perpendicular. This would eventually result in the planar intersection of these waves with the vertical surfaces of structures.

Figures 59A and 59B depict interactions from the shock wave system of a body suddenly decelerated along a curvilinear diving path. Figure 59A depicts conditions for an original Mach number of 1.5 and Figure 59B for an original Mach number of 2.0. The specific interactions are difficult to photograph, but it may be seen from these pictures, which are taken just prior to the actual interaction, that the interactions cannot differ materially from those already

shown along the straight line path. Both the planar and fly-by types of interactions can be seen to exist simultaneously. The planar interaction in these cases is occuring with horizontal structural surfaces.

CONCLUSIONS

1. A water channel is a valuable aerodynamic research tool. In its simplest form it is very useful for the demonstration of known aerodynamic phenomena and for the rapid and inexpensive checking of new theories and ideas. A channel made with precision and operated with care can furnish quantitive data. A water channel permits observation of transient phenomena associated with varying "flight" paths and velocities. High supersonic Mach numbers are easily simulated at water speeds of a few feet per second.

2. After extensive trial of the photographic techniques most frequently used in the study of surface water waves, i.e., refraction through and reflection from the water surface, it was found that they were generally not suitable for qualitative investigation of hydraulic jumps where phenomena occur over an area greater than two feet square. The method which allows the best visual and photographic observation of surface wave patterns uses light reflected from a water surface covered with aluminum powder.

3. For models with small flow deflection angles, the surface wave patterns formed in a water channel compare almost identically with the shock wave patterns for the same body in air.

4. In addition to the normal shock wave system associated with a particular body, under conditions of acceleration from a subsonic to a supersonic Mach number an additional tail wave is formed and shed by the body. This second tail wave trails astern until dissipated by viscous effects.

5. To achieve the full effect from the interaction of shock wave systems projected ahead of a suddenly decelerated body in flight, it is necessary that the body decelerate to a subcritical Mach number and not only to a subsonic Mach number. Deceleration only to a supercritical subsonic Mach number results in the retention at the body of all the shock wave system aft of any small, local supercritical subsonic shock wave which may be formed on the body.

6. Planar interaction between an aircraft's shock wave system and any surface of a structure, regardless of whether it be horizontal, vertical or angled between, can be accomplished by a proper adjustment of flight conditions.

7. Regardless of the manner in which shock waves impinge on a surface of a structure, the transfer of energy is insufficient to cause even the slightest damage to the major structure. Planar interaction of the shock waves with glass areas, however, will usually result in the transfer of sufficient energy to shatter the glass.

REFERENCES

1. Lilley, G.M., Westley, R., Yates, A.H., and Bushing, J.R., "On Some Aspects of the Noise Propagation From Supersonic Aircraft". Report No. 71, The College of Aeronautics, Cranfield, England, February 1953.

2. Preiswerk, E., "Applications of the Methods of Gas Dynamics to Water Flows With Free Surfaces". Technical Memoranda Nos. 934 and 935, National Advisory Committee for Aeronautics, Washington, D.C., 1940.

3. Orlin, W.J., Lindner, N.J., and Bitterly, J.G., "Application of the Analogy Between Water Flows With a Free Surface and Two-Dimensional Compressible Gas Flow". Report N. 875, National Advisory Committee for Aeronautics, Washington, D.C., 1947.

4. Bruman, J.R., "Application of the Water Channel-Compressible Gas Analogy". Report No. NA-47-87, North American Aviation, Inc., Los Angeles, California, 1947.

5. Einstein, H.A. and Baird, E.G., "Progress Report of the Analogy Between Surface Shock Waves on Liquids and Shocks in Compressible Gases". Laboratory Report No. N-54, Hydrodynamics Laboratory, California Institute of Technology, Pasadena, California, September 1946.

6. Crossley, H.E.Jr., "The Analogy Between Surface Shock Waves in a Liquid and Shocks in Compressible Gases". Report No. N-54.1, Hydrodynamics Laboratory, California Institute of Technology, Pasadena, California, August 1949.

7. Crossley, H.E. Jr., and Harleman, D.R.F., "Studies on the Validity of the Hydraulic Analogy to Supersonic Flow". Technical Report No. 11, Hydrodynamics Laboratory, Massachusetts Institute of Technology, Boston, Massachusetts, December 1952.

8. Rouse, Hunter, "Fluid Mechanics for Hydraulic Engineers", McGraw-Hill Book Co. Inc., 1938.

9. Matthews, Clarence W., "The Design, Operation and Uses of the Water Channel as an Instrument for the Investigation of Compressible-Flow Phenomena". Technical Note 2008, National Advisory Committee for Aeronautics, Washington, D.C., January 1950.

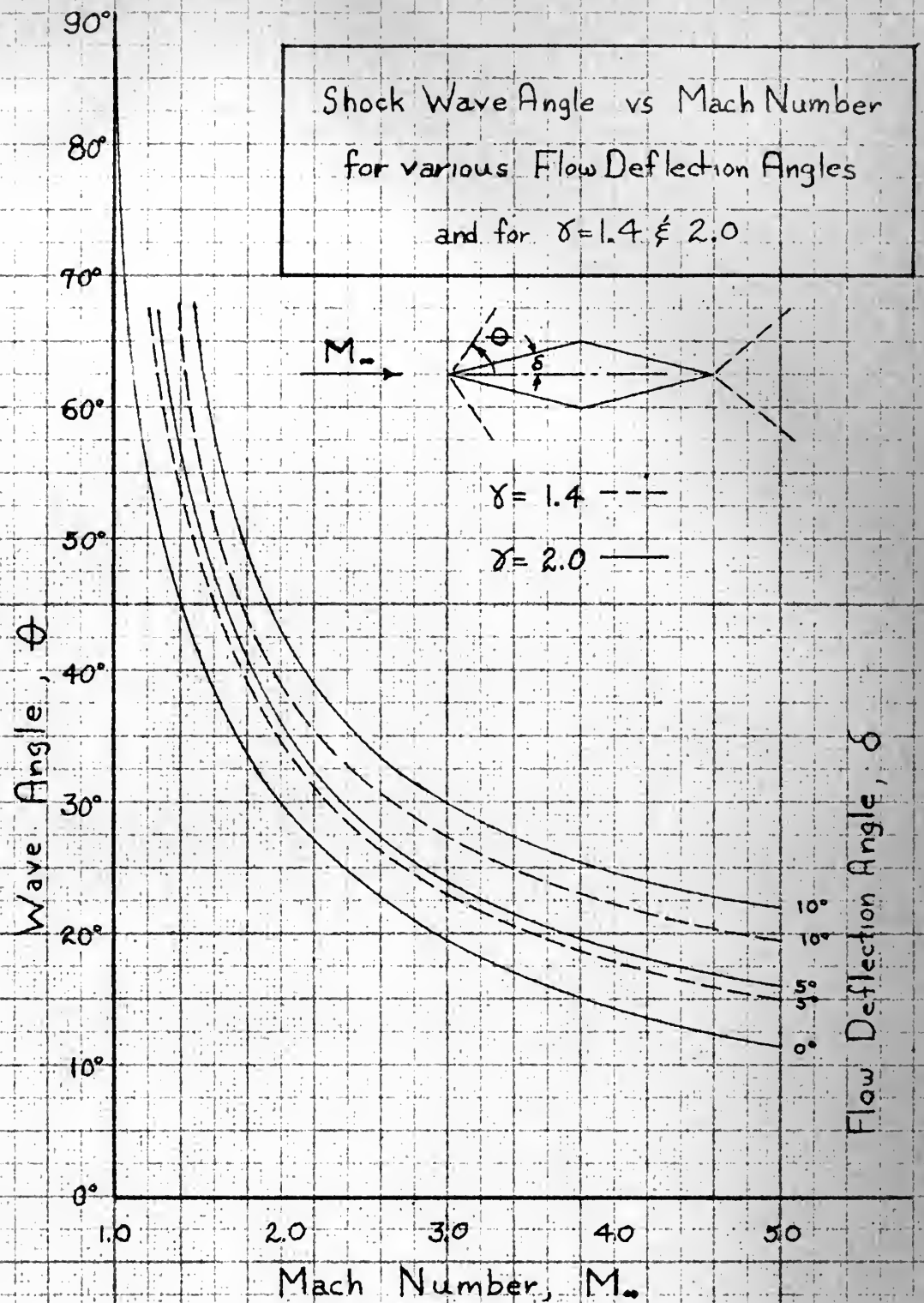
Shock Wave Angle vs Mach Number
for various Flow Deflection Angles
and for γ = 1.4 & 2.0
M∞
θ
δ
γ = 1.4 - - -
γ = 2.0 ——
90°
80°
70°
60°
50°
40°
30°
20°
10°
0°
Wave Angle, Φ
10°
10°
5°
5°
0°
Flow Deflection Angle, δ
1.0
2.0
3.0
4.0
5.0
Mach Number, M∞

FIGURE 1

Perspective View of Curvilinear Water Channel Installation.

FIGURE 2

Perspective View of Curvilinear Water Channel Installation.

FIGURE 3

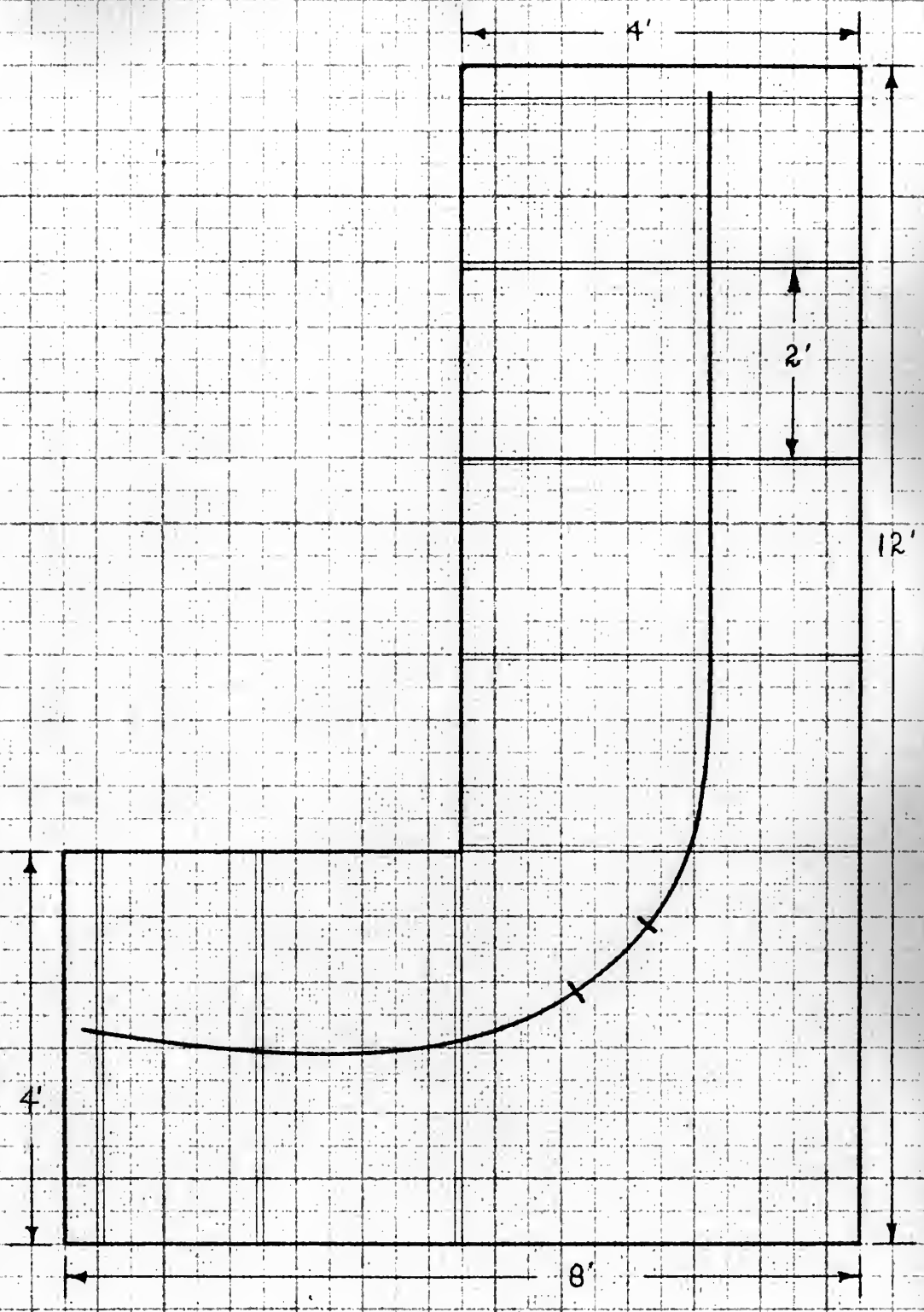

FIGURE 4

Plan View of Water Channel with Scale Drawing of the Curvilinear Path Used in the Investigation and with the Location of Certain Streamwise Members Noted to Aid in the Analysis of Results.

Perspective View of Adjustable Model Track and Track Suspension System.

FIGURE 5

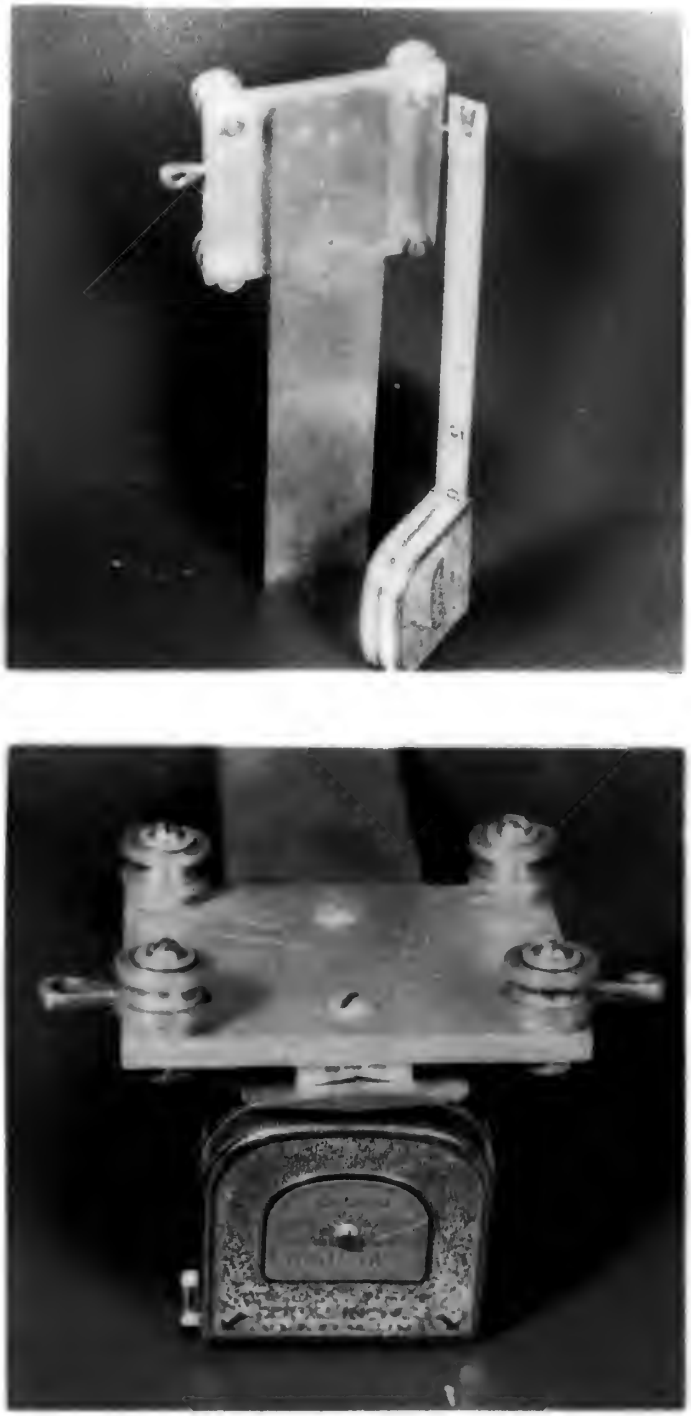

Perspective Views of Model Carriage and Test Model

FIGURE 6

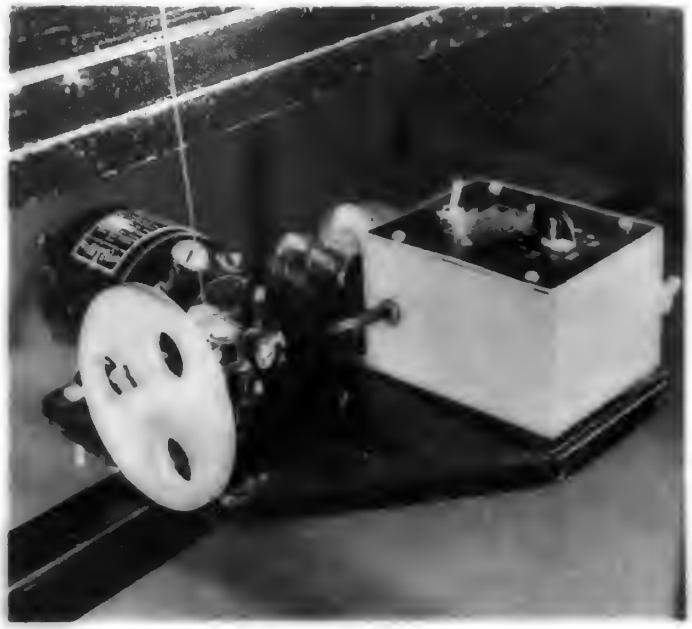

Fig. 7-A: Power and Speed Control Unit for Towing Model.

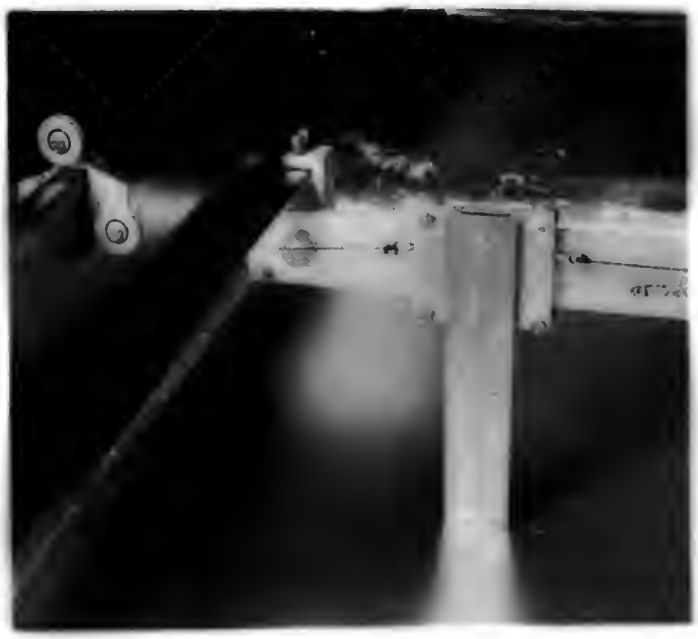

Fig. 7-B: Perspective View of Model and Carriage Mounted in Position on Model Track.

FIGURE 7

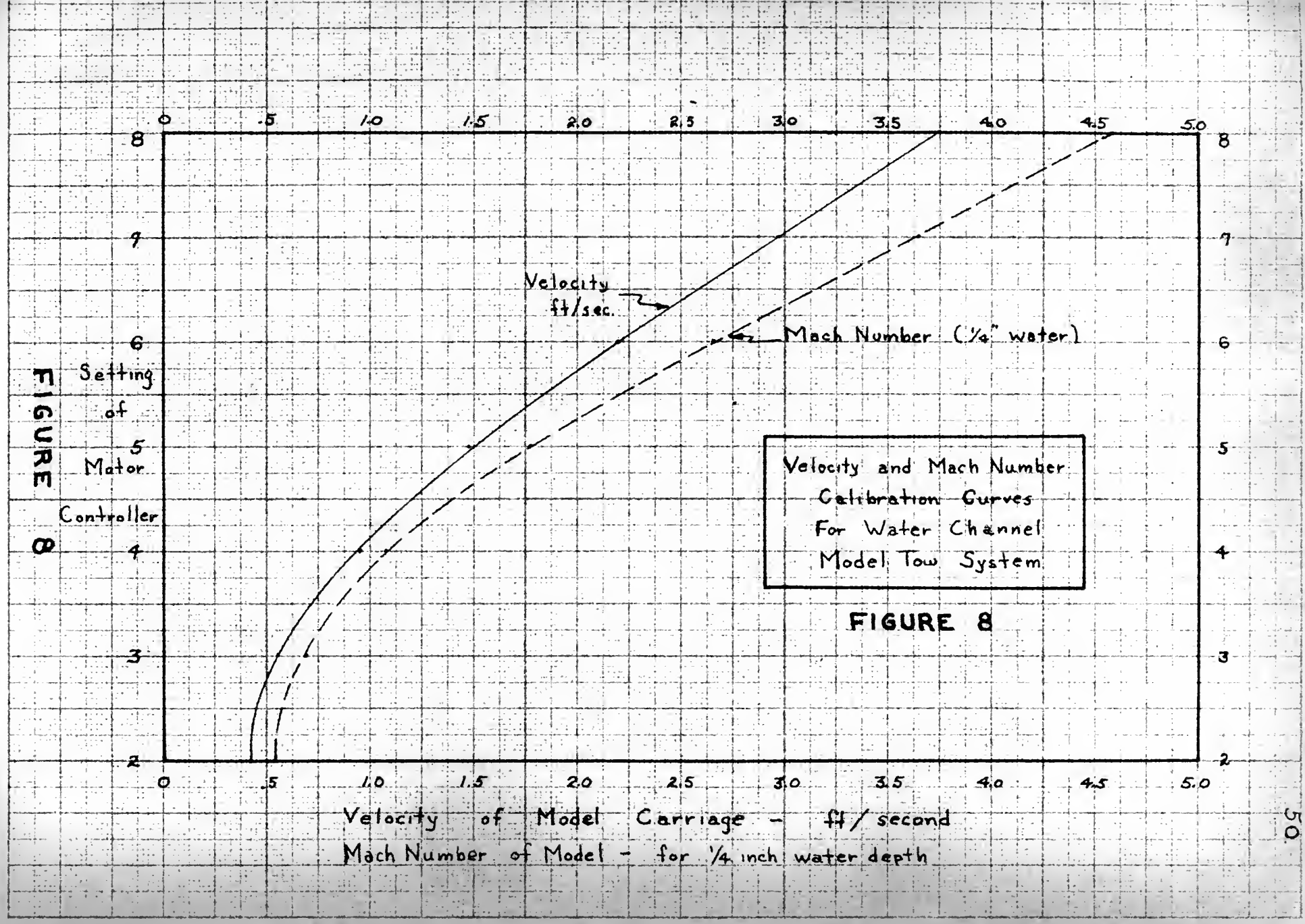
0 .5 1.0 1.5 2.0 2.5 3.0 3.5 4.0 4.5 5.0
8 9 6 5 4 3 2
Velocity ft/sec.
Mach Number (¼" water)
Setting of Mator Controller
Velocity and Mach Number Calibration Curves For Water Channel Model Tow System
FIGURE 8
Velocity of Model Carriage - ft/second
Mach Number of Model - for ¼ inch water depth

FIGURE 8

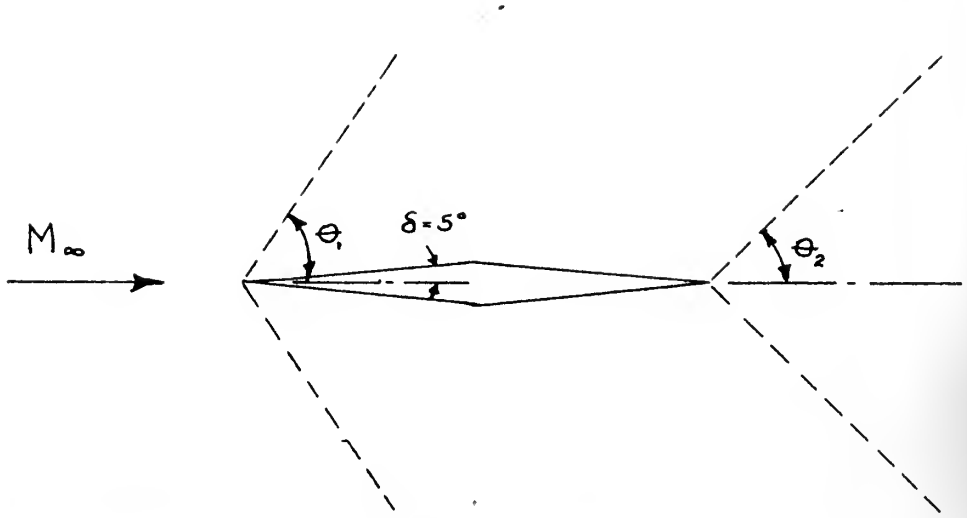

Free Stream Mach Number	Shock Wave Angles Computed for Air		Shock Wave Angles Experimental from Water Channel	
M_∞	θ_1	θ_2	θ_1	θ_2
1.25	66°	50.2°	64.5°	49°
1.50	48°	42.5°	45°	39°
1.75	40.5°	35°	39°	34°
2.00	34.5°	31.4°	35°	30°

Minimum Mach number for attachment of L.E. shock is ≈ 1.23

FIGURE 9

Cross-Section of Test Model with a Comparative Tabulation Between the Calculated Shock Wave Angles for the Body in Air and Experimental Values for the Same Conditions Simulated in the Water Channel.

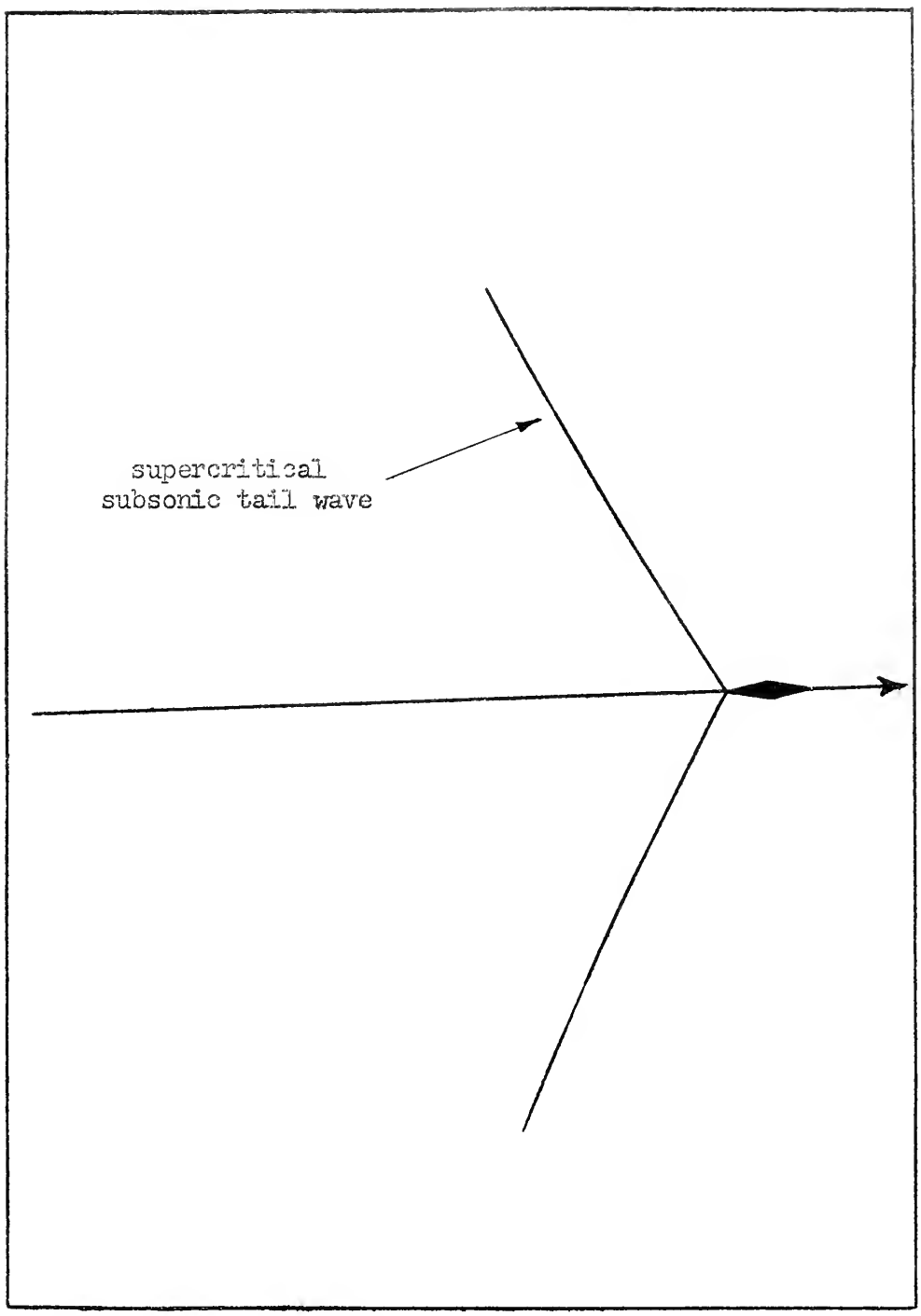

Line Drawing of Wave Pattern in Figure 11

FIGURE 10

Water Wave Pattern for a 5° Double Wedge at a Constant Mach Number of 0.95 Along a Straight Line Path.

FIGURE 11

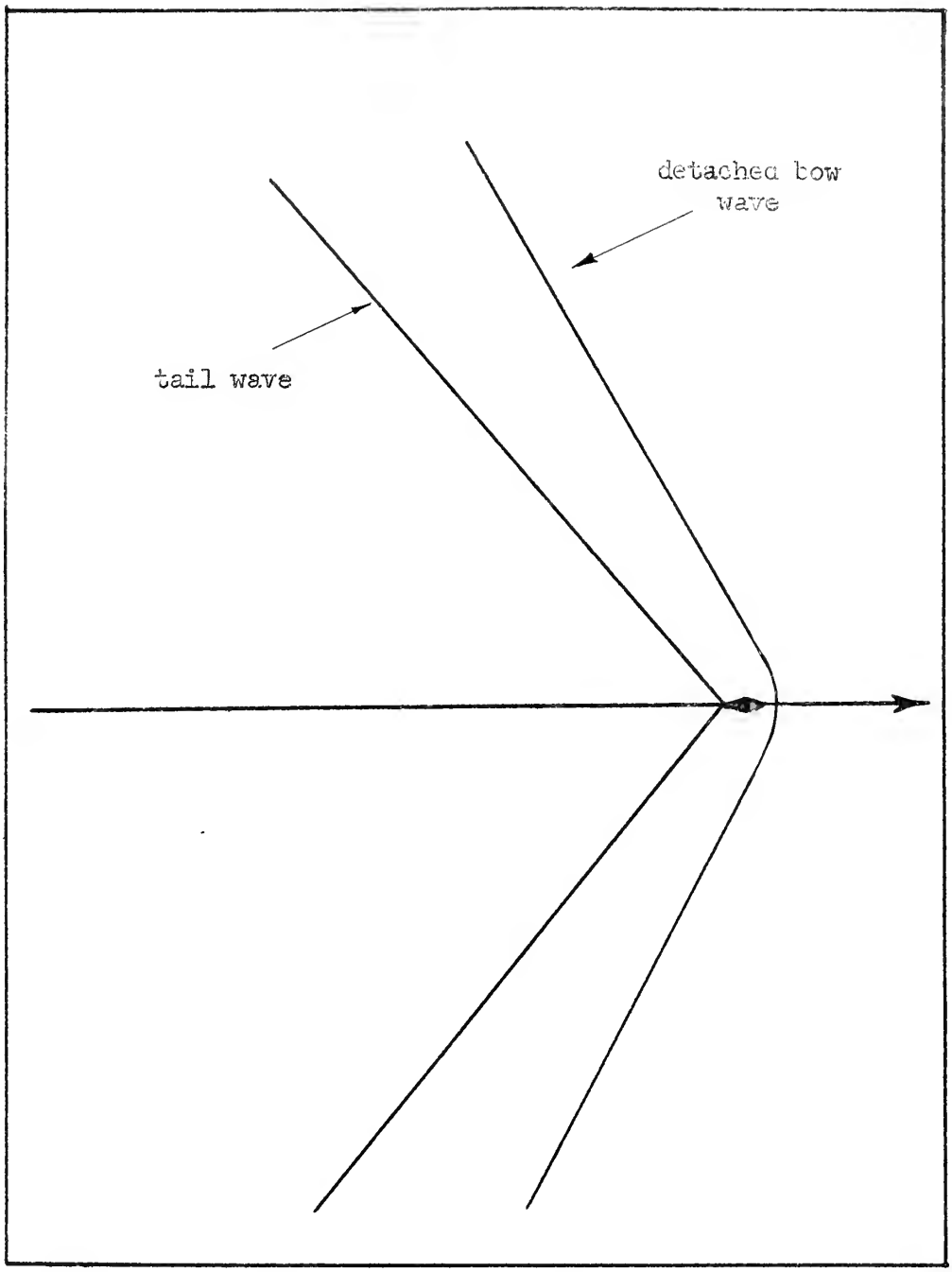

Line Drawing of Wave Pattern in Figure 13

FIGURE 12

Water Wave Pattern for a 5° Double Wedge at a Constant Mach Number of 1.1 Along a Straight Line Path.

FIGURE 13

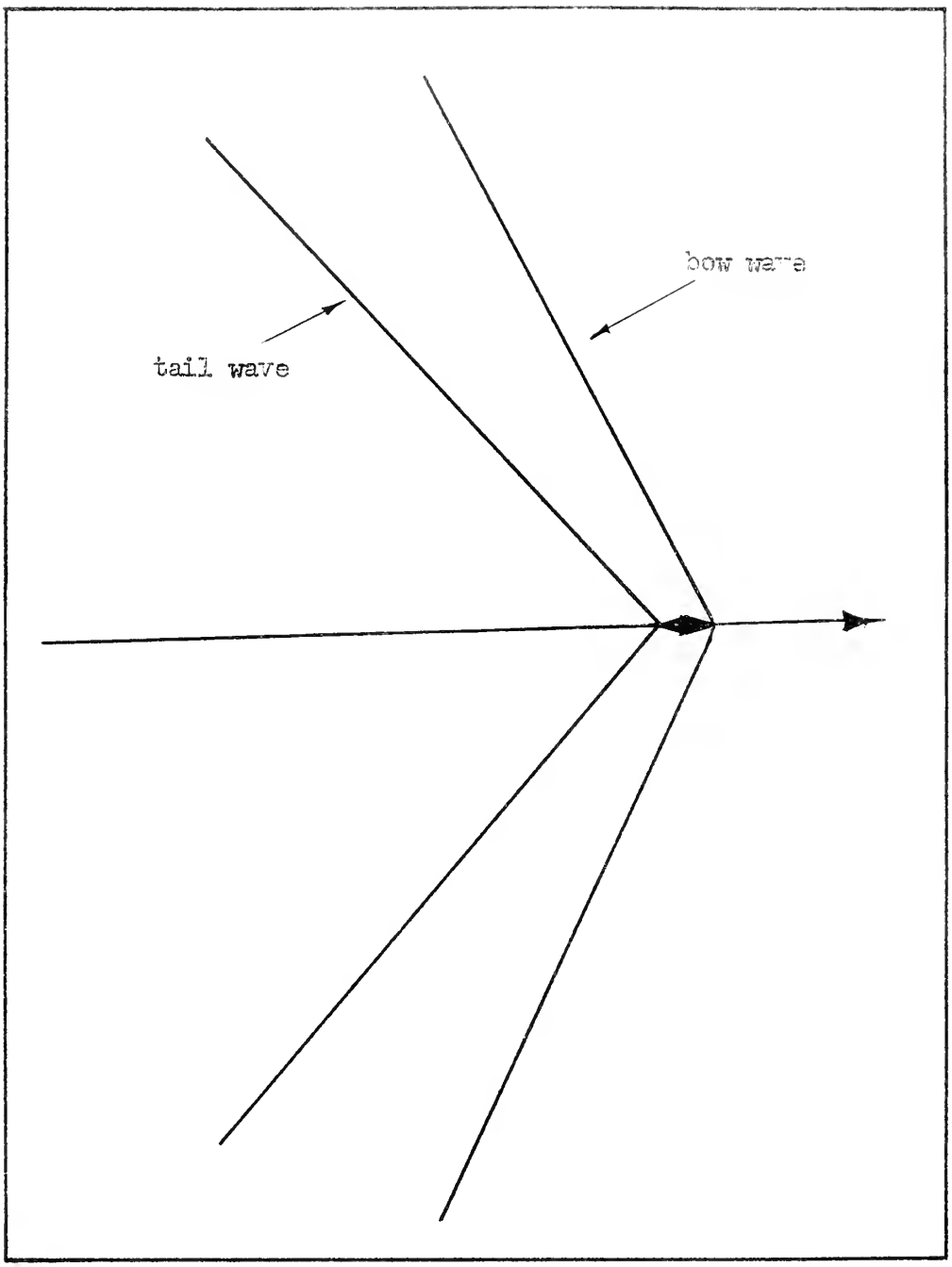

Line Drawing of Wave Pattern in Figure 15

FIGURE 14

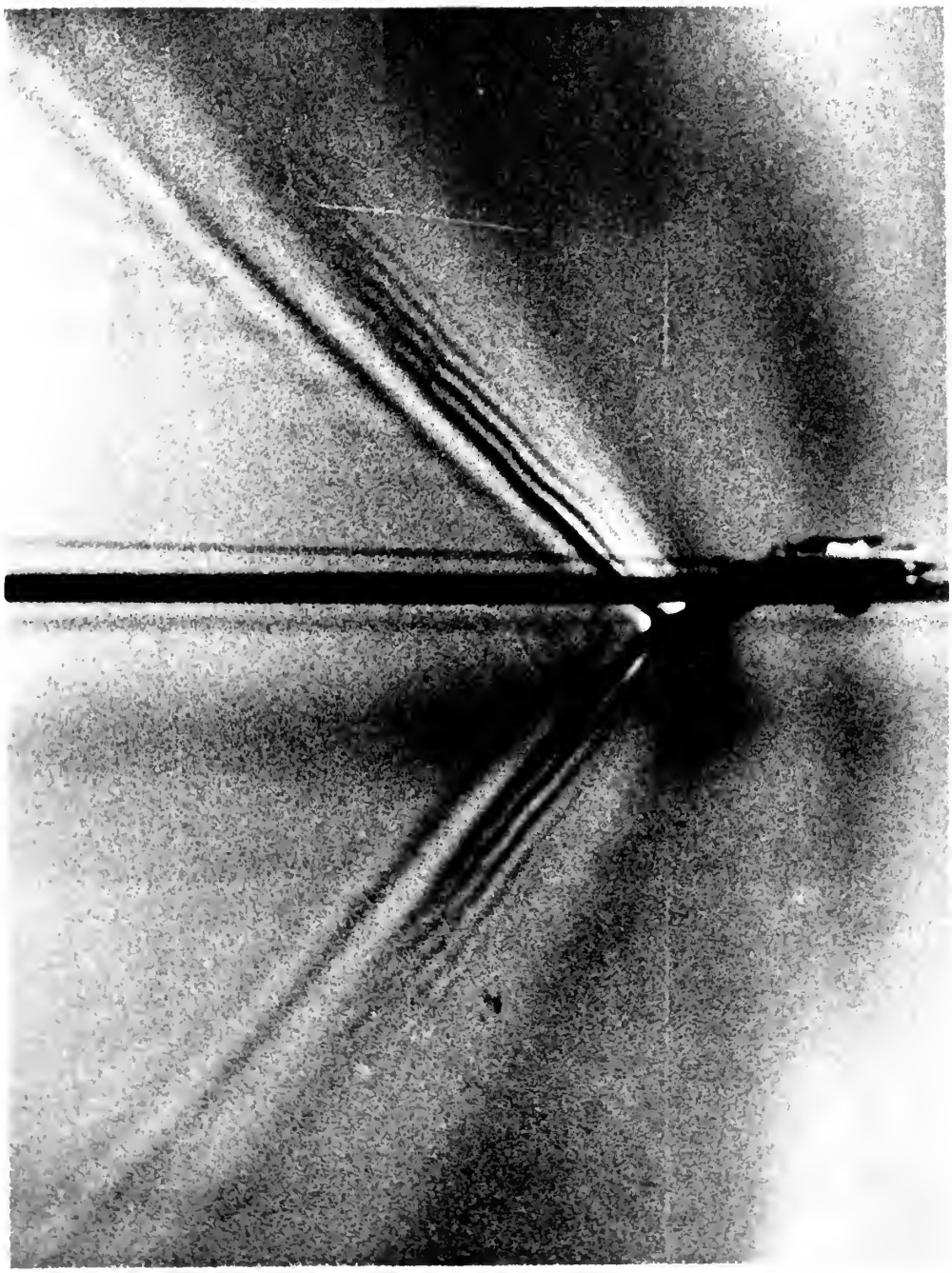

Water Wave Pattern for a 5° Double Wedge at a Constant Mach Number of 1.25 Along a Straight Line Path.

FIGURE 15

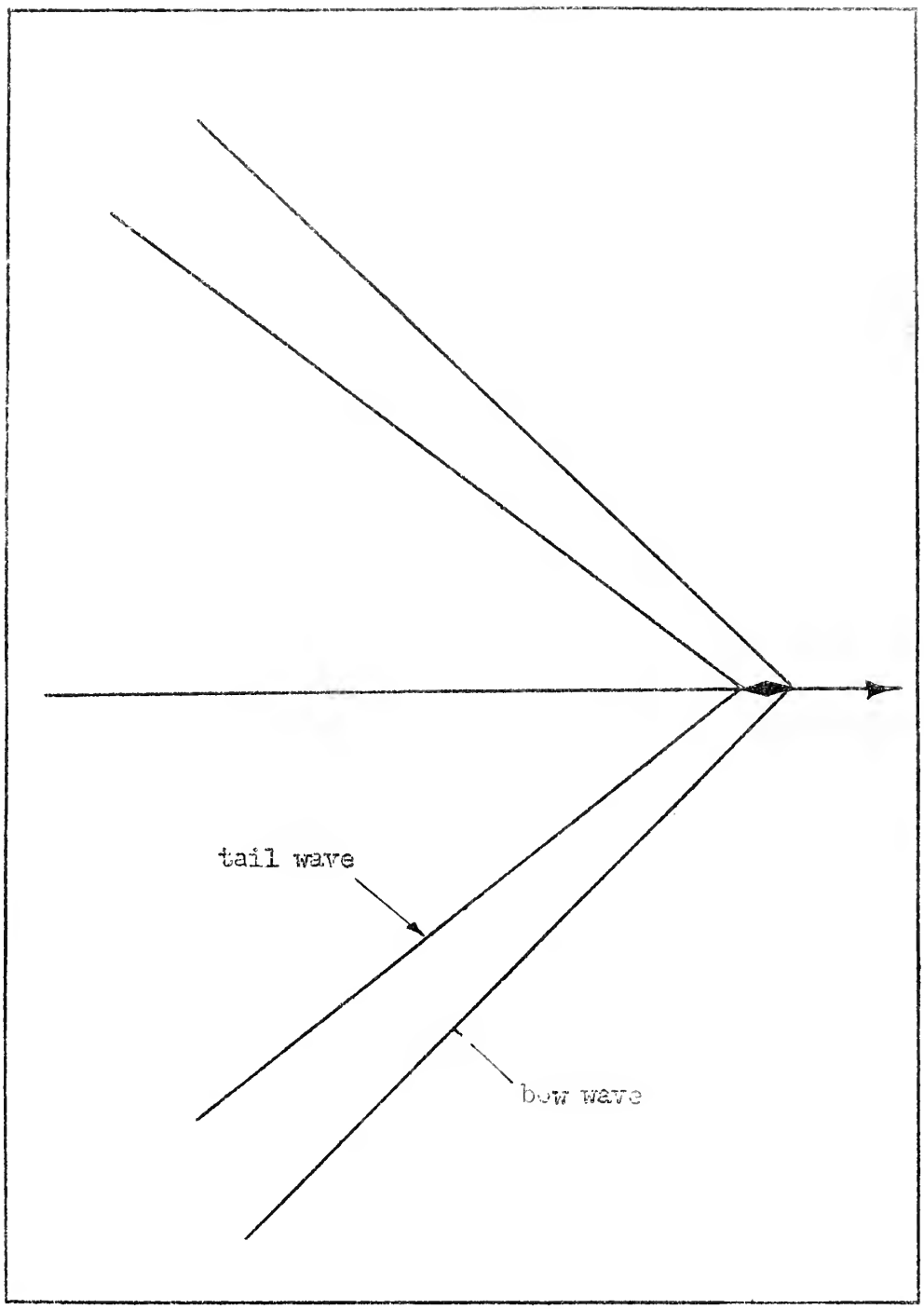

Line Drawing of Wave Pattern in Figure 17

FIGURE 16

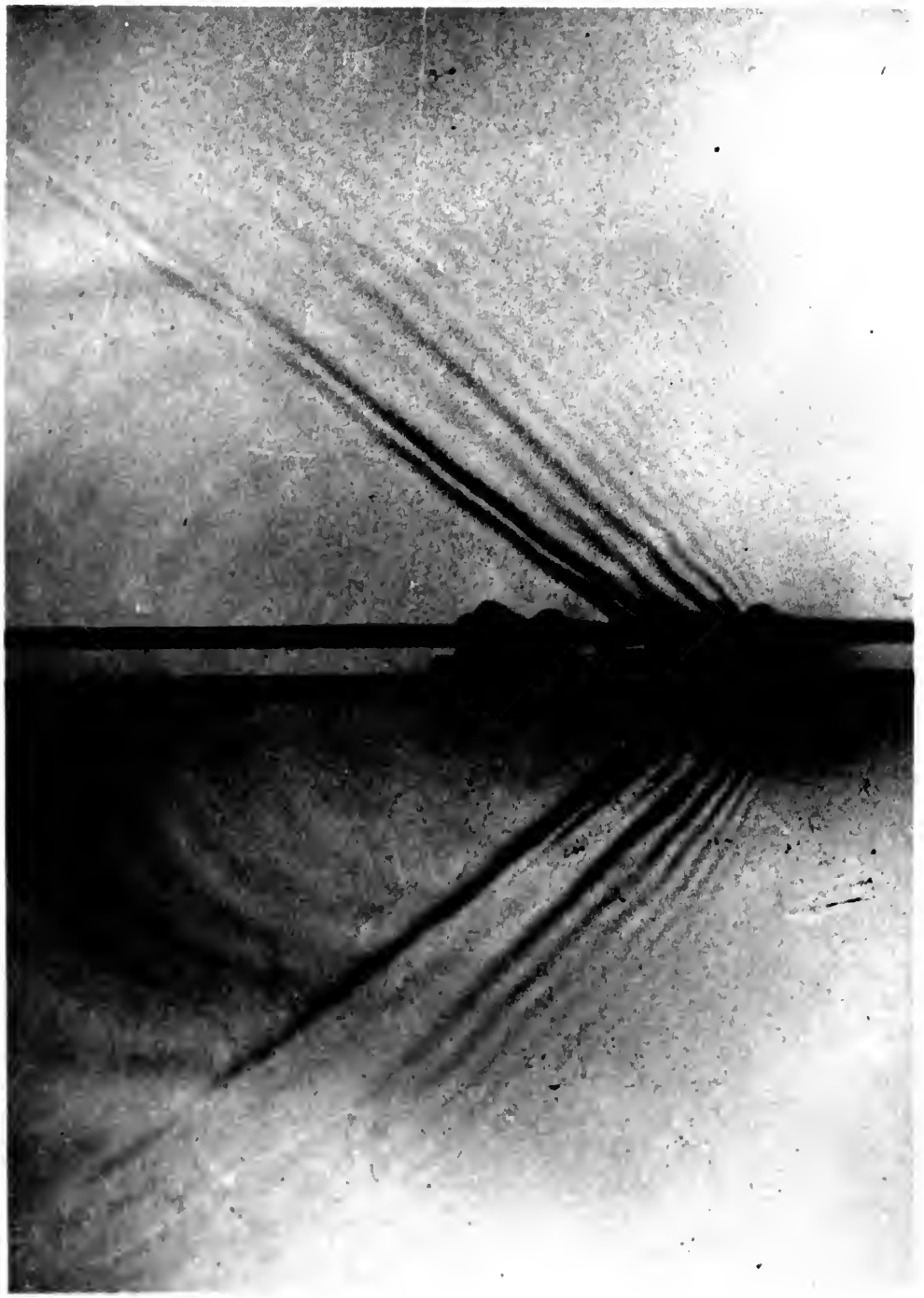

Water Wave Pattern for a 5^{o} Double Wedge at a Constant Mach Number of 1.5 Along a Straight Line Path.

FIGURE 17

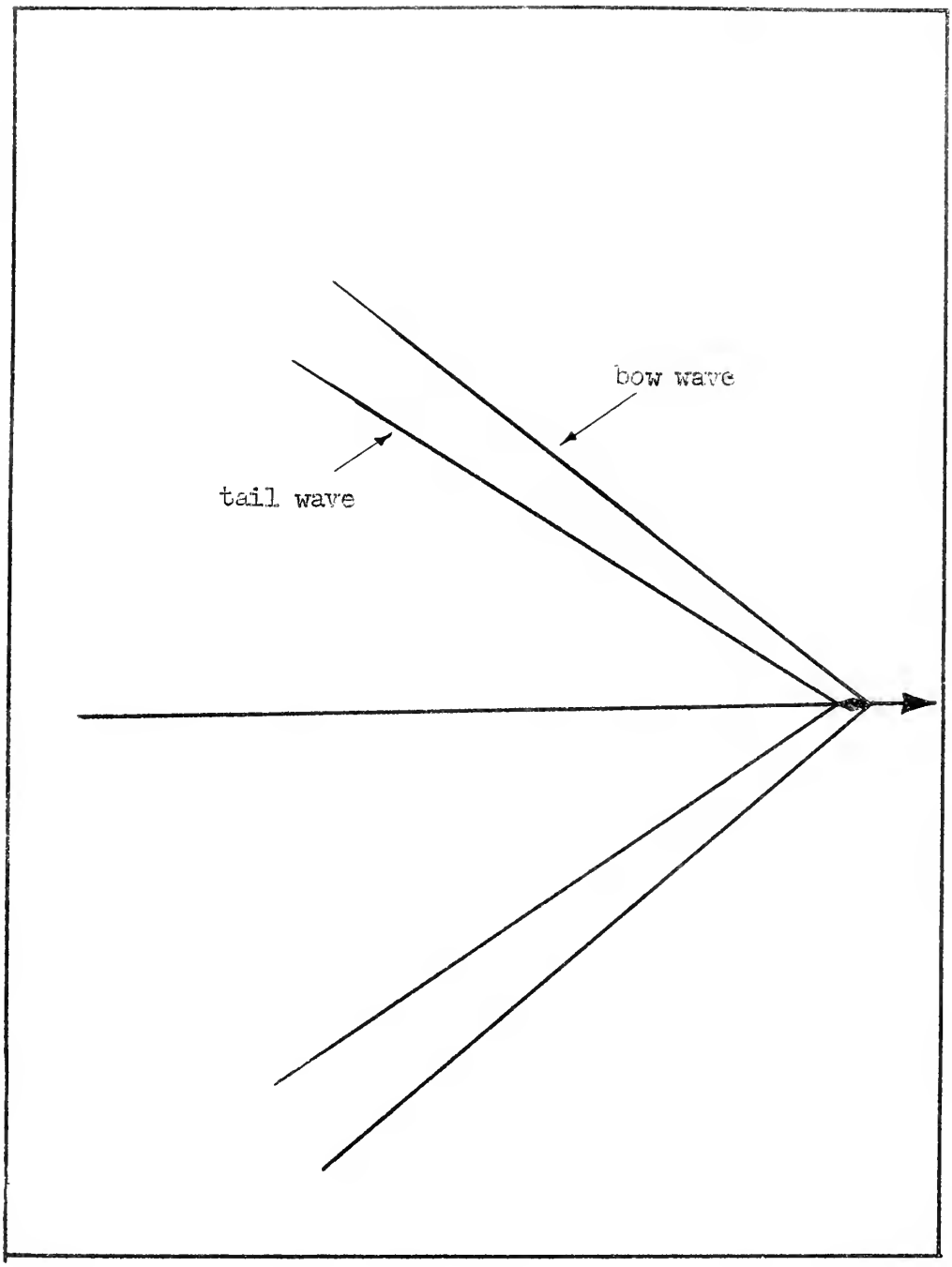

Line Drawing of Wave Pattern in Figure 19

FIGURE 18

Water Wave Pattern for a 5° Double Wedge at a Constant Mach Number of 1.75 Along a Straight Line Path.

FIGURE 19

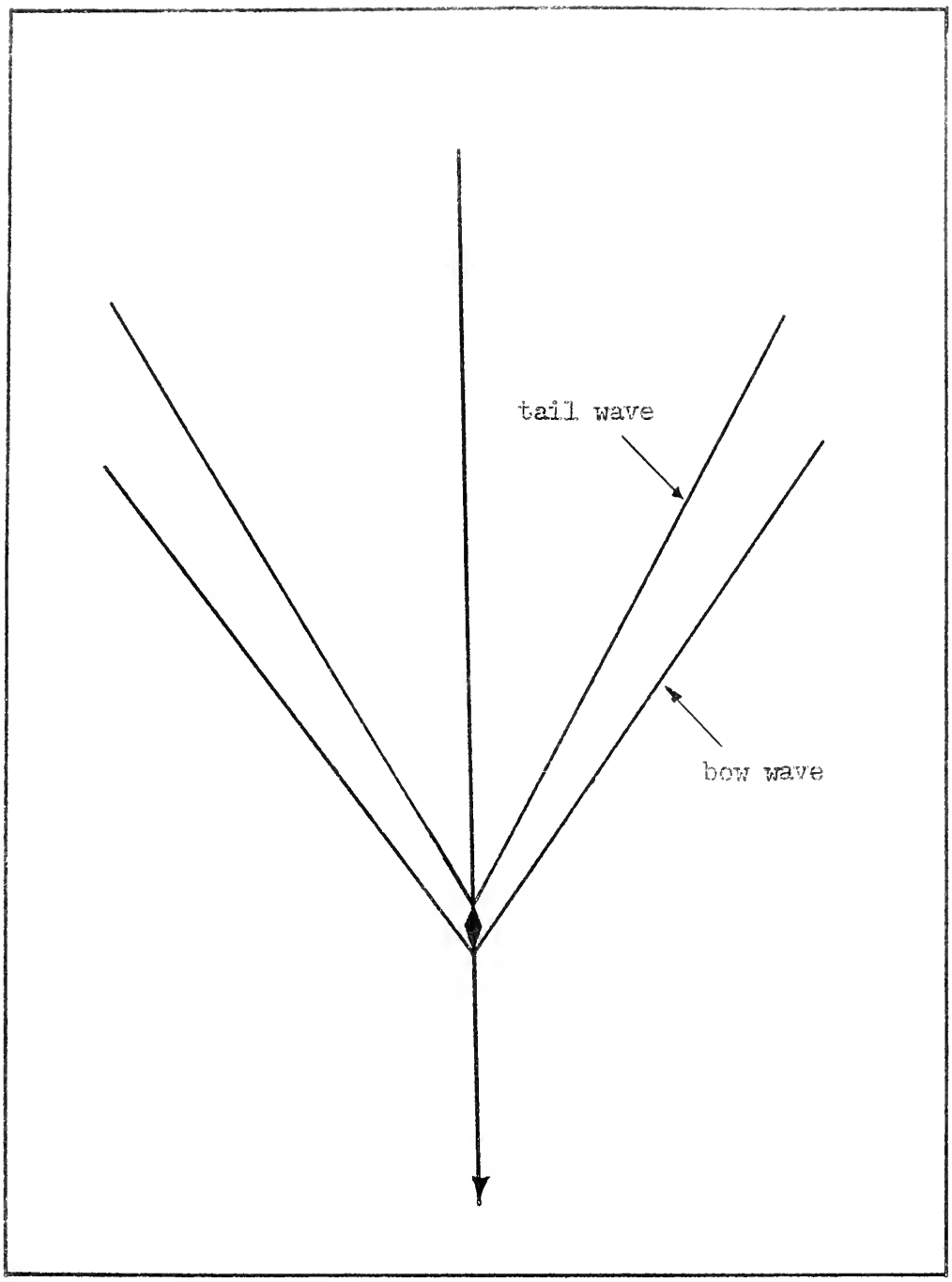

Line Drawing of Wave Pattern in Figure 21

FIGURE 20

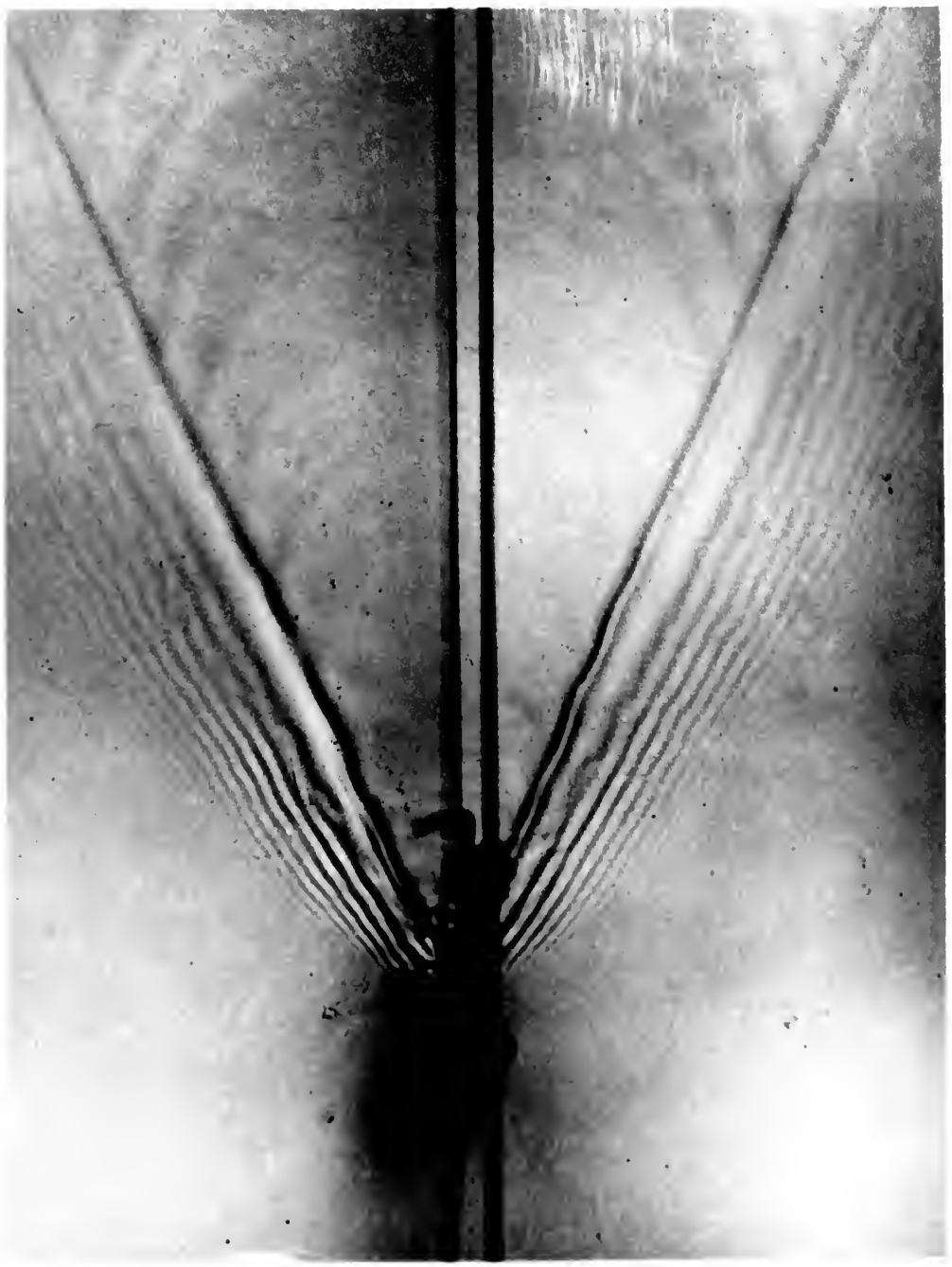

Water Wave Pattern for a 5° Double Wedge at a Constant Mach Number of 2.0 Along a Straight Line Path.

FIGURE 21

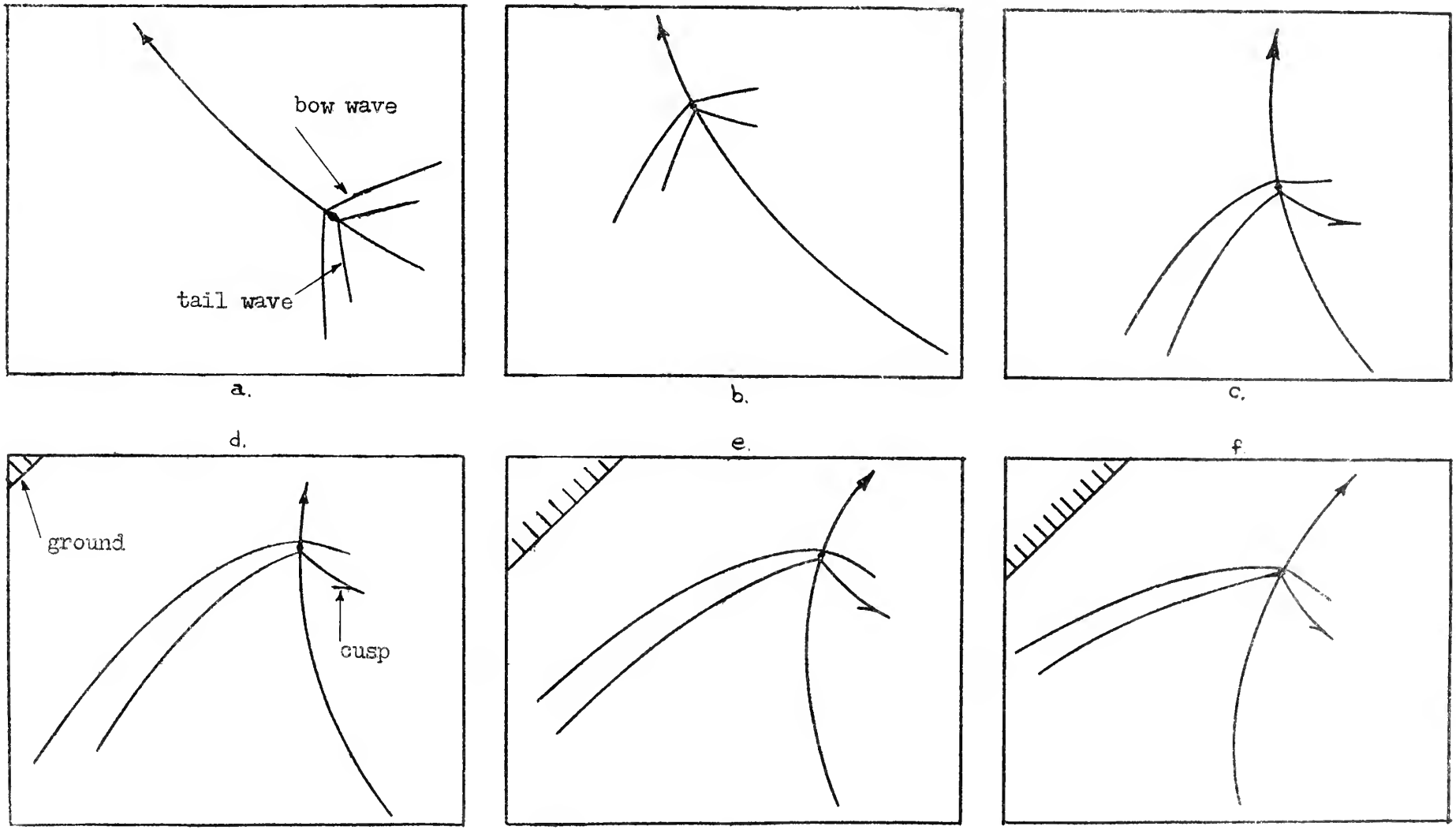

Line Drawings of Wave Patterns in Figure 23

FIGURE 22

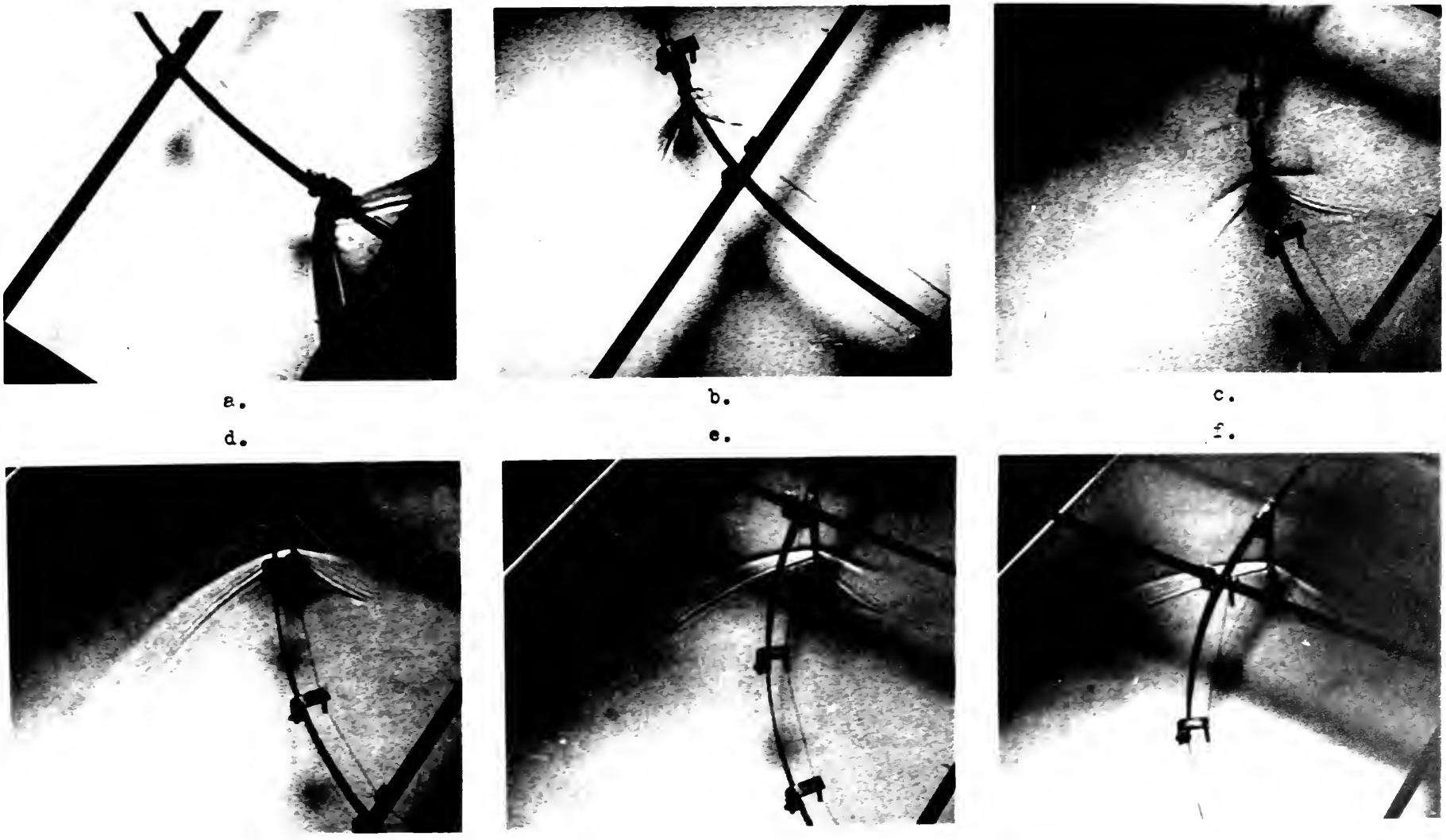

Water Wave Patterns for a 5° Double Wedge at a Constant Mach Number of 1.1 Along a Curvilinear Dive Path.

FIGURE 23

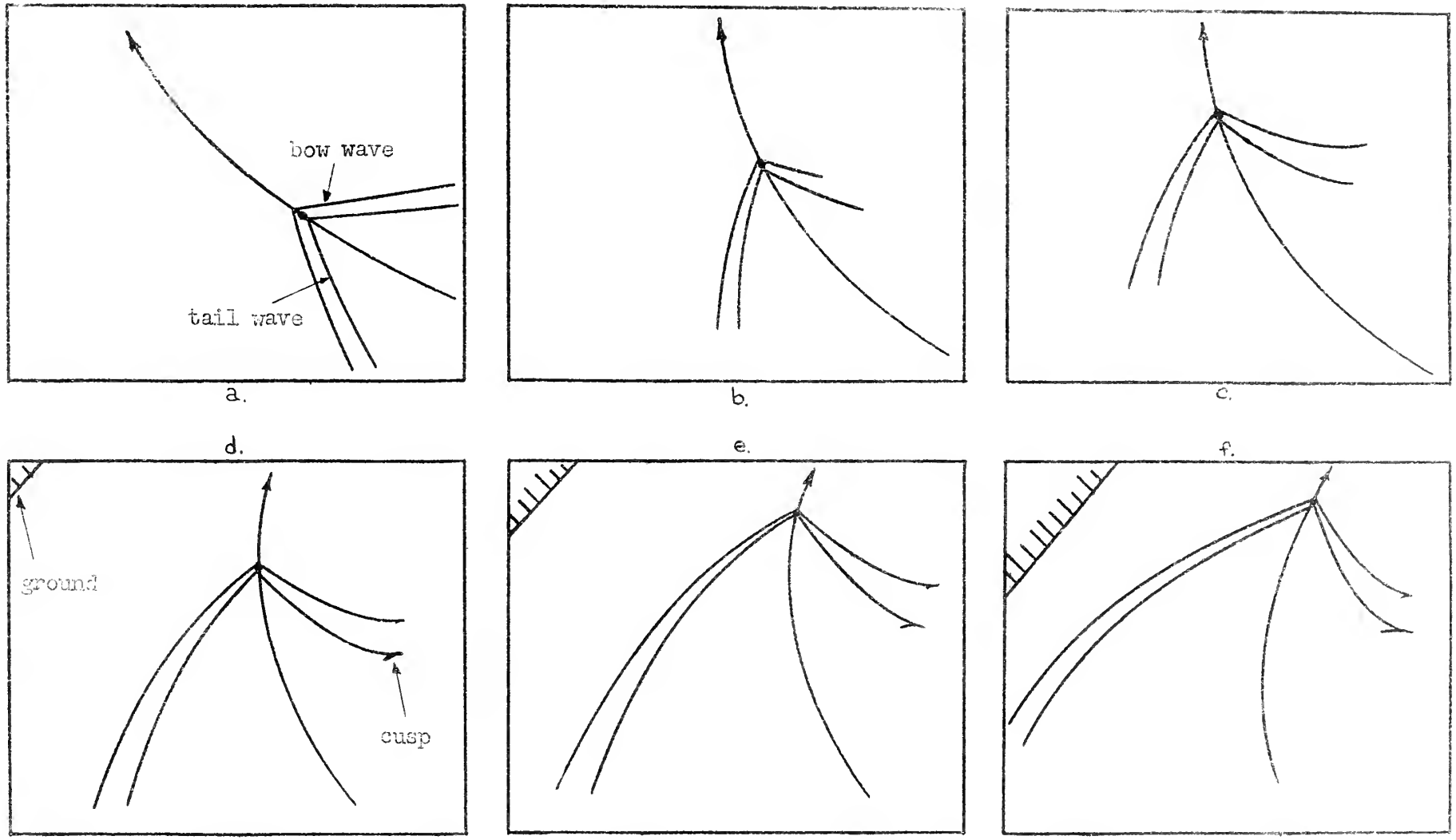

Line Drawings of Wave Patterns in Figure 25

FIGURE 24

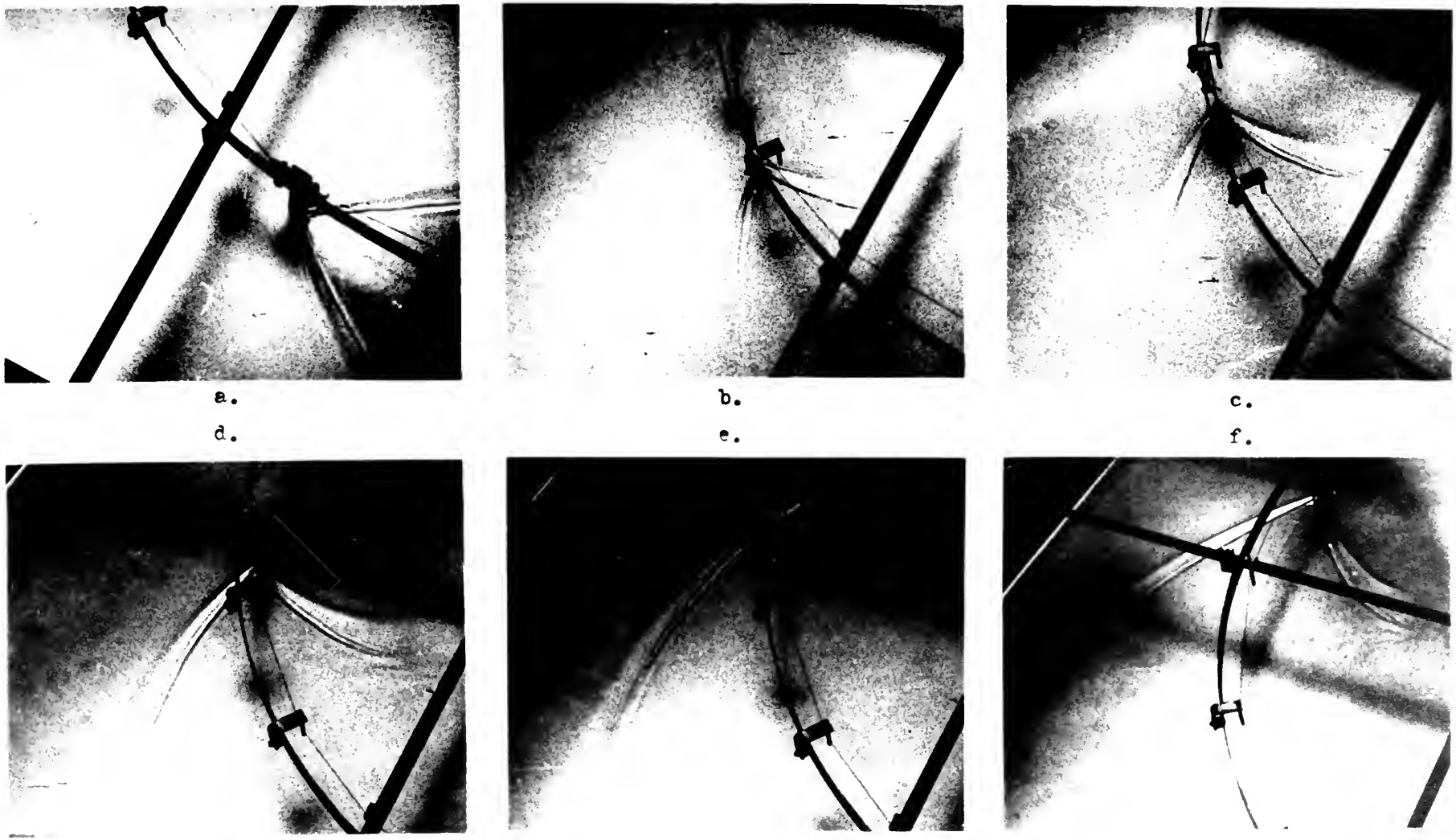

Water Wave Patterns for a 5° Double Wedge at a Constant Mach Number of 1.5 Along a Curvilinear Dive Path.

FIGURE 25

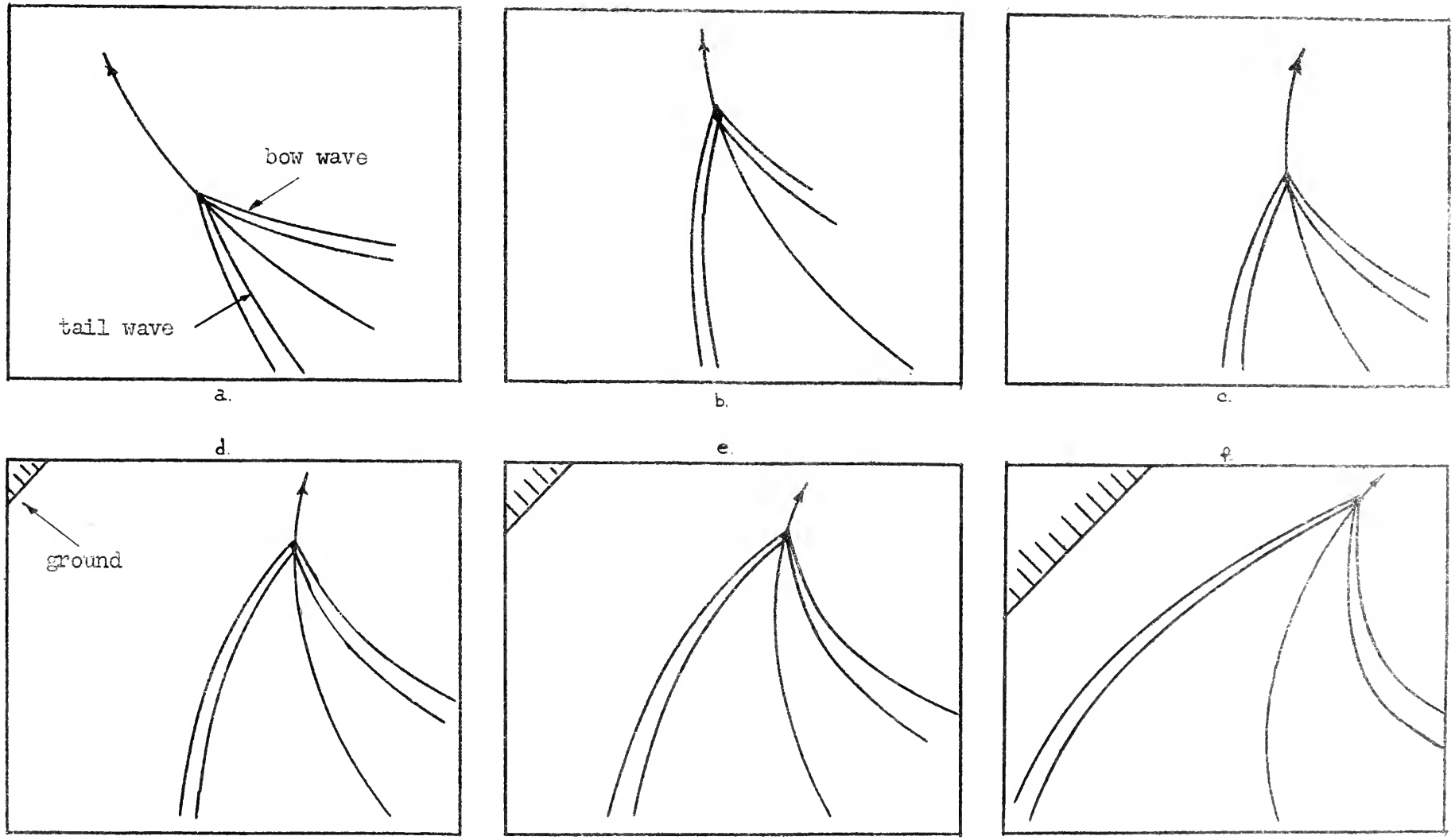

Line Drawings of Wave Patterns in Figure 27

FIGURE 26

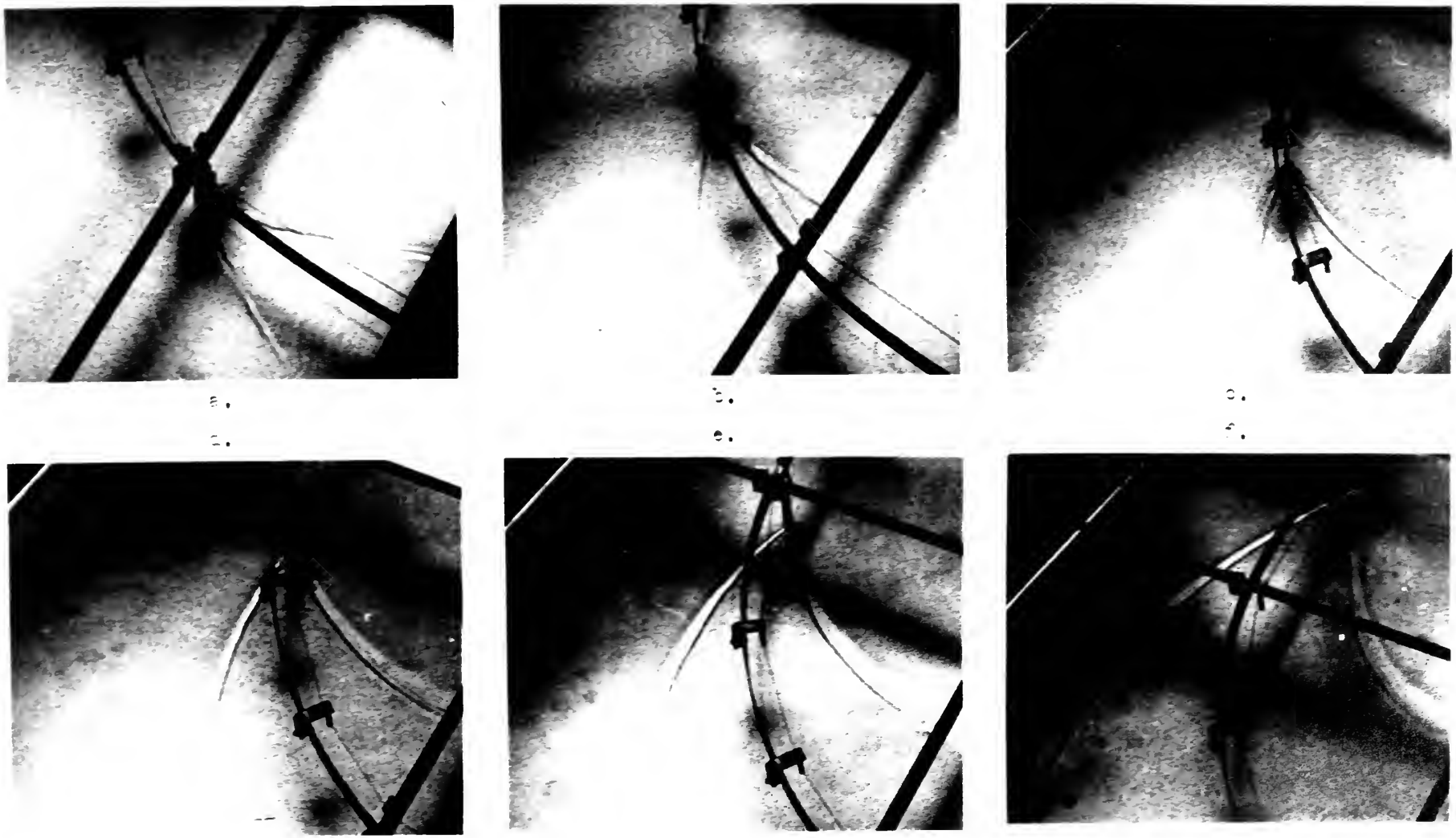

Water Wave Patterns for a 5° Double Wedge at a Constant Mach Number of 2.1 Along a Curvilinear Dive Path.

FIGURE 27

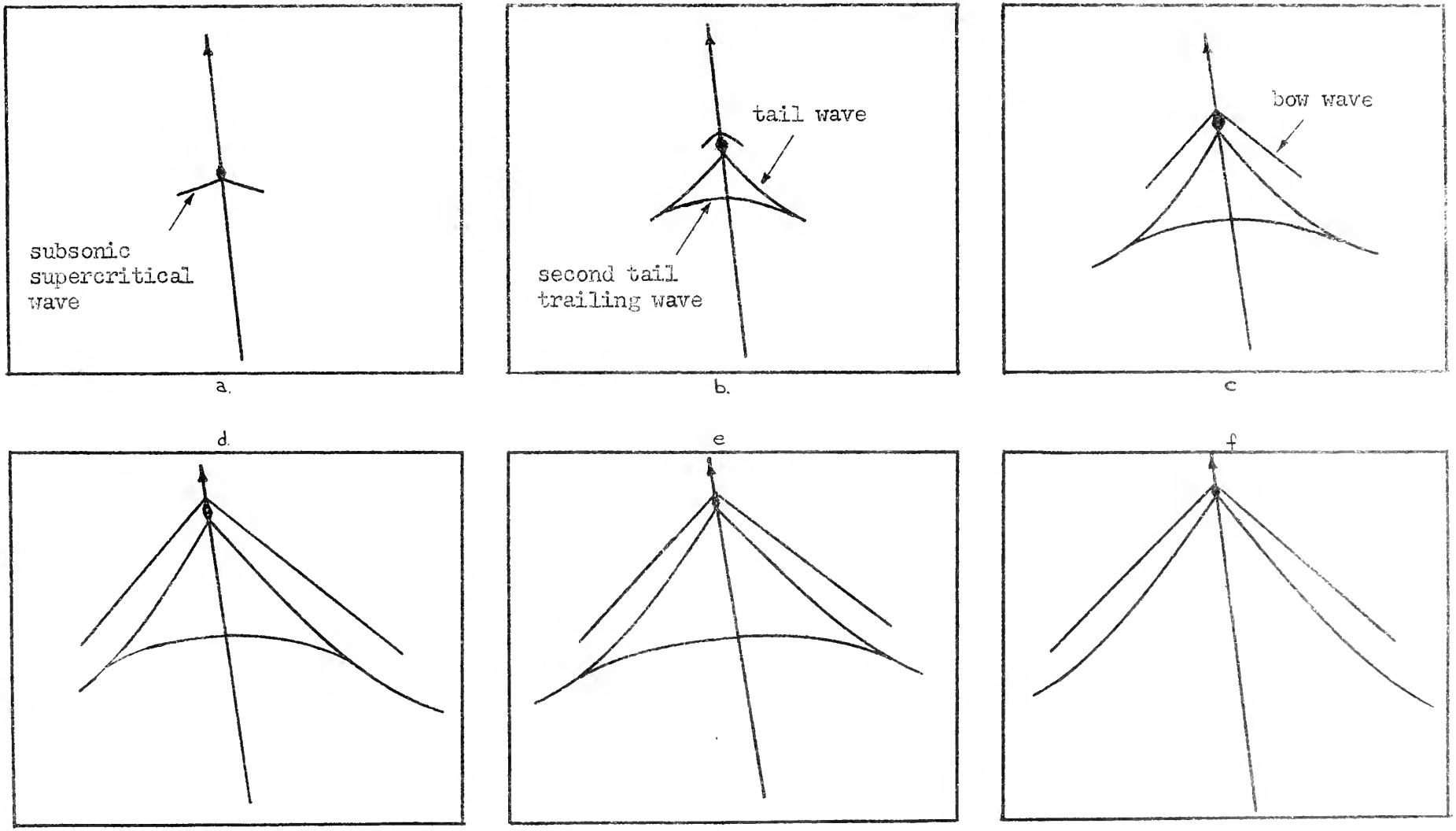

Line Drawings of Wave Patterns in Figure 29

FIGURE 28

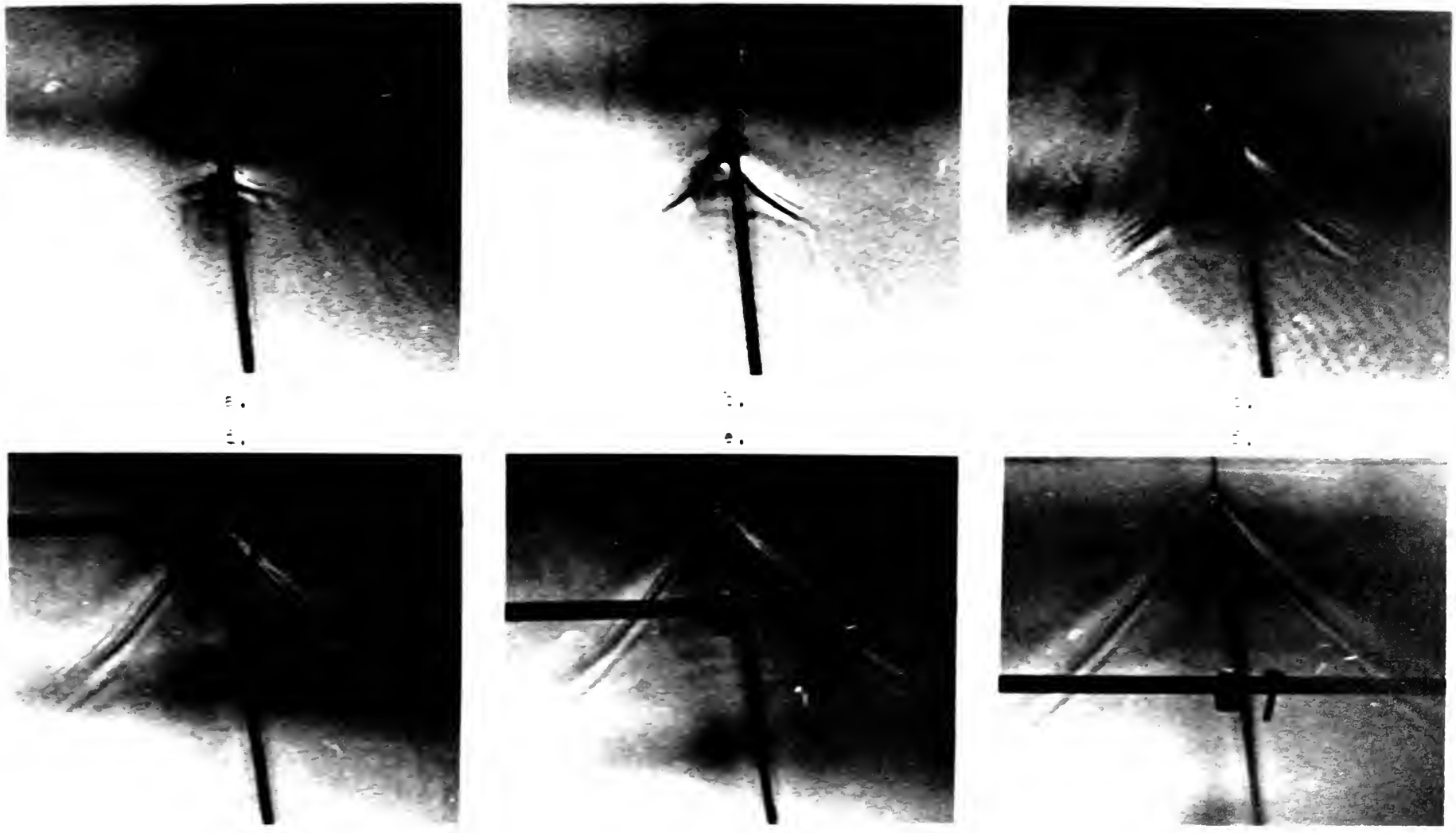

Shock Wave Patterns for a 5° Double Wedge Accelerating From a Mach Number of 1.15 to a Mach Number of 2.1 Using a Straight Line Path.

Figure 20

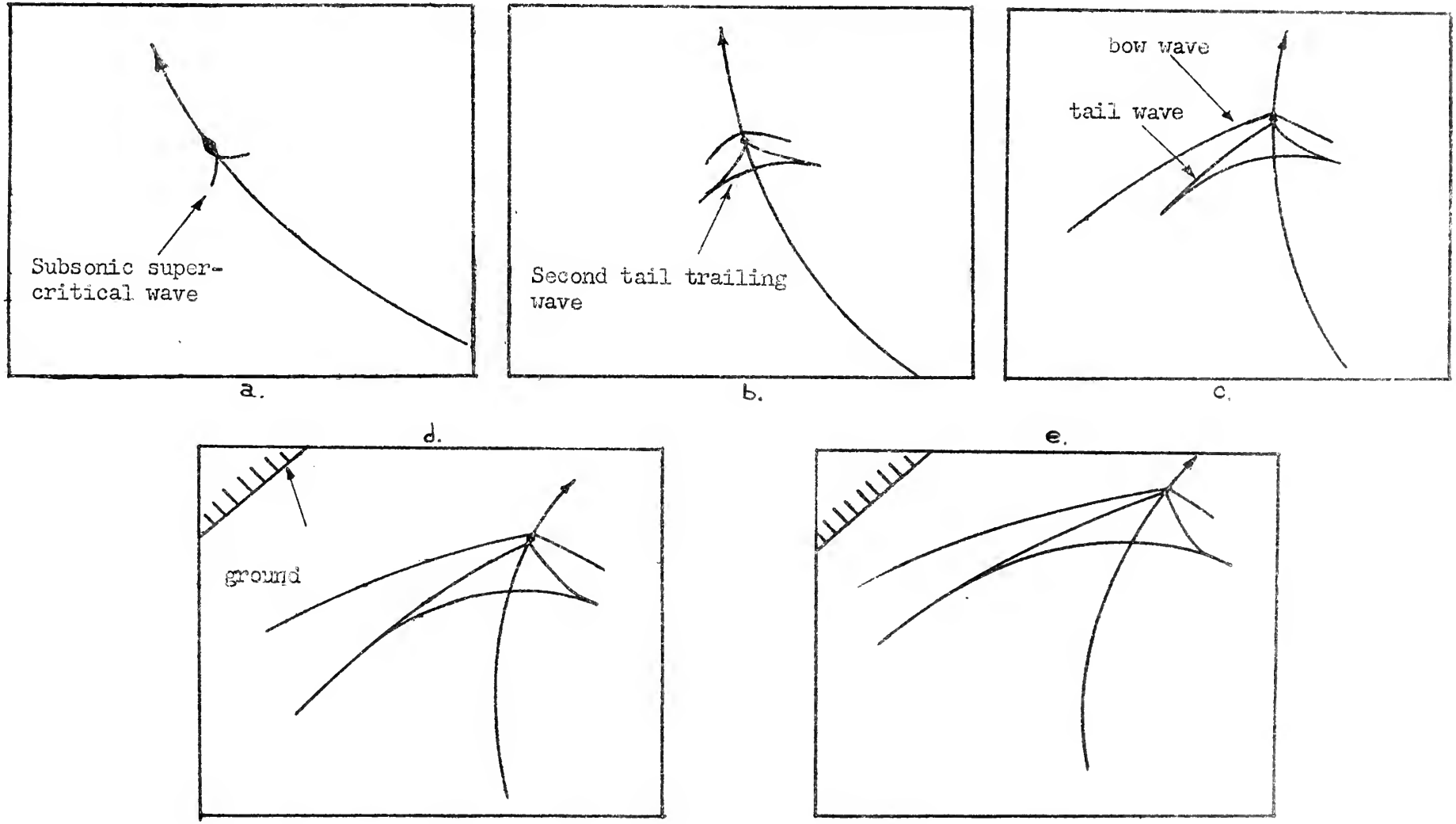

Line Drawings of Wave Patterns in Figure 31

FIGURE 30

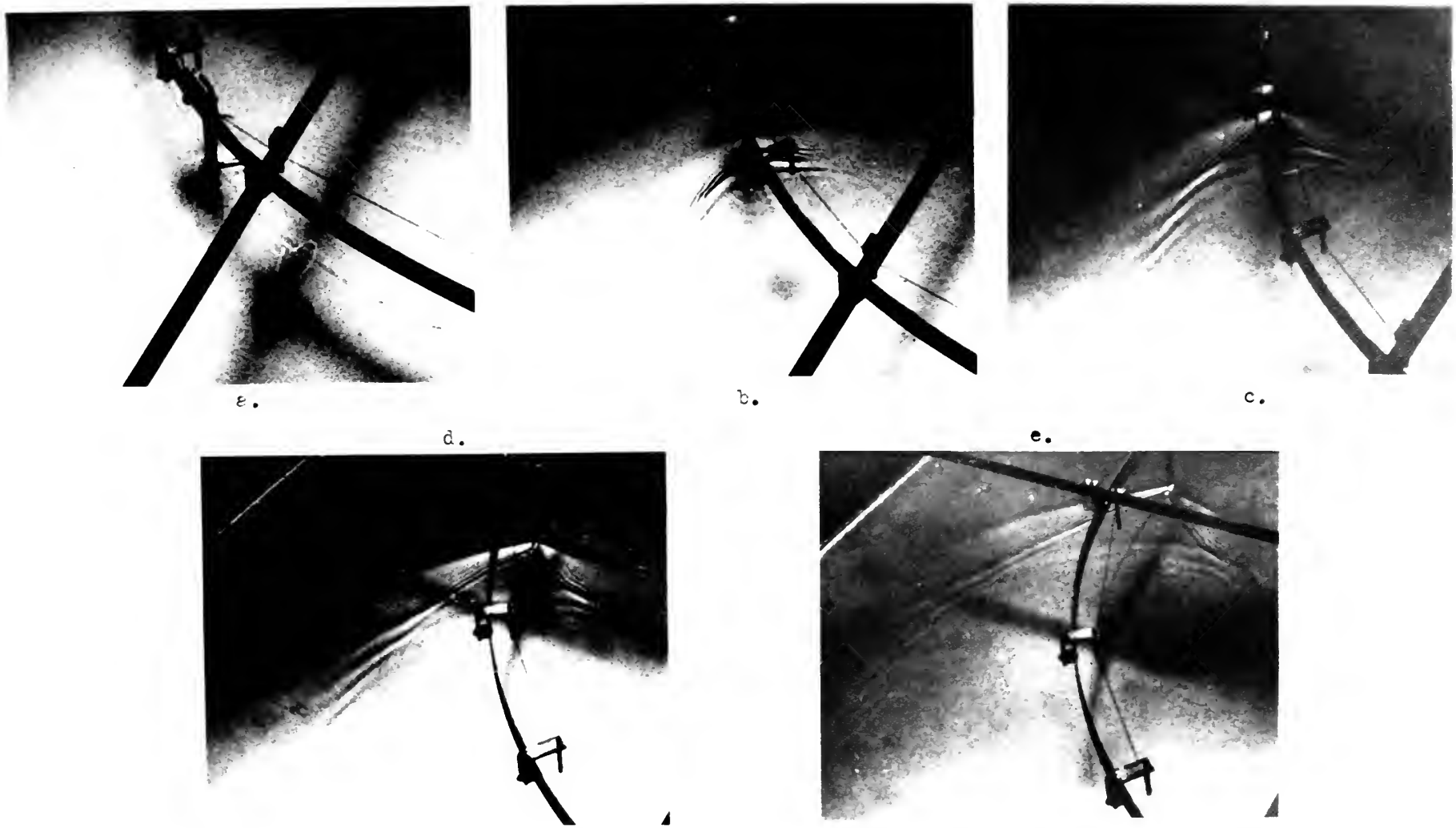

Water Wave Patterns for a 5° Double Wedge Accelerating From a Mach Number of 0.85 to a Mach Number of 1.5 Along a Curvilinear Dive Path.

FIGURE 31

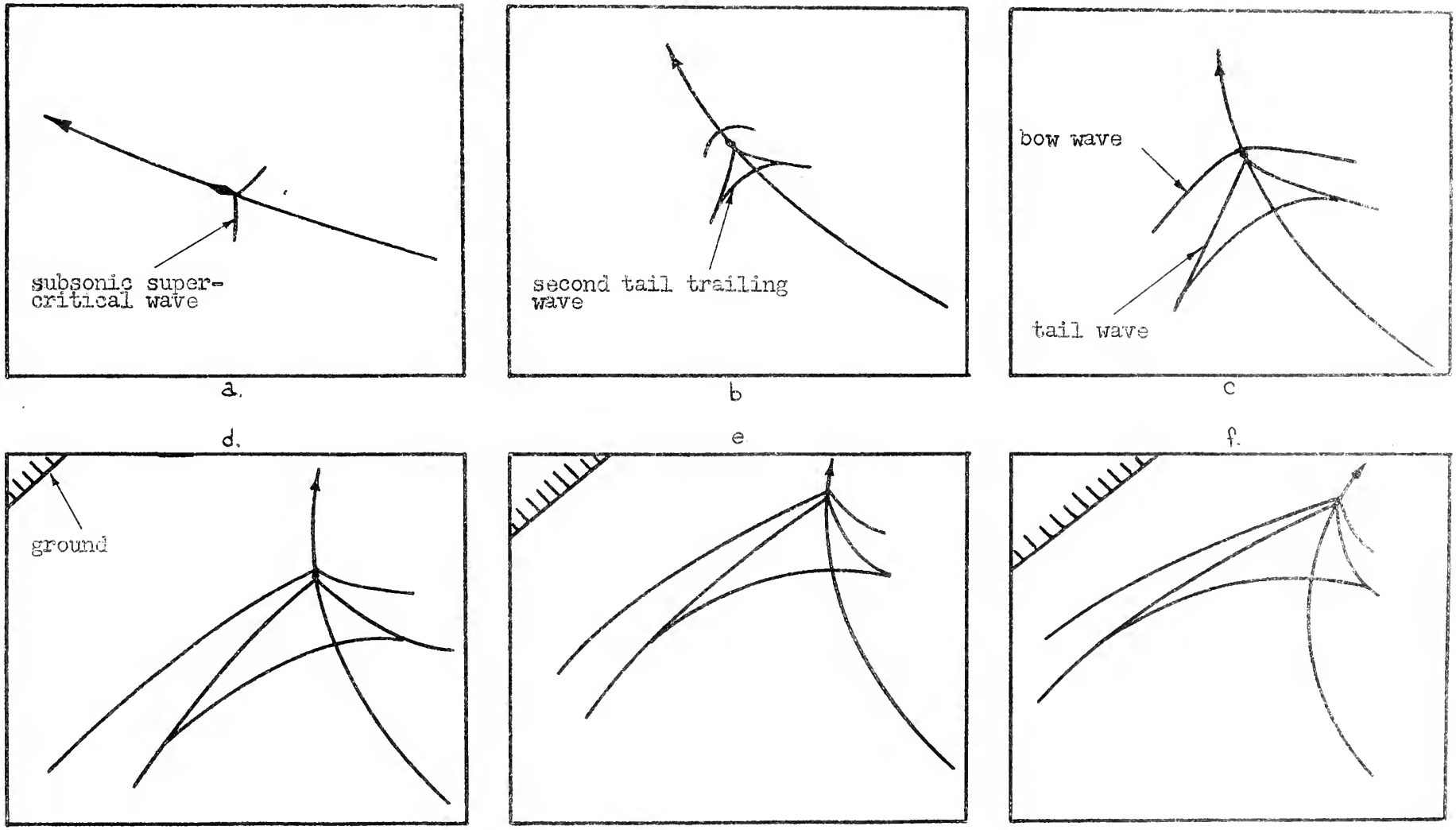

Line Drawings of Wave Patterns in Figure 33

FIGURE 32

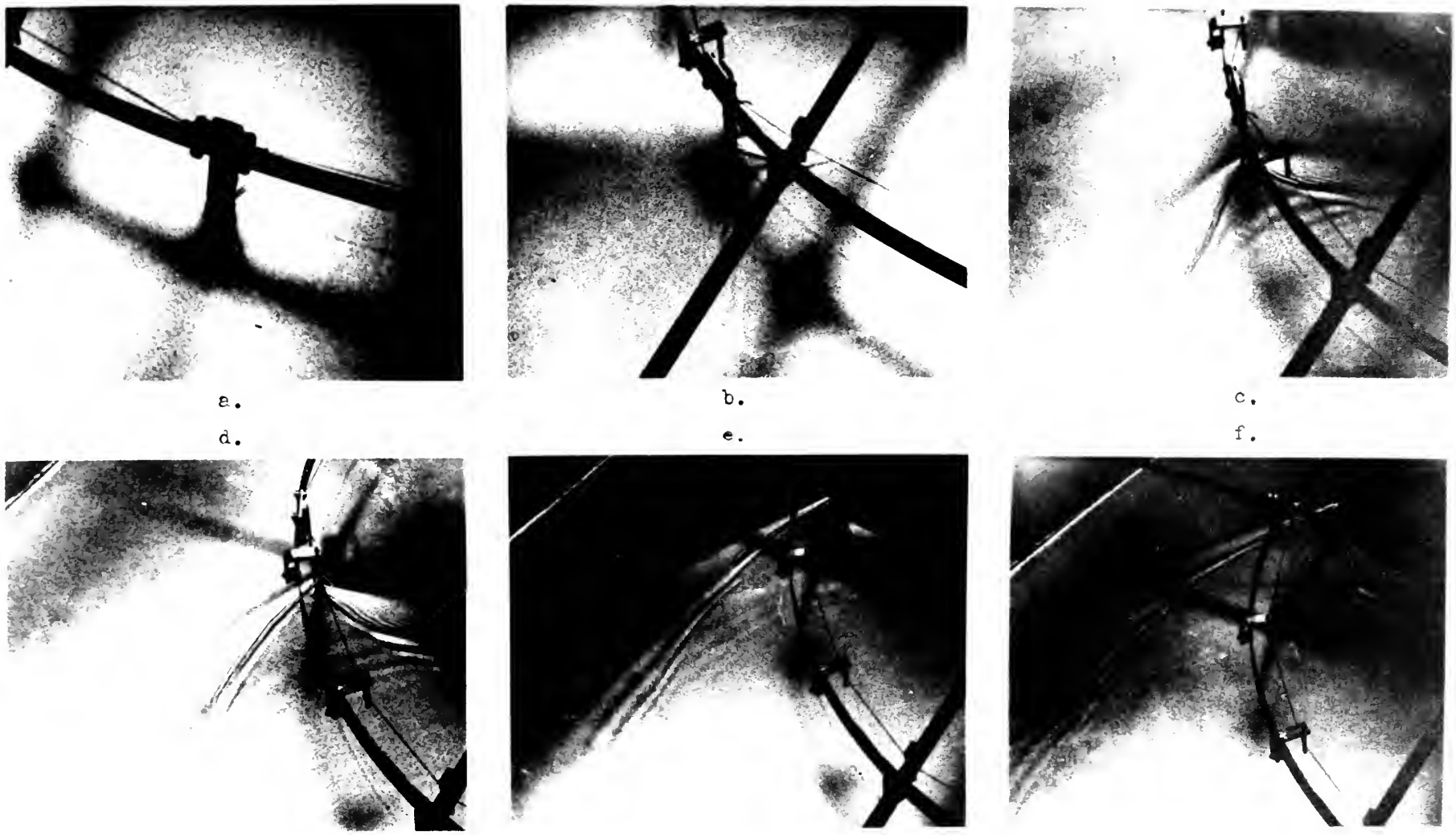

Water Wave Patterns for a 5° Double Wedge Accelerating From a Mach Number of 0.85 to a Mach Number of 2.0 Along a Curvilinear Dive Path.

FIGURE 33

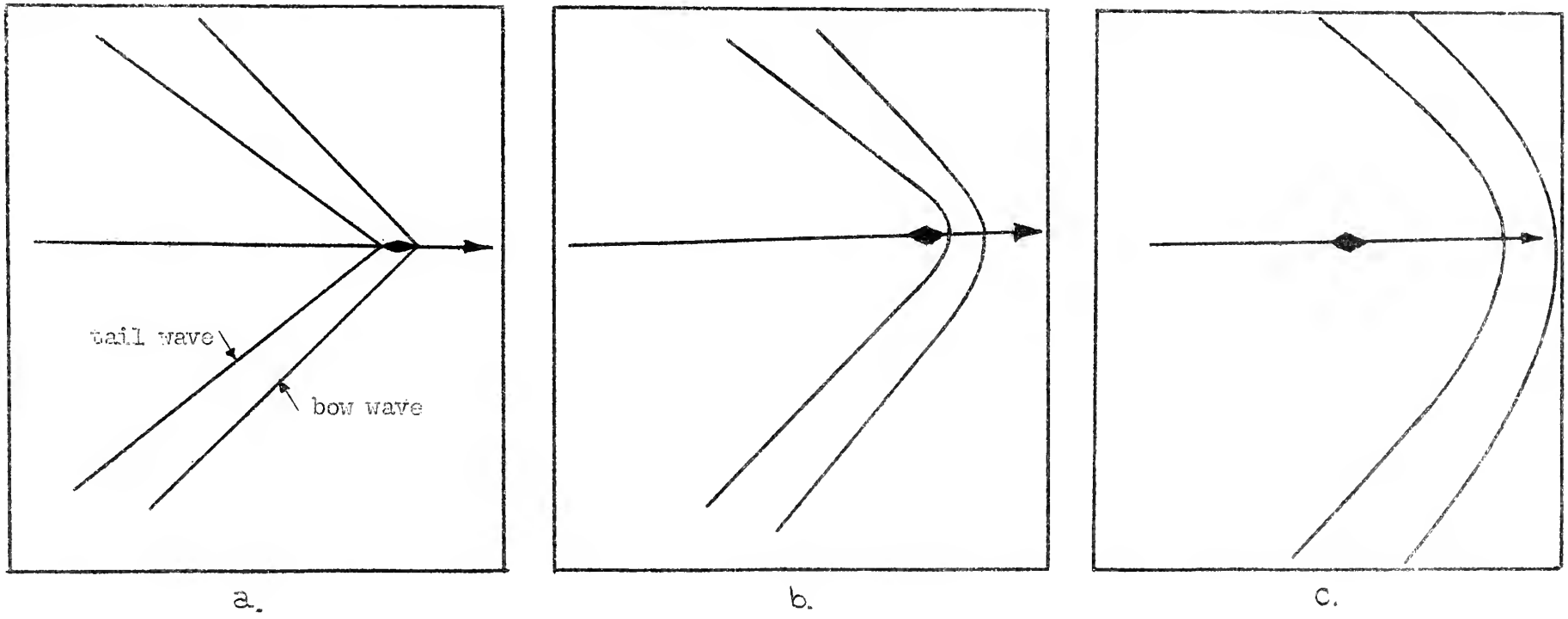

Line Drawings of Wave Patterns in Figure 35

FIGURE 34

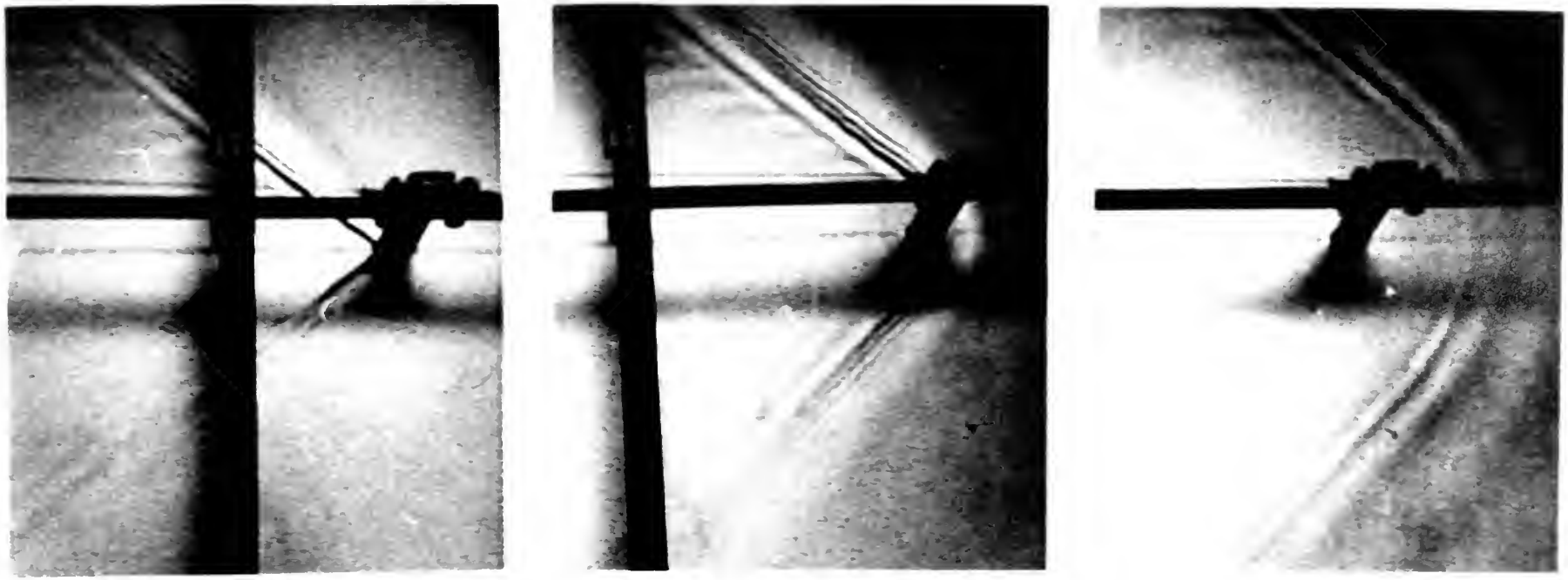

a. b. c.

Water Wave Patterns for a 5° Double Wedge Decelerating Suddenly From a Mach Number of 1.5 to a Subcritical Mach Number Along a Straight Line Path.

FIGURE 35

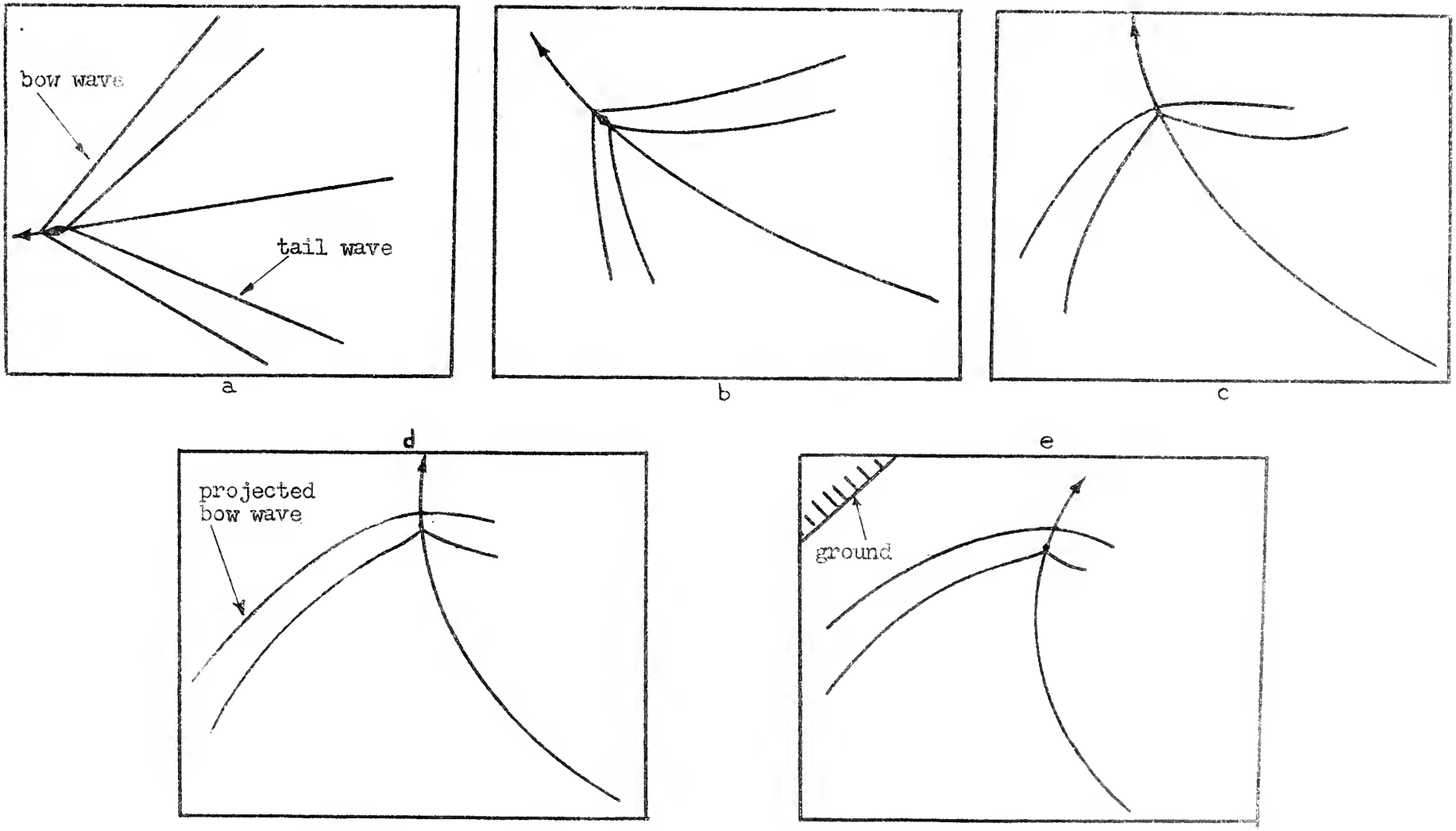

Line Drawings of Wave Patterns in Figure 37

FIGURE 36

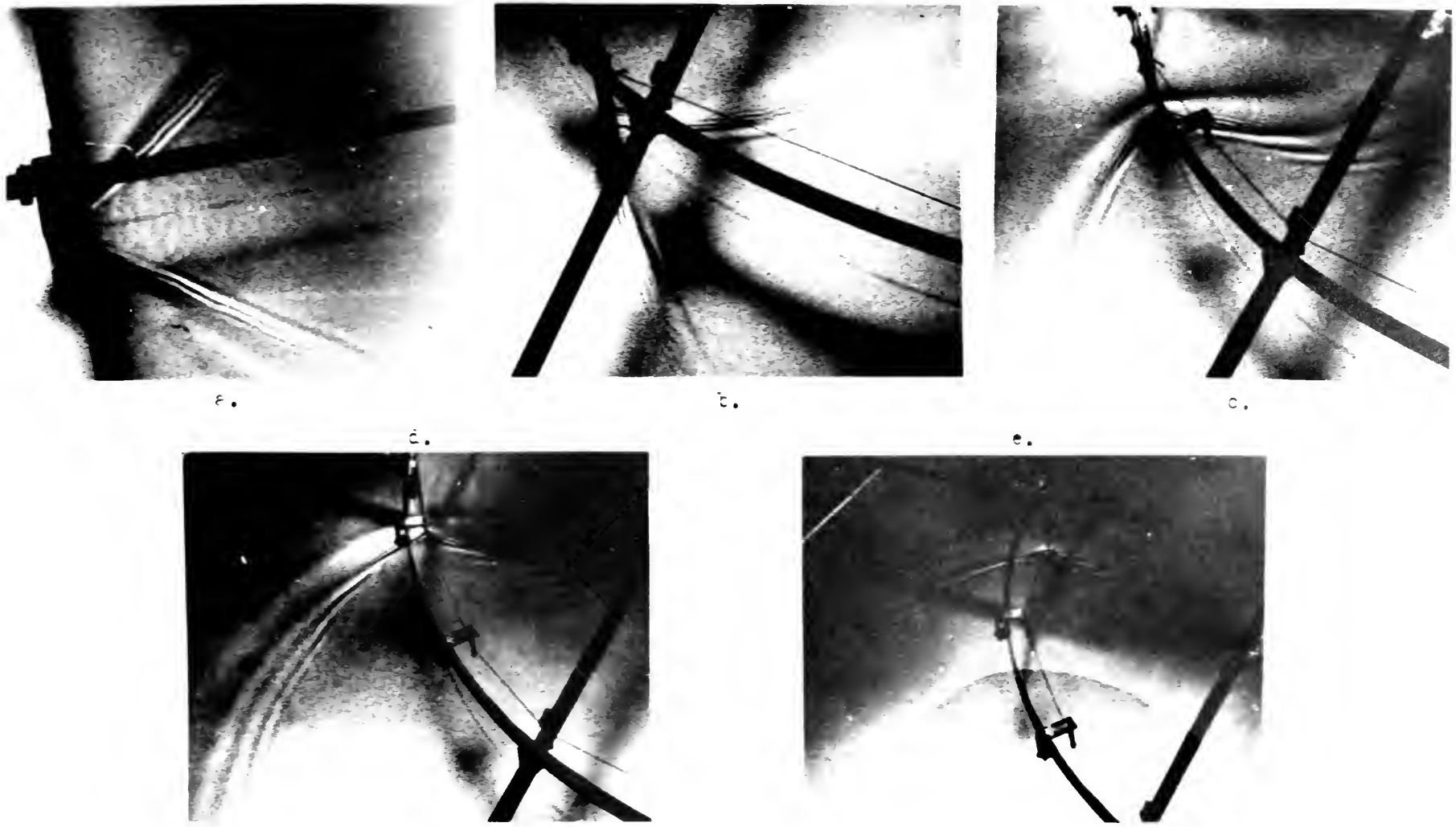

Water Wave Patterns for a 5° Double Wedge Decelerating Suddenly From a Mach Number of 1.5 to a Supercritical Mach Number of 0.85 Along a Curvilinear Dive Path.

FIGURE 37

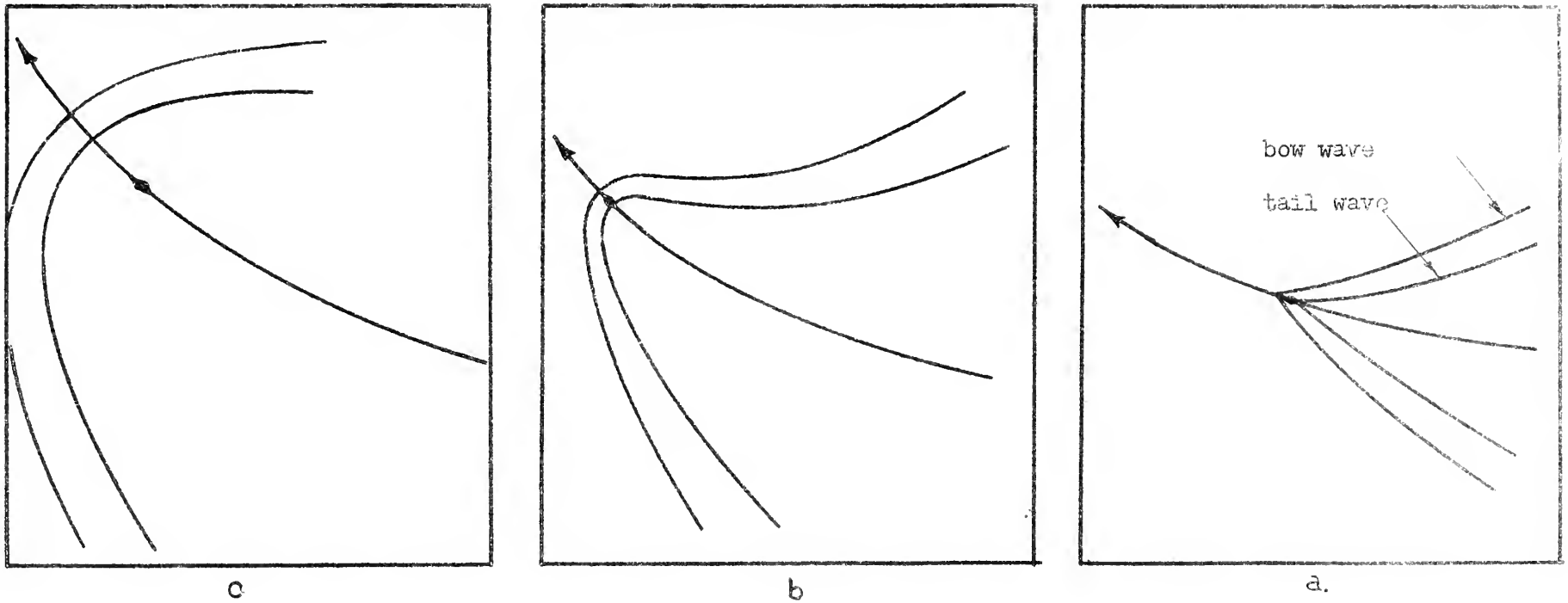

Line Drawings of Wave Patterns in Figure 39

FIGURE 38

c. b. a.

Water Wave Patterns for a 5° Double Wedge Decelerating Suddenly From a Mach Number of 2.0 to a Subcritical Mach Number Along a Curvilinear Dive Path.

FIGURE 39

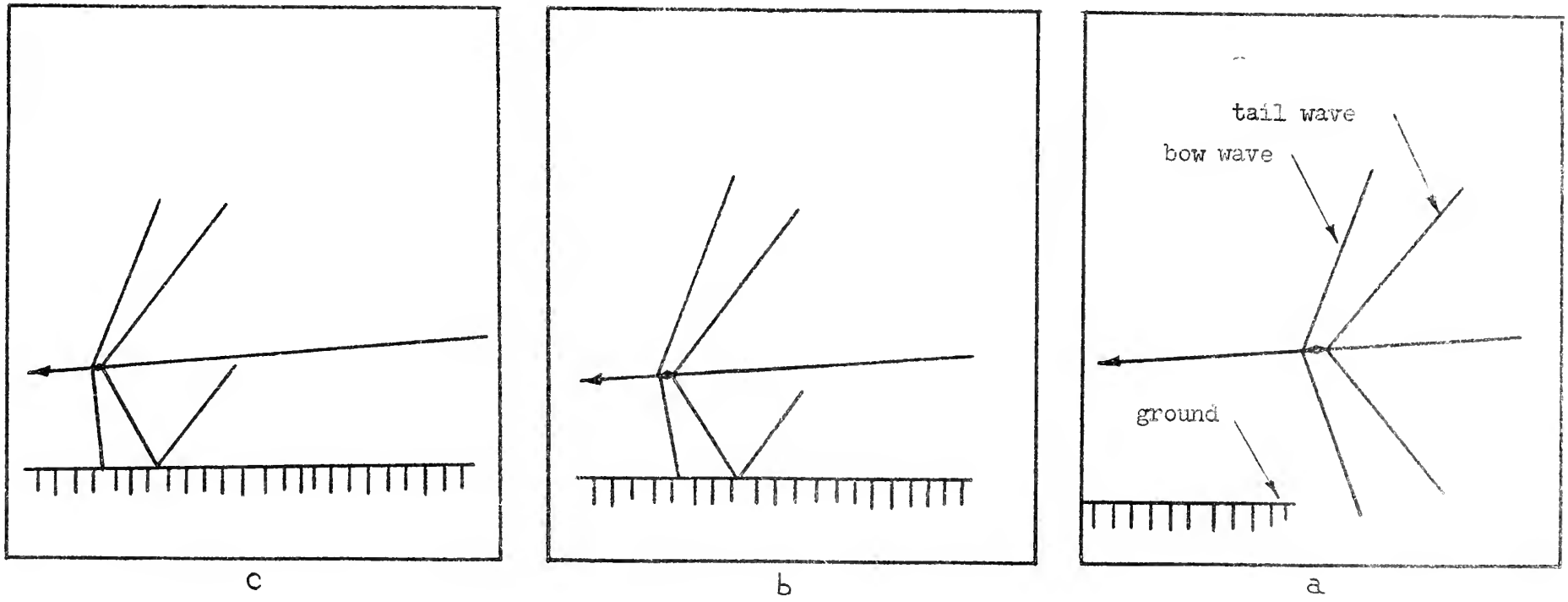

Line Drawings of Wave Patterns in Figure 41

FIGURE 40

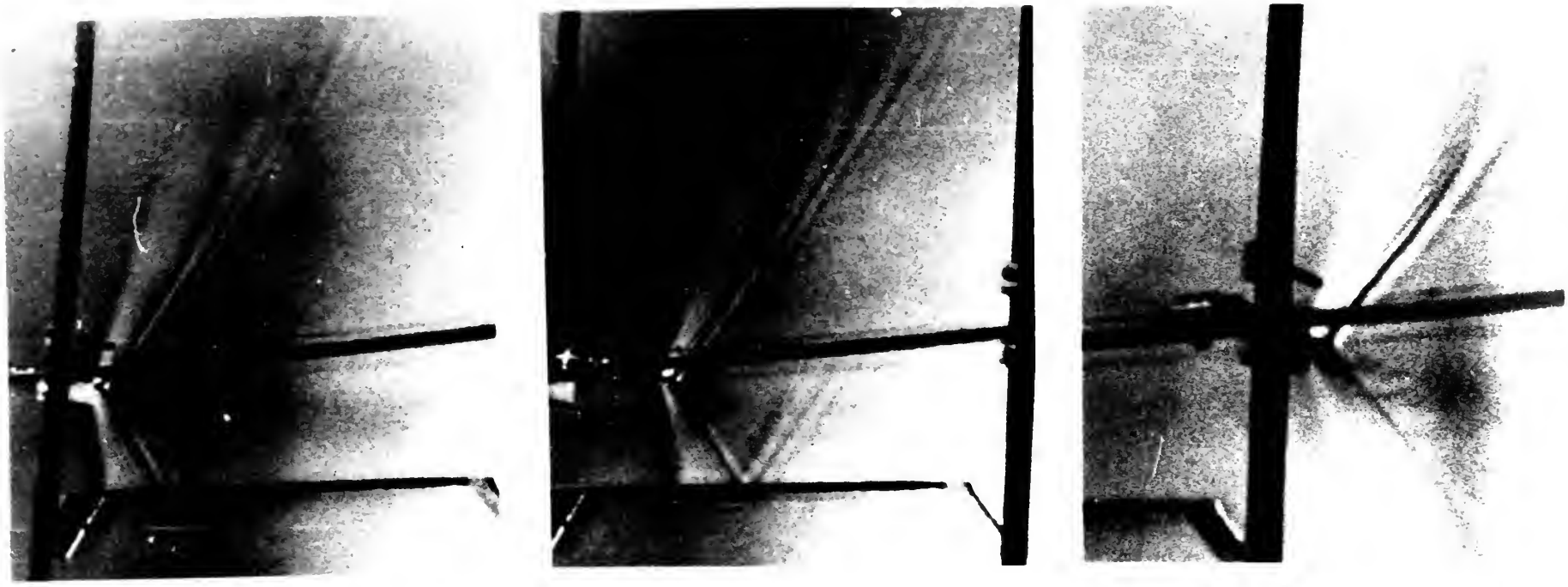

c. b. e.

Water Wave Patterns for a 5° Double Wedge Showing Shock Wave Interactions with the Ground for a Constant Mach Number of 1.25 Along a Straight Line Path Parallel with the Ground.

FIGURE 41

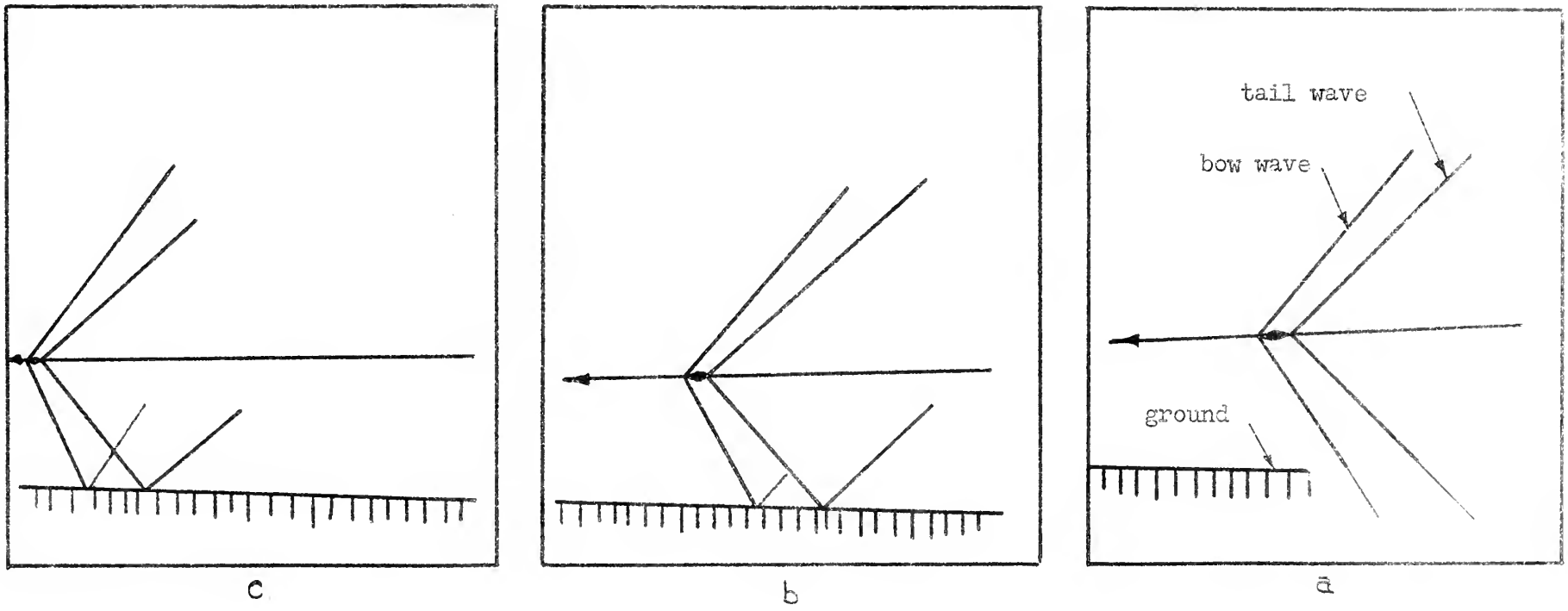

Line Drawings of Wave Patterns in Figure 43

FIGURE 42

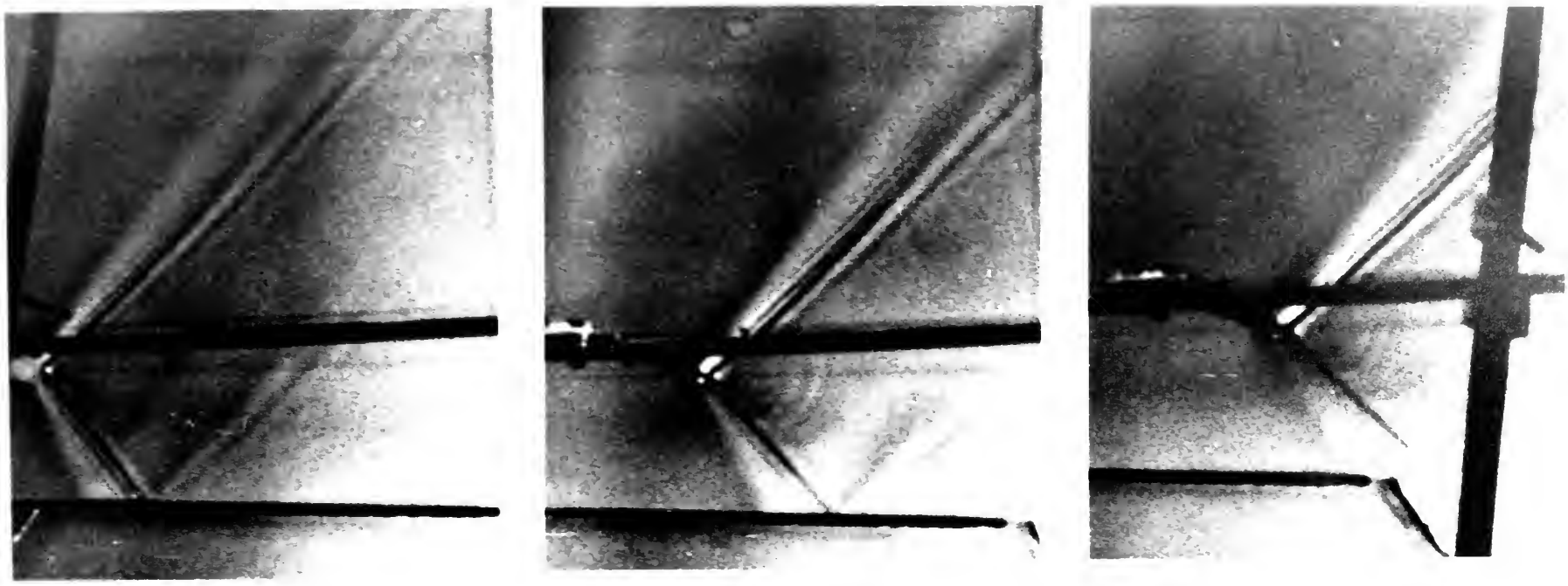

c. b. a.

Water Wave Patterns for a 5° Double Wedge Showing Shock Wave Interactions with the Ground for a Constant Mach Number of 1.5 Along a Straight Line Path Parallel with the Ground.

FIGURE 43

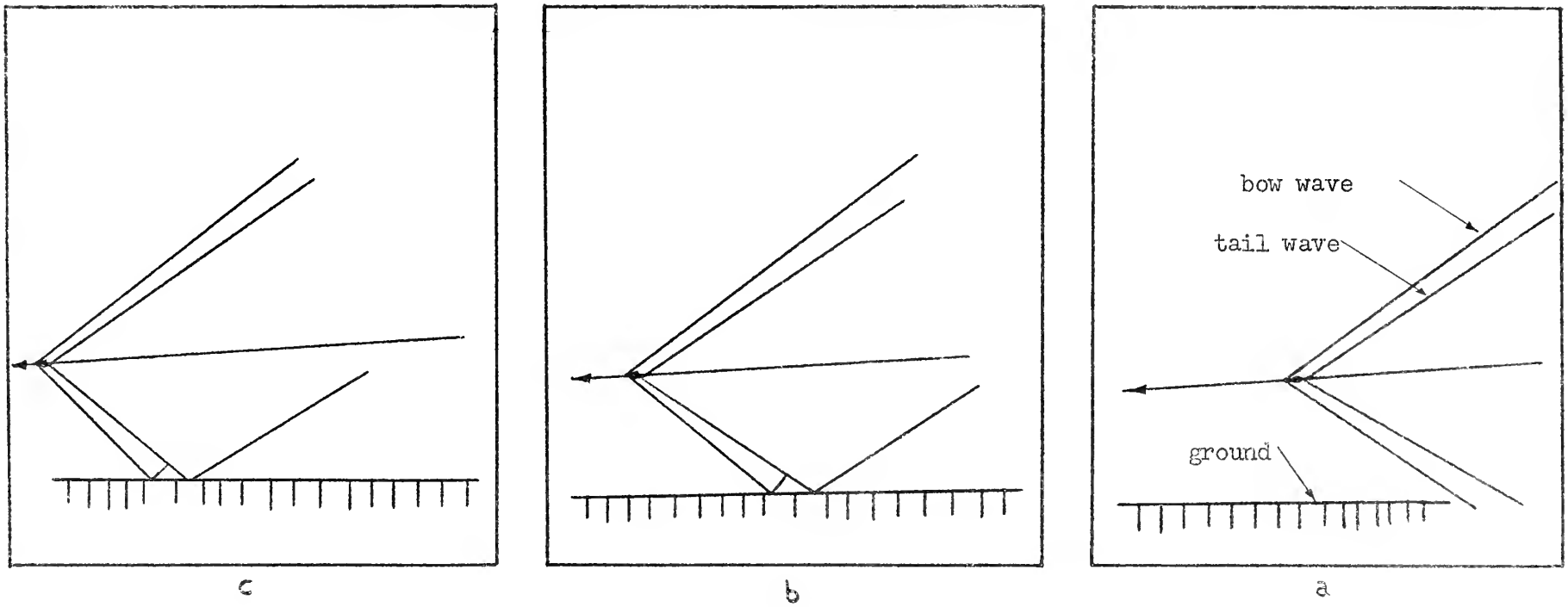

Line Drawings of Wave Patterns in Figure 45

FIGURE 44

c. b. a.

Water Wave Patterns for a 5° Double Wedge Showing Shock Wave Interactions with the Ground for a Constant Mach Number of 2.0 Along a Straight Line Path Parallel with the Ground.

FIGURE 45

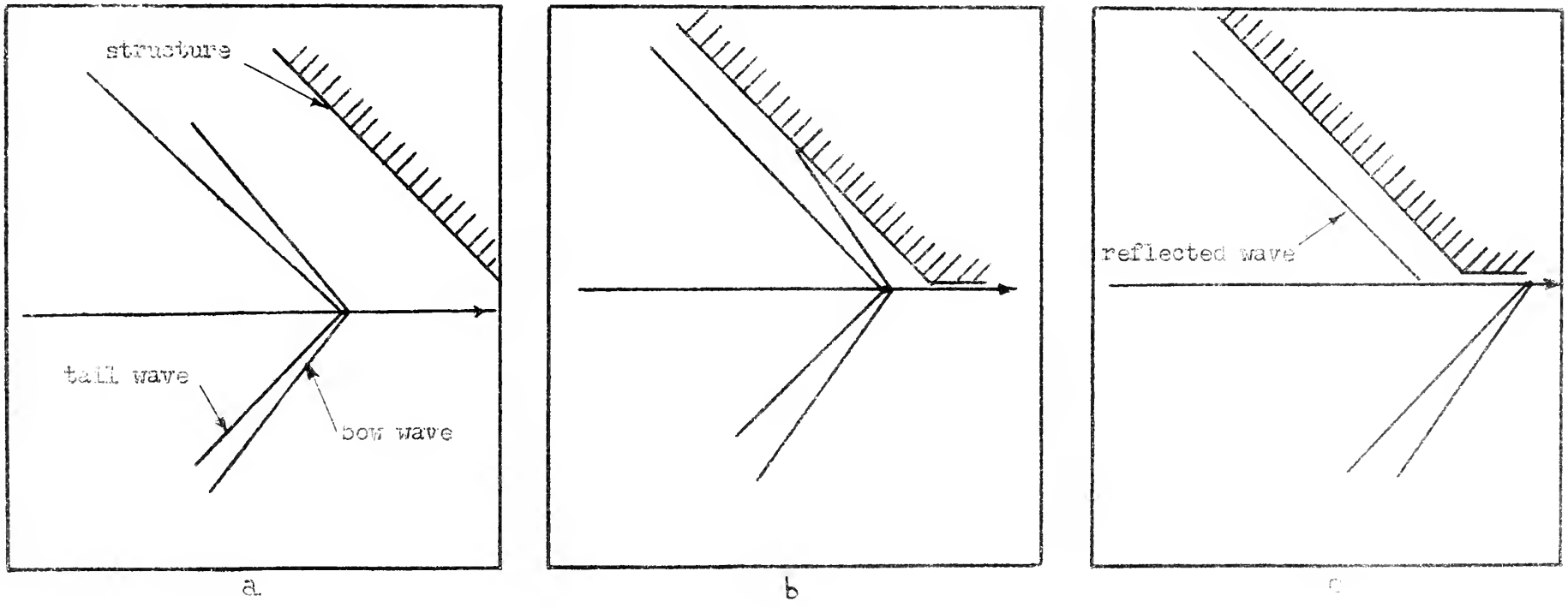

Line Drawings of Wave Patterns in Figure 47

FIGURE 48

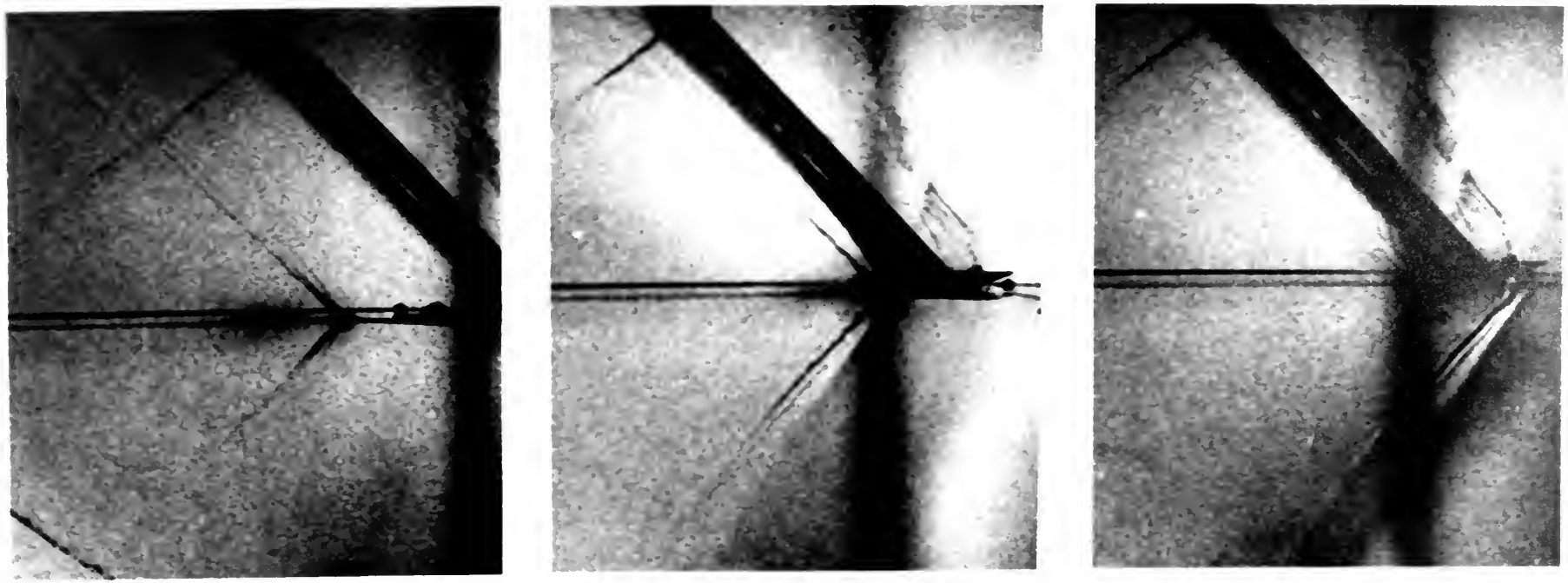

a. b. c.

Water Wave Patterns for a 5° Double Wedge Showing Plener Shock Wave Interactions with Structural Surfaces for a Constant Mach Number of 1.5 Along a Straight Line Path Parallel with the Ground.

FIGURE 47

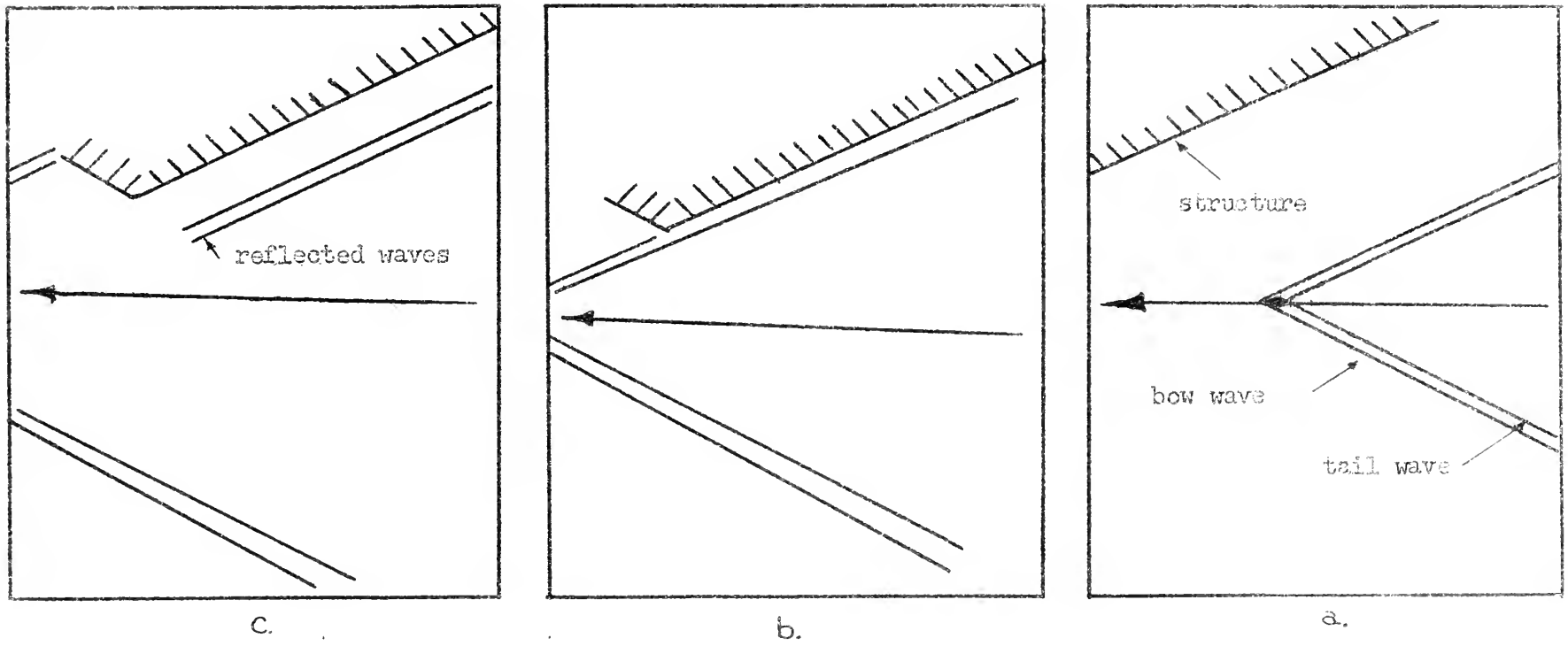

Line Drawings of Wave Patterns in Figure 49

FIGURE 48

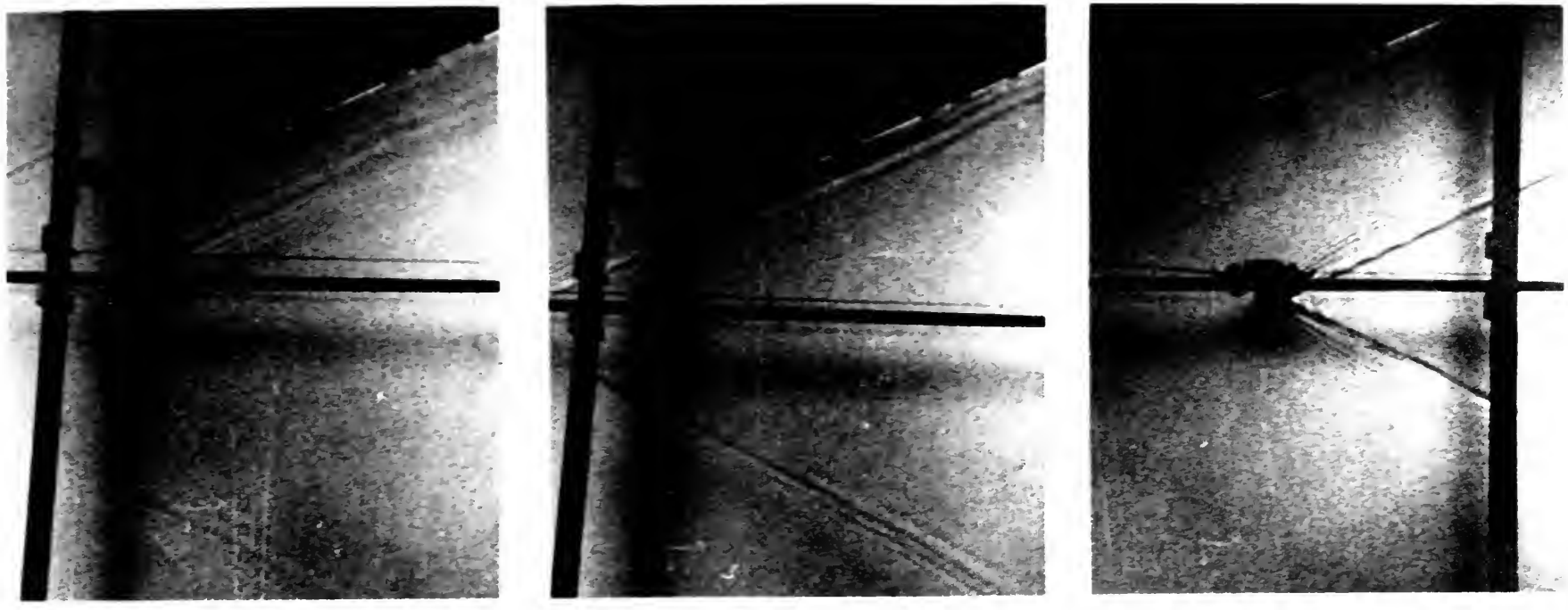

c. b. a.

Water Wave Patterns for a 5° Double Wedge Showing Planar Shock Wave Interactions with Structural Surfaces for a Constant Mach Number of 2.0 Along a Straight Line Path Parallel with the Ground.

FIGURE 49

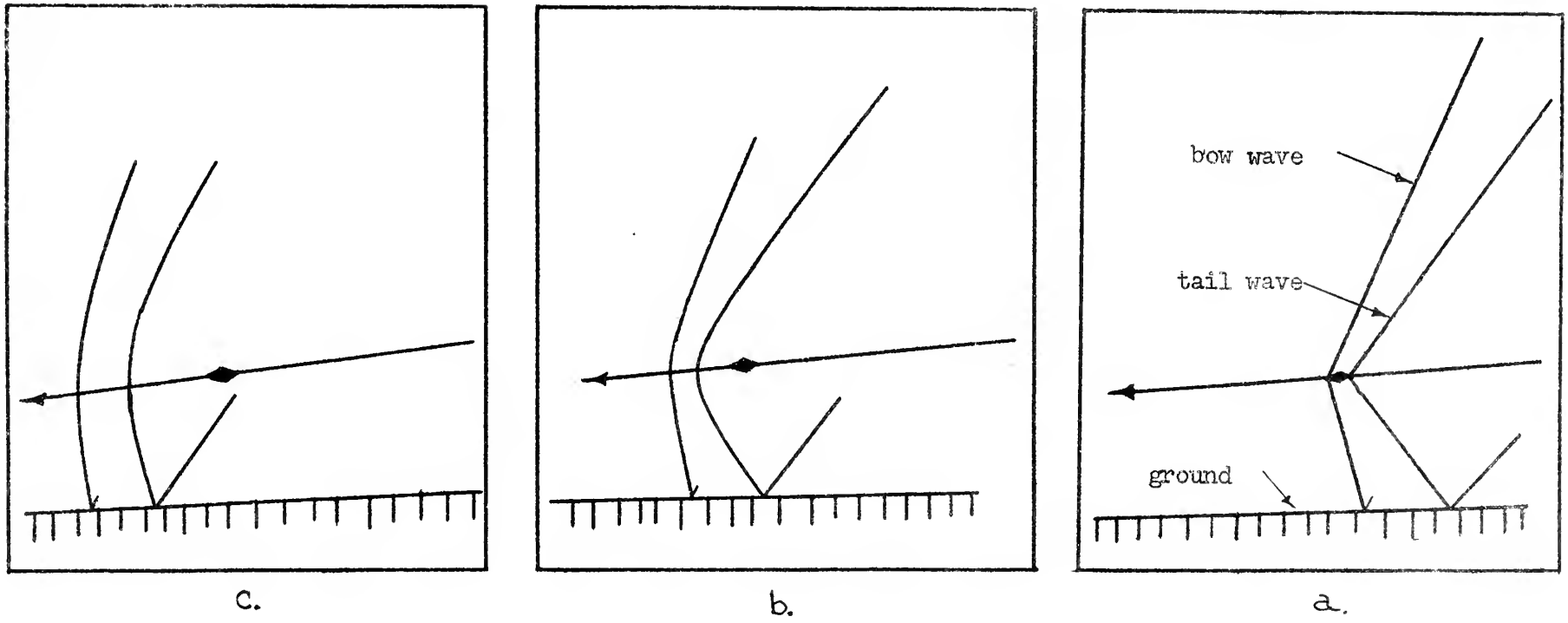

Line Drawings of Wave Patterns in Figure 51

FIGURE 50

c. b. a.

Water Wave Patterns for a 5° Double Wedge Showing Shock Wave Interactions with the Ground for Sudden Deceleration of the Wedge From a Mach Number of 1.25 to a Subcritical Mach Number Along a Straight Line Path Parallel with the Ground.

FIGURE 51

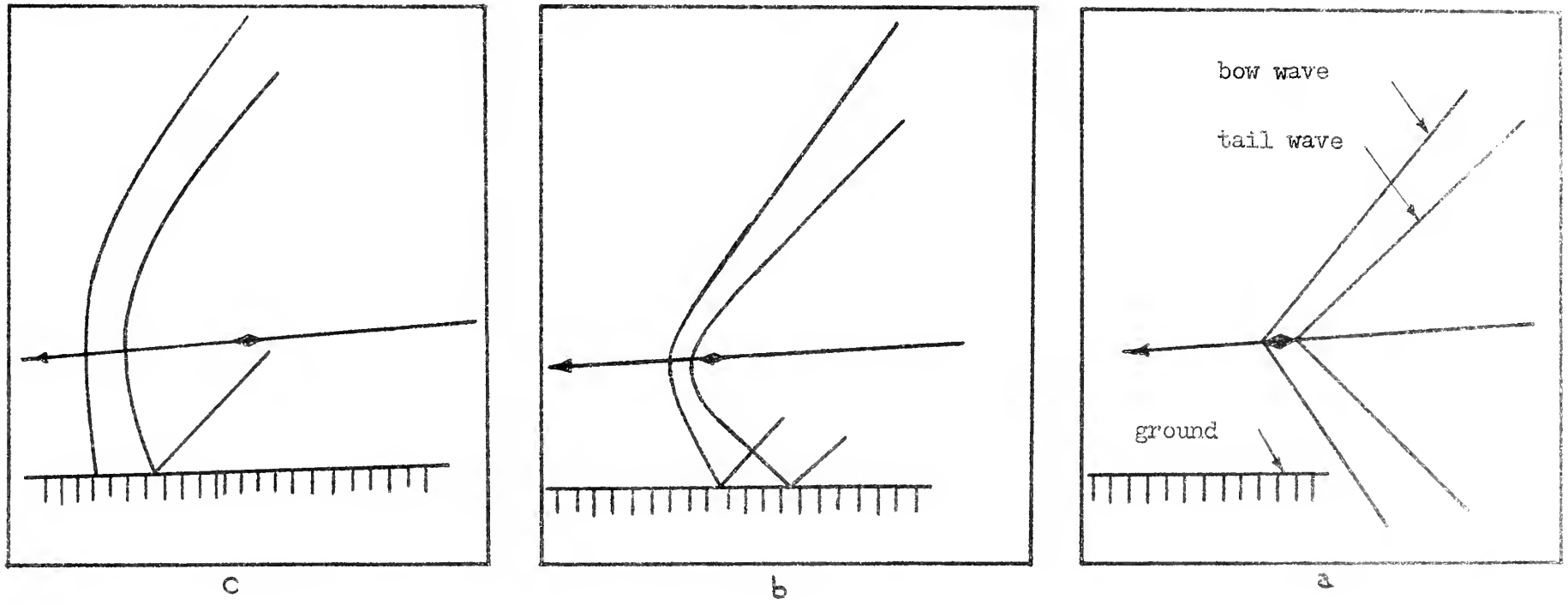

Line Drawings of Wave Patterns in Figure 53

FIGURE 52

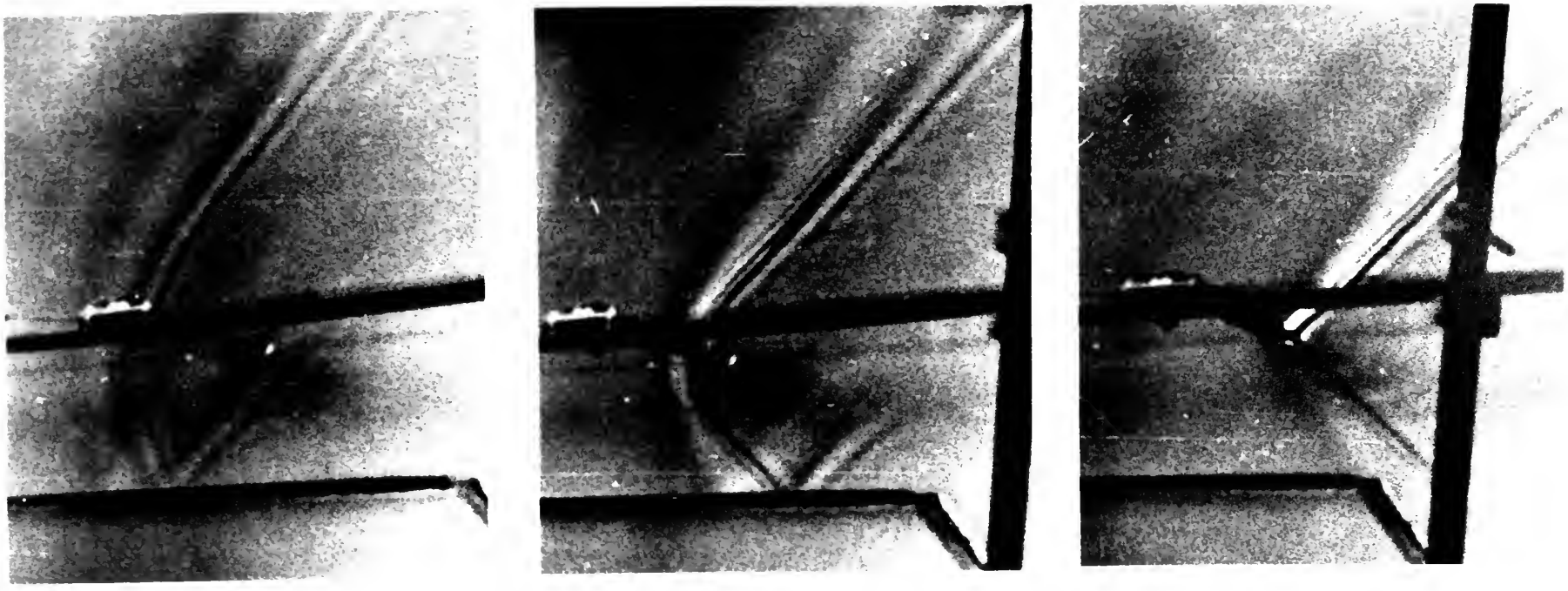

c. b. a.

Water Wave Patterns for a 5° Double Wedge Showing Shock Wave Interactions with the Ground for Sudden Deceler[illegible] of the Wedge From a Mach Number of 1.5 to a Subcritical Mach Number Along a Straight Line Path Parallel with the Ground.

FIGURE 52

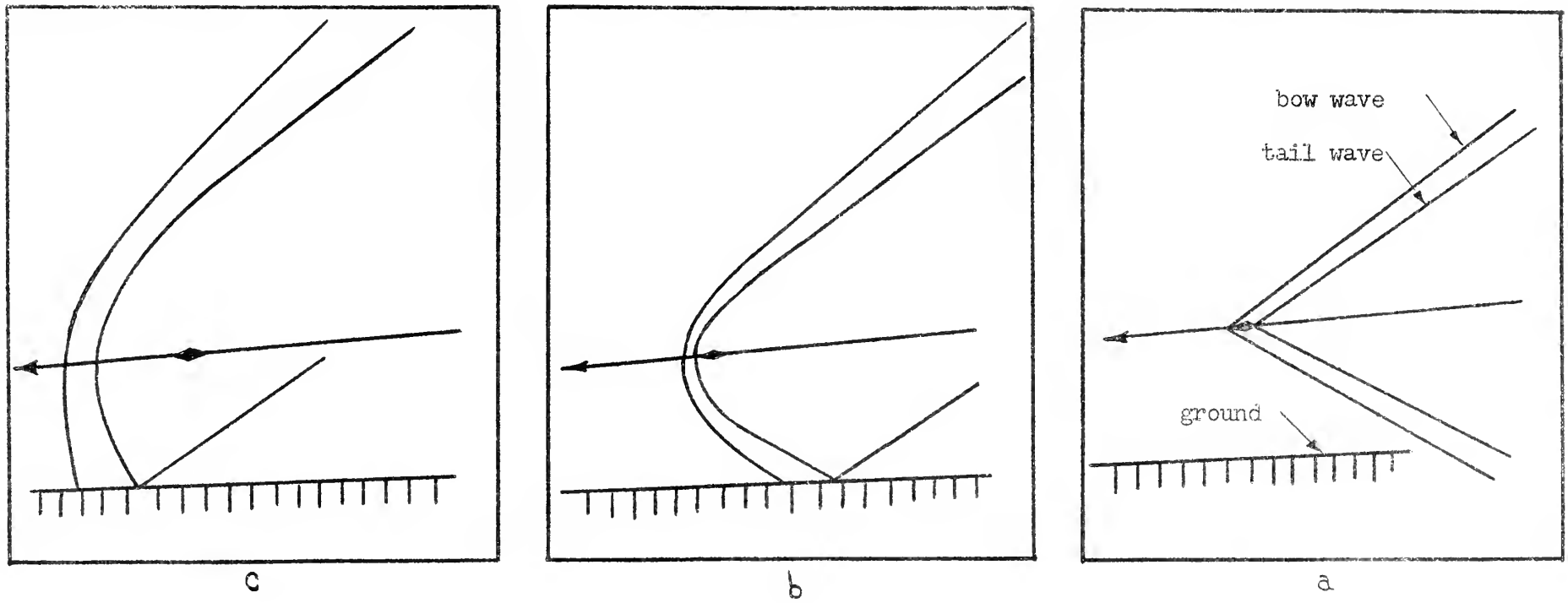

Line Drawings of Wave Patterns in Figure 55

FIGURE 54

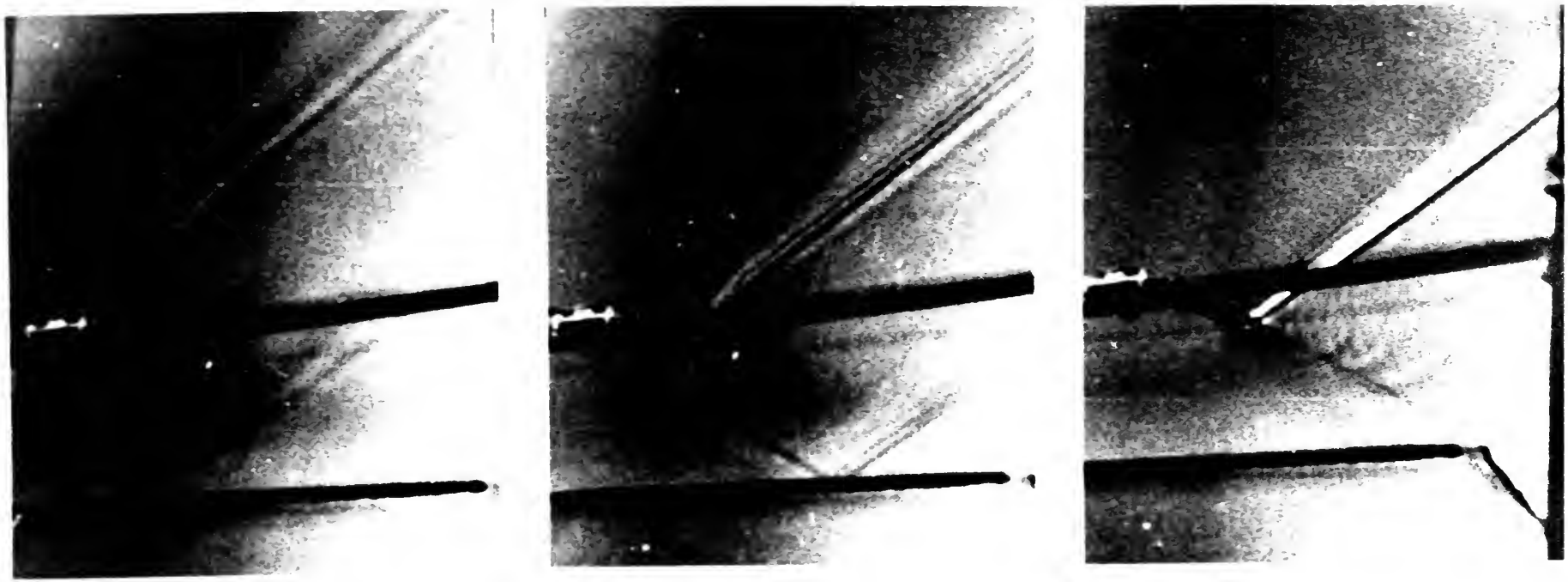

c. b. a.

Water Wave Patterns for a 5° Double Wedge Showing Shock Wave Interactions with the Ground for Sudden Deceleration of the Wedge From a Mach Number of 2.0 to a Subcritical Mach Number Along a Straight Line Path Parallel with the Ground.

FIGURE 55

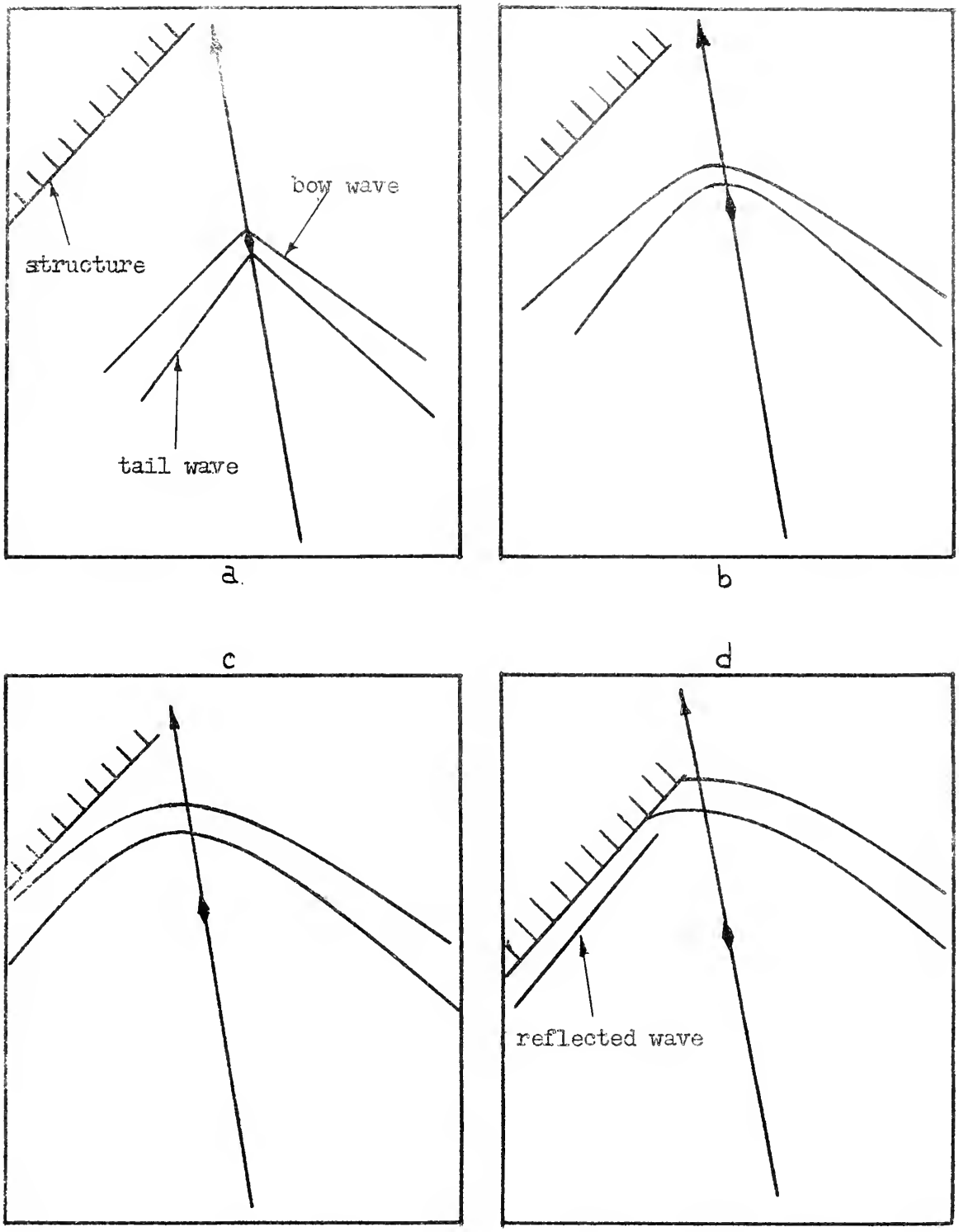

Line Drawings of Wave Patterns in Figure 57

FIGURE 56

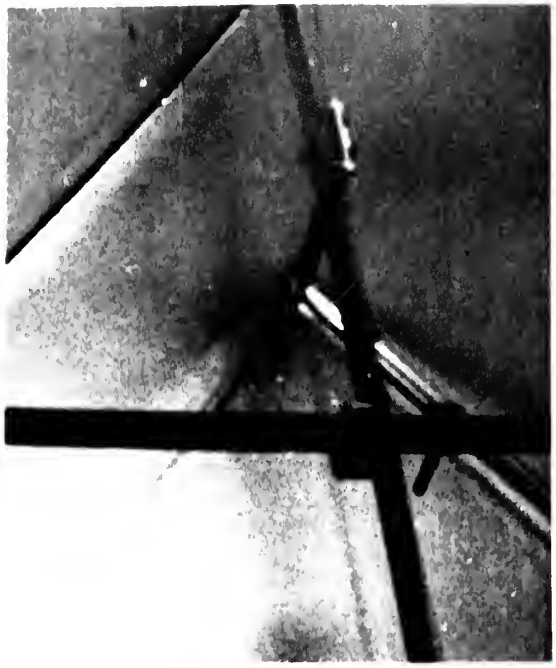

a.

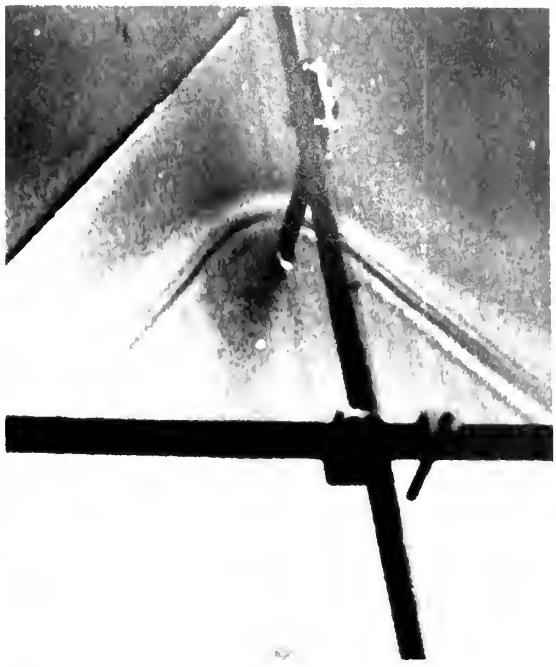

b.

c.

d.

Water Wave Patterns for a 5^{o} Double Wedge Showing Planar Shock Wave Interactions with Structural Surfaces for Sudden Deceleration of the Wedge From a Mach Number of 1.5 to a Subcritical Mach Number Along a Straight Line Path Parallel with the Ground.

FIGURE 57

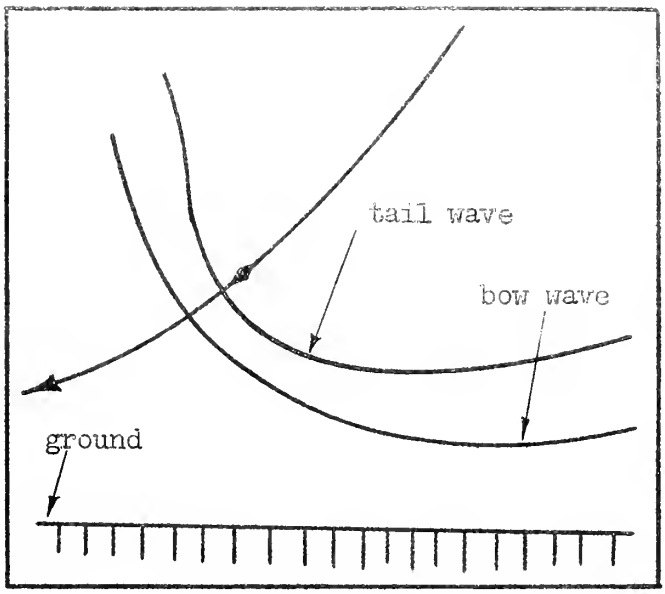

Fig. 58-A: M = 1.5

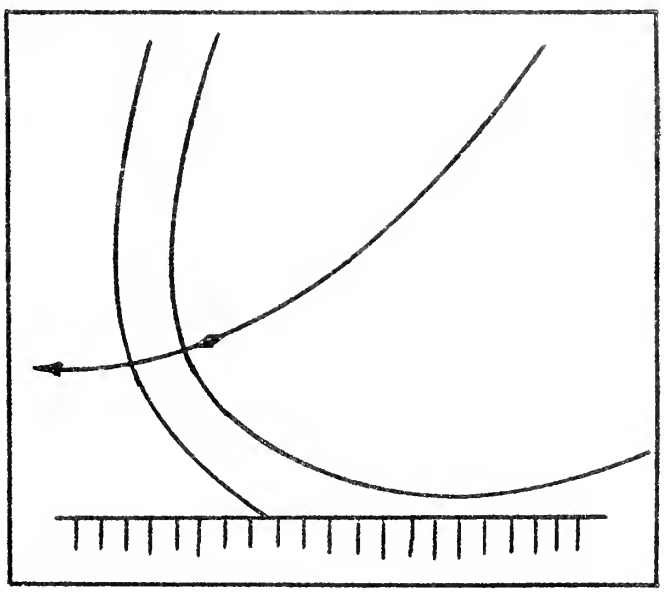

Fig. 58-B: M = 2.0

Line Drawings of Wave Patterns in Figure 59

FIGURE 58

Fig. 59-A: M = 1.5

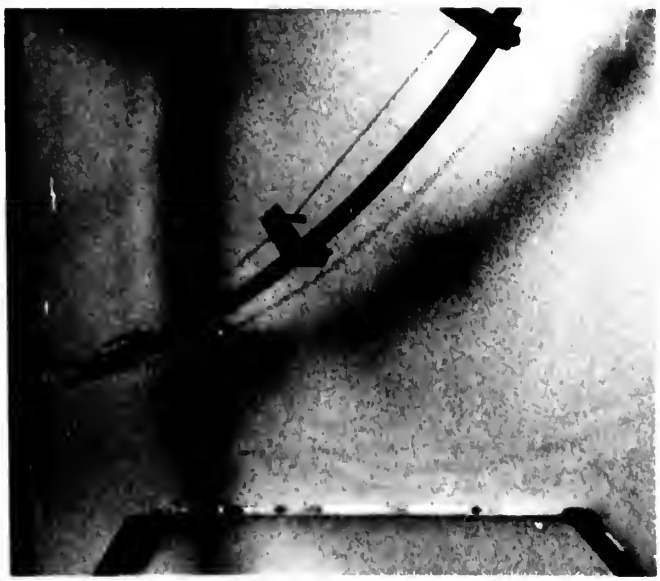

Fig. 59-B: M = 2.0

Water Wave Patterns for a 5^{o} Double Wedge Indicating the Types of Shock Wave Interactions with Other Surfaces Which may be Expected for Sudden Deceleration of the Wedge From Mach Numbers of 1.5 and 2.0 to a Subcritical Mach Number Along a Curvilinear Dive Path.

FIGURE 59